Biological and biochemical characterization of the extracellular signal-regulated kinase 8 homolog (TbERK8) in *Trypanosoma brucei*

Ana Lisa Valenciano Murillo

Dissertation submitted to the faculty of the Virginia Polytechnic Institute and State University in partial fulfillment of the requirements for the degree of

Doctor of Philosophy
In
Biochemistry

Zachary B. Mackey, Chair
Maria Belen Cassera
Jianyong Li
Paul R. Carlier

March 24, 2016
Blacksburg, VA

Keywords: *Trypanosoma brucei,* Extra-cellular signal regulated kinase 8 *(*ERK8), Proliferating cell nuclear antigen (PCNA), PIP-box, phosphorylation

Biological and biochemical characterization of the extracellular signal-regulated kinase 8 homolog (TbERK8) in *Trypanosoma brucei*

Ana Lisa Valenciano Murillo

Academic Abstract

Trypanosoma brucei species are vector-borne protozoan parasites that cause Human African trypanosomiasis (HAT) and nagana in cattle. In humans, the diseases caused by these parasites are fatal if left untreated. Treatments for these diseases are complicated because the approved drugs for treatment are ineffective against the parasites and have many toxic side effects associated with their use. There is a clear need to identify new therapeutics that are less toxic and more effective against *T. brucei*. Our approach for identifying new therapies is to identify novel targets in the parasite that can be modulated by small molecules. The mitogen-activated protein kinases (MAPK) pathway is a three-tiered signaling cascade that regulates cell responses to stimuli and are involved in essential processes. MAPKs can regulate differentiation, virulence, apoptosis, cell cycle and gene expression, which makes MAPKs interesting drug targets in *T. brucei.* The extracellular-signal regulated kinase 8 homolog in *T. brucei* (TbERK8) is essential for survival in the bloodstream form parasites. The work in this dissertation involves characterizing this *T. brucei* MAPK to better understand its biological function and identify small molecules that can inhibit its activity to kill the parasite. Here, we report that TbERK8 is an atypical MAPK kinase that is able to autophosphorylate and no upstream kinases that activate TbERK8 have been identified. We have demonstrated that TbERK8 is able to phosphorylate the proliferating cell nuclear antigen homolog in *T. brucei* (TbPCNA). This is in contrast to the reported function the human ERK8 and PCNA homologs that form a stable complex in normal breast cells which does not result in PCNA phosphorylation. We also report here that TbPCNA is phosphorylated on three residues localized to a unique insertion loop by TbERK8. TbPCNA is tightly regulated in the parasites such that either upregulating or downregulating its expression arrests *T. brucei* proliferation. Although, this mechanism of phosphorylation is unique to TbPCNA, the role that such phosphorylation has in regulating TbPCNA is not known. Finally, we have identified small molecules that can selectively inhibit either TbERK8 or

HsERK8, demonstrating that TbERK8 can be selectively inhibited to kill the parasite. The unique properties of TbERK8 can be exploited by small molecules that can be developed into new parasite-specific therapies that kill *T. brucei* with fewer side effects to the patients.

Biological and biochemical characterization of the extracellular signal-regulated kinase 8 homolog (TbERK8) in *Trypanosoma brucei*

Ana Lisa Valenciano Murillo

General Audience Abstract

Trypanosoma brucei is a protozoan parasite the causes the fatal disease human African trypanosomiasis (HAT) also known as sleeping sickness. It is transmitted by the tsetse fly and is endemic to the Sub-Saharan region of Africa where over 65 million people live at risk of infection. Although treatments are available, they cause toxic side effects that can in some cases lead to death. In addition, the administration of each of the available treatments requires a clinical setting. These problems associated with treatments clearly show the need for developing new treatments. This dissertation project, involved studying the extracellular-signal regulated kinase 8 homolog in *T. brucei* (TbERK8), a protein that is critical for the bloodstream form parasites, which thrives in humans to survive. Without the expression of this protein, the bloodstream form parasites cannot proliferate normally and will die. Because this protein is essential for the parasite's survival, it is an interesting target to inhibit in the parasite. We think that identification of compounds that inhibit the activity of this protein could result in new treatments. My work has revealed that TbERK8 has several unique properties that can be taken advantage of to create *T. brucei*-specific therapies. We have found that mutating several key residues that have an effect on its activity results in decreased growth of the parasites. We have also identified the proliferating cell nuclear antigen homolog (TbPCNA) as the first parasite substrate for TbERK8. We revealed that this relationship between the ERK8 and PCNA homologs in *T. brucei* is quite different than their relationship in human cells. In human cells, ERK8 and PCNA interact to form a tight and stable complex that does not lead to PCNA phosphorylation. Finally, we identified compounds that are capable of killing the parasites and inhibiting the activity of TbERK8. The discovery of these inhibitors gives us a potential starting point for developing new treatments that can kill the parasites by inhibiting TbERK8 in the parasite.

Acknowledgements

I would like to thank a number of people that have been with me through this journey. I would like to thank my advisor Dr. Zachary Mackey, for taking me into his lab where I was able to develop as a scientist in the field I am most passionate about, for his support and guidance, I am very grateful for everything I have learned. I would like to thank all the lab members that in one way or another helped me out and were here for me during these five years, including Julie Walker, Nathan Roberts, Aaron Ramsey, Sabrina Hill and Hyun Kang. A special thanks to Dr. Phoebe Williams, Aaron Ramsey, Michelle Pasier, Hyun Kang and Anne Brown for comprehensive reading, editing and formatting advice of this dissertation. I would like to thank my committee members Dr. Belen Cassera, Dr. Paul Carlier and Dr. Jianyong Li. Thank you for your advice during these 5 years and your willingness to help. I would also like to thank Dr. Pablo Sobrado who just believed in me as an undergraduate student coming from Costa Rica. And to our irreplaceable collaborator who also became a mentor through all these years, thank you Dr. Giselle Knudsen.

Graduate School would not have been possible with the support of my family, my parents Marita and Felix, my sister Juliana and brother Luis, my niece Sofia and sister in law Silvia, grandparents Tita Cata and Tito Vidal. Their understanding and encouragement to pursue my dreams even if it was far away from home is what kept me going through these years. Thank you for your unconditional support, multiple sacrifices and trips to Blacksburg to make sure I was doing well. As well as to my extended family and all my friends back at home. GRACIAS!!! The friendships I have made through these six years in Blacksburg from people all over the world are irreplaceable and an a huge part of me being able to reach this goal. Your support and continuous encouragement helped me through the difficult times and I will always be thankful. You are so many it would be impossible to list you by name but thank you!

Table of Contents

Attributions

Several chapters in this dissertation were done in collaboration and expert advice with others in both research and writing. The contributing researchers and experts include: Assistant Professor Zachary Mackey, Associate Professor Richard Helm, Professor Zhijian Tu, Senior Research Associate Keith Ray, undergraduate student Hyun Kang, former graduate student Aaron Ramsey, former lab technician Nathan Roberts, former lab technician Sabrina Hill from the Department of Biochemistry at Virginia Tech; Assistant Adjunct Professor Giselle M. Knudsen from the Department of Pharmaceutical Chemistry at the University of San Francisco California. All the co-author contributions are explained in each chapter. The publish work is used with permission from the publishers. I performed all the work on this dissertation unless highlighted in each chapter.

1. Introduction

1.1 The Parasite and the Disease

Trypanosoma brucei is a single-cell flagellate protozoa that belongs to the class kinetoplastida (1). Members of this class are Bodonida (free living) and Trypanosomatidae (which are human and veterinary pathogens). The Trypanosomatidae order include the pathogens *T. brucei*, *Trypanosoma cruzi* and species of the *Leishmania* genus, each of which are vector-borne pathogens that cause a range of diseases that affect humans and animals (2,3). There are three sub-species of *T. brucei* which cause disease in cattle and humans*:* (1) *T. brucei brucei* causes Nagana in cattle, while (2) *T. brucei rhodesiense* and (3) *T brucei gambiense* cause Human African Trypanosomiasis (HAT) also known as African sleeping sickness (4,5).

T. brucei is a heteroxenous parasite, meaning that the life cycle requires two different hosts that include an insect vector and a mammalian host (6). The vector *T. brucei* relies on is the blood-feeding tsetse fly from the genus *Glossina* (7). The fly carries the metacyclic trypomastigotes, infective stage to mammalian host, in the salivary glands and are injected in the host when the fly takes a blood meal. Once in the bloodstream, parasites differentiate to the trypomastigote stage where they multiply by binary fission. The trypomastigote stage exists in two forms in the blood: long slender form and stumpy form. Long slender form parasites can cross the blood brain barrier and infect the Central Nervous System (CNS) (6) and the quiescent short-stumpy form are infective to the tsetse fly (8). Parasites ingested by the fly during a blood meal enter the midgut and transform into the replicative procyclic trypomastigotes. The procyclic parasites transform to epimastigote stage and migrate to the salivary glands and transform into the infective metacyclic trypomastigotes (7).

Human African Trypanosomiasis is endemic in 36 sub-Saharan African countries where it has a negative impact on health and economic development of the population (9,10). In this area, over 65 million people are at risk of infection from *T. brucei*. *T.b gambiense* is responsible for 95% of the current cases. This subspecie is endemic to West and Central Africa and a total of 57 million people live in the

risk area. The remaining 5% of cases are caused by *T. b. rhodesiense*, which is endemic to East and South Africa, where 12.3 million people are at risk of infection. There are less cases because the vector control has been very effective (11). A big number of cases go unreported due to the remote areas where infection occurs, and the lack of health care services of the endemic areas that are able to diagnose and confirm cases. The reported cases have decreased in the recent years thanks to effective vector control and aggressive treatment programs. Currently there are approximately 10,000 cases reported per year, reduced from over 35,000 cases declared 15 years ago (12). African Trypanosomiasis can also affects animals, when causing the disease named Nagana. This disease affects livestock and results in an economic burden for the affected areas, which are mainly already poor rural regions (13). Infected cattle are non-productive, which deprives the population in these countries of milk and meat (14).

HAT presents itself in two different stages in the host; the early hemolymphatic stage and the late encephalitic stage. In the early stage of the disease, the parasites live in the bloodstream of the host and the lymphatic system invading different surrounding areas of the organs like the liver, spleen and skin. Patients develop a range of symptoms such as headaches, fever, malaise and sleeping disorders (9). The late stage takes place when the parasite crosses the blood-brain barrier and invades the CNS residing in the cerebrospinal fluid (CBF). The resulting disease is most often fatal if left untreated (10,15). In addition to the symptoms of the early stage disease, symptoms of the late stage include adenopathy, pruritus, tremor and neurological effects such as motor weakness and speech disorders(16). When HAT is caused by *T brucei gambiense*, the disease has a more slow chronic progression, taking an average of 3 years until it is fatal if untreated (17), while the infection of *T. brucei rhodesiense* has a faster progression, taking only a few months to reach the second stage, resulting in death of the host if he is not treated.

1.2 Diagnosis

Due to the endemic area of HAT and the lack of healthcare facilities with all the necessary tools, an accurate diagnose on confirming the stage that the disease is at is hard to come by. The diagnosis is

done first through elimination of other diseases as the cause of the symptoms. Some symptoms are easy to detect such as enlarged lymph nodes during the hemolymphatic stage. This is followed by trying to observe the parasites in the bloodstream using parasitological tests like microscopic examination of blood films; the results obtained are not always accurate because it depends on the level of parasitemia which constantly varies. These parasitological tests have limitations because the techniques and equipment are not accessible in all the regions where the infection is prevalent and it is more accurate for the *T. b. rhodesiense* infection. For *T.b. gambiense* infection, the use of the antibody-detecting card agglutination trypanosomiasis test (CATT) is used to try to identify specific antibodies against the parasite (18), but more accurate and practical parasitological tests to confirm HAT diagnosis are missing. The most reliable method to detect the late stage infection is the lumbar puncture, this is done to examine the cerebrospinal fluid for increased white-blood-cell count, elevated protein levels and the presence of trypanosomes (19). The use of PCR to detect trypanosomes is also being studied but has not yet proved to be of easy access on field (20). There is research on going to identify new and better approaches, such as the Molecular Dipstick test that identifies the presence of *T. brucei* DNA from samples of blood of infected patients; and it is rapid, simple and highly sensitive (21). And more practical serological tests, such as lateral flow tests, where you can obtain a result from an optical read, (22) and multiplex assays (23) to identify presence of *T. brucei* antigens in patients' blood are also being actively studied.

1.3 Treatment

Differentiating the early stage from the late stage is a key factor to apply the available treatment, since either lack of treatment or use of the wrong treatment on the early stage can result in death. The drugs that are used to treat HAT have been around for decades, however toxicity and the side effects caused by the drugs are still the main concern (24). Administration of these drugs is through parenteral route (intravenous or intramuscular) and requires a clinical setting, which is not always available in endemic regions.

There are two main treatments for early stage HAT. Pentamidine is used to treat the early stage of *T.b. gambiense*, and is administered via intramuscular (i.m.) injection during seven consecutive or

alternate days (25). This drug seems to be well tolerated by the patients and does not cause serious side effects other than hypotension and hypoglycaemia. However, there is evidence that parasites are becoming resistant to this treatment (26). Suramin has been the drug of choice to treat the early stage of *T.b. rhodesiense* since 1920, and it has not been noted to develop drug resistance (27). Adrenal failure is the most serious side effect developed by the use of this drug, however other less common problems can occur such as diarrhea, high fever, tiredness, anorexia (5,25). This drug has to be administered by intravenous injections (i.v) because it irritates the muscles. The treatment is given during 10-day intervals at 1-2 g; it possesses an extremely long half-life, which explains its efficacy. Although there is not an actual mode of action known for this drug, a wide range of serum proteins have been found to be inhibited by it (25).

There are two main treatments for late stage HAT. Melarsoprol was introduced as treatment in 1949 and is still used in both *T. b. rhodesiense* and *T. b. gambiense* infection. The treatment is administered in 3-4 different intravenous (i.v.) injections in series and repeating the series ten days after each time, for a total of four rounds of treatment. Patients given this treatment have a 5-10% chance of developing encephalopathy and the mortality rate of this group is greater than 50% (9,25). Patients who survived need to be examined for the following 2 years to check for absence of the infection (9). In addition to the serious side effects, drug resistance has also been reported (26,28).

Eflornithine came along in the 1980s, it was approved to be used for HAT by the FDA in the 1990s but it is only active against *T.b. gambiense* infection. Eflornithine targets the ornithine decarboxylase enzyme (ODC), enzyme in charge of the rate limiting factor in the polyamine pathway. This enzyme converts ornithine to putrescine. ODC is essential in all eukaryotic cells (29). The rapid turnover of this enzyme in *T. b. rhodesiense* prompts the parasite to be resistant to the drug (30), however it is highly effective against *T.b. gambiense*, The treatment is given at 400 mg/kg/day divided in 4 different doses for a total of 14 days (31). The major drawback is that the cost of the treatment is extremely high and the administration requires extensive care. Oral administration has been studied in both humans and rats but the patients relapsed, proving that this treatment is only effective through I.V.

administration (32,33). As a result, melarsoprol is still the drug of choice because it is more accessible to the populations at risk for HAT (24,31). Due to all the negative aspects of the treatments being used now, new treatments need to be developed, for which reason the identification of important pathways that can be targeted by inhibitors that could kill the parasites is a growing field of study.

1.4 Mitogen Activated Protein Kinases

Protein kinases phosphorylate proteins and are classified based on the specific residues they act on: serine, threonine or tyrosine. The mitogen activated protein kinases (MAPKs), are a family of protein kinases found only in eukaryotes, which contain both serine/threonine and dual-specificity kinases that also phosphorylate tyrosine residues (34). Signal transduction pathways communicate external signals that affect changes within the cell, MAPK are in charge of regulating these pathways. They can regulate many cell process such as apoptosis, cell proliferation, cell division and gene regulation (35-37). MAPK are part of a three-tiered cascade involving a MAPK kinase kinase (MAPKKK), a MAPK kinase (MAPK or MEK) and a MAPK. MEK have dual kinase activity, being able to phosphorylate threonine (T) and tyrosine (Y) residues at the same time. MEKs are the kinases in the second step of the pathway in charge of activating the MAPK. MAPK need two phosphorylation events in their activation loop to be fully activated. This activation occurs after the phosphorylation of the common TxY motif, where the kinases are activated after both the threonine (T) and the tyrosine (Y) are phosphorylated by an upstream MEK, however MAPK can also autophosphorylate. There are three subfamilies of MAPKs and these are categorized by the amino acid in the middle of the activation motif (TxY) where x can be either proline (P), glycine (G), or glutamic acid (E). The c-Jun aminoterminal kinases (JNK) have the TPY motif, p38 have the TGY motif, while ERKs present the TDY (ERK1/2) or TEY (ERK5 and ERK8) motif (38,39).

1.5 MAPKs in the *T. brucei*

There are 156 identified kinases in the *T. brucei* genome, which translates to close to 2% of its whole genome. Moreover, unlike humans, receptor-linked tyrosine and tyrosine-like kinases have not been identified in trypanosomes (40,41). The variety of kinases present in *T. brucei* suggests that phosphorylation pathways might be present in the parasites and have a role in cell regulation. The way in

which the parasites sense and respond to their environment is poorly understood. MAPK have been identified in the parasites and are known in other eukaryotes for their role in reacting to environmental changes by activating essential pathways (41). Having a better understanding on this area and targeting this responses by using protein inhibitors could develop new treatments.

T. brucei encodes genes for 10 MAPK and for 5 MAPK-like proteins, showing that basic components of the MAPK signalling pathways are present in the parasites, but the roles of most of this kinases and their respective substrates remain unknown; a functional network has not been demonstrated (41). MAPK is found throughout eukaryotes, however there has been divergence of these genes across plants, animals, fungi and unicellular organisms. Although the sequences are similar between host and parasite MAPK, key structural differences in their polypeptide sequences suggest they have unique features that contribute to functional differences that can be exploited to identify inhibitors that can kill the parasite with no effect on the human counterpart (42-44). The Extracellular-signal-regulated Kinases (ERKs) belong to the family of the MAPKs and are involved in signalling cascades that inform the cells how to respond to external signals. In the parasite genome, homologues of the human ERK1, ERK2, ERK4 and ERK8 have been identified. TbERK4 is needed for normal differentiation of the parasites into bloodstream form (45,46); while TbERK8 is the only that is essential for survival of bloodstream form parasites (47-49).

1.6 Extracellular-signal regulated Kinase 8 (ERK8)

ERK8 was first identified and studied in humans; it was discovered by using rat cDNA of ERK7 to screen a human cDNA library. ERK8 is the most divergent from the other ERKs with only 67% homology compared to up to 99% homology in other members of the ERK family (50). Common characteristics of the ERKs are a long C-terminal extension found in human and rat ERK8 and the two SH3-binding motifs found in both ERK7 and ERK8 (50,51). Human ERK8 is able to autophosphorylate and apparently, the known MEKs are not in charge of this activation. Several studies report that ERK8 is activated by Src-dependent signalling pathway, serum stimulation (50) and by an activated form of the

RET proto-oncogene (52). Other study suggests that ERK8 might have a role on DNA repair (53). After exposing the cells to H_2O_2, levels of phosphorylated ERK8 transiently increase to its maximum, followed by an accumulation of DNA double strand breaks (DSBs), suggesting a role for ERK8 in DNA repair (53).

A number of groups have studied the role of ERK8 in different types of cancer cells. In the HCT15 colorectal cancer cell lines; ERK8 is highly expressed compared to two other cell lines. The high levels of ERK8 promoted cancer progression; knocking down the kinase resulted in decrease of tumorigenic properties of HCT15 cells together with increased c-Jun phosphorylation. And in the other cell lines studied, that had normal levels of ERK8, the cancer developed less aggressively, suggesting a direct role of ERK8 in the progression of these cancer cells (54). Other reports have studied the binding abilities of ERK8. It was found to be a corepressor by binding to the ERRα and inhibiting it to localize to the nucleus (55). On the other hand, silencing ERK8 from this cells resulted in amplified cell motility and aggressive cancer (56).

ERK8 has two chromatin binding domains and a PCNA interacting peptide (PIP-box). The latter is a motif present in over 200 proteins that interact with proliferating cell nuclear antigen (PCNA), the homotrimeric clamp that is involved in DNA synthesis and repair pathways (57). Human ERK8 has a functional PIP-box that interacts with PCNA but only in the form of chromatin-bound ERK8; free ERK8 does not interact with PCNA. They concluded that in human breast cancer cells, ERK8 protects PCNA from the E3 ligase. Knock down of ERK8 decreases cell proliferation in approximately two fold but does not cause a lethal phenotype (57).

The first substrate phosphorylated by HsERK8 was recently identified. The RNA-binding protein that belongs to the family of the Hu/embryonic lethal abnormal vision (ELAV) genes named HuR was phosphorylated by HsERK8; preventing it from binding to the tumour suppressor PDCD4 (Programmed cell death 4) mRNA. The exact residues that are phosphorylated by HsERK8 were not described (58).

1.7 ERK8 in *Trypanosoma brucei*

ERK8 was recently identified in *T. brucei* while performing a small RNAi kinase screen. ERK8 and CRK12 where the two kinases identified that develop an interesting phenotype in the parasites. In the case of ERK8 the parasites stopped proliferating resulting in a lethal phenotype (47). ERK8 homologs have also been studied in other two protozoan parasites, *Entamoeba histolytica* (*Eh*MAPK) (59) and *Toxoplasma gondii* (*tg*MAPK2) (60); but their role on the cells has not yet been described. The essential role of this kinase has also being confirmed by other two groups using targeted parallel sequencing RNAi and by a kinome wide RNAi screen (48,49).

TbERK8 shares a number of characteristics of ERKs found in other eukaryotes. Just like other ERKs in protozoan organisms, the motif in the activation loop is TxY. In *T. brucei*, the loop of ERK8 is TDY in contrast to the TEY motif in the human protein (61). TbERK8 has a long C-terminal extension, but lacks a chromatin-binding region found in the human homolog. The PIP-box, motif on proteins that interact with TbPCNA, is highly conserved, with 75% sequence similarity to the motif in HsERK8.

1.8 Proliferating Cell Nuclear Antigen and its role in the parasites

Proliferating Cell Nuclear Antigen (PCNA) is the central component of the DNA replication machinery, involved in the recruitment of key factors into the fork during DNA replication and repair such as polymerases. Inside the cell, it forms a homotrimeric sliding clamp that wraps DNA; each of the monomers is composed of domains I and II that are linked by the inter-domain connecting loop (62). PCNA has been found in almost all the eukaryote organisms studied thus far, in humans there are over 200 proteins known to interact with PCNA (63). Due to the wide number of interacting proteins, process where PCNA is involved need to be tightly regulated in order for each of them to proceed as expected (64). Proteins that have a PCNA-interacting peptide (PIP-box) motif bind to this homotrimeric clamp by an interaction between the hydrophobic inter-domain connecting loop localized between the two domains of PCNA and the PIP-box from the interacting protein (65). One tightest binding of PCNA to a protein is the interaction with $p21^{CIP1/WAF1}$, because it has a canonical PIP-box motif. The consensus sequence for the PIP-box motif is QxxΨxxϑϑ (Ψ= hydrophobic residues and ϑ= aromatic residues) (63).

Conformational changes on PCNA can occur to promote a specific interaction or a choice of pathway, post-translational modifications such as ubiquitylation, sumoylation, (66) and phosphorylation (65) can take place to promote these changes. In human cells, the Y211 is phosphorylated by the Epidermal Growth Factor receptor (EGFR) tyrosine kinase. An increase in phosphorylated PCNA correlates to a lack of chromatin-bound PCNA stability, resulting in uncontrolled cell proliferation (67) and inhibition of mismatch repair (68). Phosphorylation of PCNA occurs through the receptor tyrosine kinase, Recepteur d'Origine Nantais (RON)/ C-Abl pathway (69). The phosphorylated PCNA promotes binding of the clamp to chromatin and an increase in DNA replication (69,70). In TbPCNA, this residue is substituted by a phenylalanine, suggesting that activation through this phosphorylation site is not conserved and this mechanism of phosphorylation in the parasite is not possible.

Although there is plenty of information regarding cell cycle regulators, there is a lack of information on DNA replication in *T. brucei*. The research regarding DNA replication is mostly limited to proteins in the origin of replication complex (ORC) that have been identified in the parasites, including Orc1b and Orc1/Cdc6, who interact with the Mcm2-7 component of the CMG (Cdc45·Mcm2-7·GINS) complex (71), but PCNA was not studied with these other DNA replication factors. In the protozoan parasites, *Leishmania donovani* and *Trypanosoma cruzi,* PCNA has been found to localize to the periphery of the nucleus during DNA replication and remain in the cells during all the stages of the cell cycle, unlike what has been previously reported for *T. brucei* (72,73). There is only one study that has investigated the role of PCNA in *Trypanosoma brucei* in order to use TbPCNA as a cell cycle marker. They have reported that TbPCNA localizes to the nucleus during DNA replication in the G1/S phase but is degraded during cell division (73). There is a clear need to have more insight into what happens during the parasites DNA replication and cell cycle, and the identification of more of these proteins involved in this process. Through understanding how DNA replication and the cell cycle is controlled in the parasite, we may discover new targets for therapeutics.

1.9 TbERK8 and TbPCNA interaction: targeting these proteins for drug discovery

By studying TbPCNA and TbERK8 we expect to elucidate the role of these proteins in the parasite; and if the mechanism of action in the parasite is similar to that in human cells. Polβ has a non-canonical PIP-box, were the binding between this proteins is very tight but instead of having two residues between the hydrophobic and the aromatic residues it has three (74). This is the type of PIP-box that is found in TbERK8 and HsERK8. Groehler *et al* (57) reported the ability of HsERK8 to bind to HsPCNA by the PIP-box motif when HsERK8 has bound to chromatin. We will attempt to understand the function of TbERK8 and TbPCNA in the parasites, the importance of TbPCNA and study if and how they interact. Both of these proteins are essential for parasite survival, have unique properties that make them different from their human homologs and have the potential to be involved in essential pathways in the parasite. They could be drug targets for which inhibiting the interaction could culminate in the death of the parasite.

1.10 Organization of the dissertation

The dissertation is organized as follows: in order to understand the roles of both of these proteins and their interactions we started by studying the biological role of TbERK8 in the parasite. In Chapter Two you will find studies that include protein localization, the effect of TbERK8 depletion on DNA replication and the effect of overexpressing single point mutations in the conserved residues of the kinase domain. Before understanding the TbERK8/TbPCNA interaction we established the essential role of TbPCNA in the parasites. Chapter Three studies the effects of downregulating or upregulating TbPCNA, as well as its physical localization in the parasite throughout the stages of the cell cycle. In Chapter Four we show the mechanism of interaction of TbERK8 with TbPCNA and unique properties of TbERK8. For Chapter Five we present the results of a focused kinase inhibitor screening in the parasites and recombinant proteins. Finally in Chapter Six you will find what we concluded from this project and what the future work should be.

2. TbERK8 is an essential MAP Kinase in bloodstream form *Trypanosoma brucei*

Author Contributions:

Ana Lisa Valenciano performed all the research except for the experiments mentioned below and wrote the article.

Nathan Roberts performed the FBS titration on wild type parasites.

Sabrina Salisbury did the RNA quantification experiment.

Zachary Mackey performed the RNAi experiment on the procyclic form parasites. Oversaw, edited and directed the writing of the article.

Abstract

The previous studies show that TbERK8 is essential for bloodstream form *T. brucei* survival, this prompt us to try to understand the biological role of this kinase in the parasite. We found that the phenotype displayed after silencing TbERK8 is only present in bloodstream form parasites and not in the procyclic form. We found TbERK8 localized in the cytoplasm and nucleus. After silencing by RNAi its absence promoted defects in DNA replication. Lastly, we identified the activation loop residues T174A and Y176A to be important for the normal proliferation of the parasites, overexpressing this mutant developed a dominant negative affect.

2.1 Introduction

Mitogen activated protein kinases (MAPK) regulate signal transduction, gene expression, the cell cycle, and apoptosis; there are several MAPKs in different systems that have been found to be indispensable for cell survival (43). These characteristics make MAPK good drug targets. MAPK regulate these processes by a signalling cascade activated by a three-tiered phosphorylation process. Extracellular signal regulated kinases (ERK) are activated by an external stimuli. ERK1/ERK2 (45,75), ERK5, and ERK8 homologs have been identified in *T. brucei*, the cause of African Sleeping Sickness, but only ERK8 has been found to be essential in bloodstream form parasites (47).

The recent identification of ERK8 in *T. brucei* together with the lack of information on its homolog in Kinetoplastid parasites awoke our curiosity to answer questions about this MAPK deviant to typical ERK1/ERK2s (47). In this study, we showed TbERK8 is only essential in the bloodstream form parasites, and that it acts like other ERK8 homologs regarding localization to the cytoplasm. Our studies confirm that TbERK8 is a good drug target because changes in its integrity, besides RNAi silencing, promote proliferation defects.

2.2 Materials and methods

2.2.1 Culturing of *T. brucei*

Procyclic form *T. brucei* (PF) was subcultured at 27^{o}C without CO_2 in Cunninghams medium (76) containing 10% fetal bovine serum (FBS). Bloodstream form (BSF) parasites were incubated in 5% CO_2 at 37 °C in HMI-9 medium modified to contain 20% fetal bovine serum (FBS) (77). Both digenetic stages of the parasite were cultured in media containing 100 U/ml penicillin/ and 100 µg/ml streptomycin. Selection medium contained 5 µg/ml hygromycin B, 2.5 µg/ml G418 and 2.5 µg/ml phleomycin. Recombinant proteins were expressed in BSF 90-13 strains (78) in HMI-9 medium containing 100 ng/ml of tetracycline. The recombinant open reading frames were subcloned into the Hind III and Afl II restriction sites of the C- terminal HA-tagged modified version of pLEW111 (79).

2.2.2 *T. brucei* genomic DNA extraction

Bloodstream form parasites where grown up to $1X10^7$, pelleted by centrifugation and washed three times with 5 ml of PBS. The cells were lysed in 10X Tb. Lysis buffer (PBS with 5% SDS), with 5 unit/ml final concentration of Proteinase K and RNAse, followed by incubation at 65 °C for 4 hours. The DNA was extracted using phenol:chloroform:IAA (isoamyl alcohol), phenol:chloroform and precipitated with Isopropanol. The pellet was washed with 70% ethanol and finally resuspended in Tris-EDTA (TE) buffer.

2.2.3 TbERK8 mutant constructs

The TbERK8 RNAi construct used was the one previously reported (47). To introduce mutations into the TbERK8 gene, Wild-type TbERK8 was amplified with the forward primer 5'-CGCGCCAAGCTTATGTCATCAGAAATAGAGCC-3' and the reverse primer 5'-CTTAAGTTTGTGCAACACACGAGAGGC-3' from genomic DNA. Point mutations were made in TbERK8 cDNA by the annealing overlapping PCR method (80). PCR templates used for the annealing overlapping reaction were made by combining the wild-type TbERK8 forward primer with the

appropriate mutant reverse primer or the wild type TbERK8 reverse primer with the appropriate mutant forward primer listed below:

K42A rev 5'-GCGTCGTATATCTTCGCTAACGCTACAACC-3'

K42A fwd 5'-GGTTGTAGCGTTAGCGAAGATATACGACGC-3'

D153A rev 5'-TTGAGCAATCGCTGTTTACAAGCA-3'

D153A fwd 5'-TGAAAGTGGCAGCCTTTGGGCTAG-3'

T174A rev 5'-AACGTGTCATGATGTAATCCGCGAGTACGGG-3'

T174A fwd 5'-CCCGTACTCGCGGATTACATCATGACACGTT-3',

Y176A rev 5'-AACGTGTCATGATCGCATCAGTGAGTACGGG-3'

Y176A fwd 5'-CCCGTACTCACTGATGCGATCATGACACGTT-3'. The full-length mutant TbERK8 cDNAs were subcloned into the Afl II and Hind III sites of the vector and expressed in pLEW1113HA. To make the double mutations, the previous primers were used in a copy of the gene where a mutation had been previously introduced.

2.2.4 Introduction of transgenes into *T. brucei*

To perform the transfections, 10^7 parasites were pelleted by centrifugation and washed once with 10 ml of phosphate buffered saline (4.3 mM Na_2HPO_4 137 mM NaCl, 2.7 mM KCl, 1.4 mM KH_2PO_4) pH 7.4. 1-to-10 µg of DNA (Not I linearized plasmid for tetracycline inducible constructs or with NruI for endogenously expressed genes) was nucleofected into the parasites using a Lonza Nucleofector II® and the T-cell kit. Program X-001 for bloodstream form and X-003 for procyclic form were used to pulse the parasites, then transferred to 10 ml of modified HMI-9 or Cunningham's media and incubated in the conditions previously described overnight. After 24 h, 5.0 µg/ml hygromycin B, 2.5 µg/ml G418, and 2.5 µg/ml of phleomycin was added to the media to select stable clones.

2.2.5 RNA interference (RNAi) transgenes quantification

The media was supplemented with 100 ng/ml of tetracycline to induced the RNAi and parasite proliferation was monitored by using a Multisizer™ 3 Coulter Counter®. The induced parasites and the non-induced controls were pelleted by centrifugation and resuspended with 1 ml of TRIzol reagent (Invitrogen,Grand Island, NY). 1.5 µg of total RNA was used as a template for amplifying coding regions using the SuperScript III One-Step RT-PCR kit (Invitrogen,Grand Island, NY) and gene-specific primers: (TbERK8 forward *5′- GGATCCATGTCATCAGAAATA GAGCC-3′* and reverse *5′-GTCGACAATTTCTTGGTATAGCCGCT-3′*), (TbPCNA forward *5′-AAGCTTATGCTTGAGGCTCAGGTTCT -3′* and reverse *5′-CTTAAGCTCGGCGTCGTCA CCTTTG -3'),* and (Tbα-Tub forward *5′-ATGCGTGAGGCTATCTGCATCCACAT -3′* and reverse *5′-AGGTTGCGGCGAGTCAAATCATAAAT -3')*. To monitor that the PCR products during amplification were still in the linear range, 5 ul from cDNA samples were collected at 20, 23, and 25 PCR cycles. The products were resolved by agarose gel electrophoresis, stained with SYBER Safe®, and quantified by ChemDoc (BioRad, Hercules, CA).

2.2.6 Statistical analysis

The Student's t-test was used to compare numerical means obtained from non-induced or induced samples.

2.2.7 Western blots

Parasites were lysed with Tb lysis buffer (1.0% Triton X-100, 10 mM Tris pH 7.5, 25 mM KCl, 150 mM NaCl, 1 mM $MgCl_2$, 0.2 mM EDTA, 1 mM dithiothreitol, 20% glycerol). Twenty-five micrograms of crude lysate was resolved by SDS-PAGE and transferred to a polyvinylidene difluoride (PVDF) membrane. After transferring and blocking, the PVDF membrane was incubated with rabbit anti-HA (hemagglutinin A) (1:2,000 dilution) for 1 h and washed three times for 5 min each with Tris-buffered saline triton-100 (TBST) (10 mM Tris, pH 7.4, 150 mM NaCl, 0.4% Tween 20). After the third wash, horseradish peroxidase-conjugated donkey anti-rabbit IgG (1:1,000 dilution) was added to the blots

for 1 h. The blots were then washed again in the same buffer 3x for 5 min each and examined by enhanced chemiluminescence (ECL) (GE Healthcare).

2.2.8 5-ethynyl-2'deoxyuridine (EdU) staining

TbERK8 RNAi clones were subcultured at $1x10^5$ /ml at T_0 in HMI-9 media, induced with a 100 ng/ml final concentration of tetracycline and without tetracycline as a control. A final a concentration of 100 µM EdU (LifeTechnologies, Grand Island, NY) was added to the media after 48 h and labeling proceeded for 2 h or 12 h. The parasites were pelleted by centrifugation, washed with 5 ml phosphate buffered saline (PBS) and fixed for 30 min with 0.5% paraformaldehyde. The fixed parasites were stained, visualized and the nuclei and kinetoplast quantified as reported before (81).

2.2.9 Overexpression of recombinant proteins in *T. brucei*

Tetracycline was added to the medium at a final concentration of 100 ng/ml to overexpress all recombinant proteins in the BSF parasites. Induced parasites were incubated in humidified chambers at 37^oC with 5% CO_2.

2.2.10 Kinase immunoprecipitation assay

Extracts from at least $5x10^7$ induced parasites were pelleted by centrifugation and lysed with 1 ml of immune-precipitation (IP) lysis buffer on ice for 30 min (1% Triton X-100, 10 mM Tris pH 7.9, 25 mM KCl, 150 mM NaCl, 1 mM $MgCl_2$, 0.2 mM EDTA, 1 mM dithiothreitol (DTT), 20% Glycerol, and 1 complete protease inhibitor tablet). Lysates were precleared with 50 µl of Protein A beads. Precleared lysates were transferred to new tubes and 5 µl of mouse anti-HA antiserum (Sigma St. Louis, Mo.) was added to the mixture and incubated for 5 h. 50 µl of a 50% protein-A agarose bead slurry were added to the mixture and rotated overnight at 4 °C. The beads were washed 5 times with 1 ml of IP lysis buffer. After the last wash, beads were resuspended in 50 µl of IP lysis buffer. Ten microliters were taken from the slurry to perform a kinase IP reaction using Buffer B (30 mM Tris, 10 mM $MgCl_2$, 1 mM DTT, 5% glycerol, and 0.1 mg/ml BSA) with 10 µCi of ^{32}P-γ-ATP in 30 µl reactions. Reactions were stopped by adding 5X SDS-PAGE loading buffer and boiled for 2-5 minutes. Ten microliters of kinase IP reaction

were resolved by SDS-PAGE and examined by autoradiography. Quantification was conducted using a Storm 820 PhosphorImager (GE Life Sciences).

2.2.11 FBS EC50 determination

Beginning from modified HMI-9 medium containing 20% FBS, 2-fold serial dilutions of FBS were done across 11 columns in a 96-well plate. The parasites were then incubated in biosafety cabinets for 48 h at 37^{o}C with 5% CO_2. After the 48 h incubation period, 50 µl of CellTiter-Glo™ reagent (Promega Inc., Madison, WI, USA) was added to each well and plates were placed on an orbital shaker at room temperature for 2 min to induce lysis. After a 10 min incubation to stabilize the signal, the ATP-bioluminescence of each well was determined using a Spectra Max L microplate reader (Molecular Devices, Sunnyvale, CA, USA). Raw values measured in relative light units (RLU) were converted to $\log_{10}$ and percentage inhibition was calculated relative to the controls. IC_{50} curve fittings were performed with Prism 4 software or Excel.

2.3 Results

2.3.1 TbERK8 is not essential in procyclic form (insect stage) *T. brucei*

Procyclic form parasites were transfected with the TbERK8 RNAi plasmid and the cells were induced for TbERK8 knock down. There is a decrease in TbERK8 mRNA levels after 48 h (Fig. 2.1 A). Parasite growth over 9 days was observed to test if knocking down TbERK8 had any effect on their proliferation. No decrease in proliferation was observed in these parasites after depleting TbERK8, which contrasts with the results reported in bloodstream form *T. brucei* by our group (Fig. 2.1 B) (47). Other groups have also reported the importance of TbERK8 in bloodstream form parasites by either RIT-seq or kinome wide RNAi screens (48,49). Because there were no significant effects on the phenotype of procyclic form parasites we continued studying the bloodstream form cells to identify the source of the lethal phenotype observed by TbERK8 knockdown.

2.3.2 TbERK8 is localized to the cytoplasm in *T. brucei*

Human ERK8 has been found to be primarily located in the cytoplasm but it can also localize to the nucleus (55,82). In order to observe the localization pattern of TbERK8, we transfected the parasites with a copy of TbERK8 labeled with an HA tag that would be endogenously expressed in the parasites (Fig. 2.2 A). The expression of TbERK8 after identification by anti-HA antibodies can be seen in figure 2.2 B. Immunostaining of fixed parasites showed that TbERK8 localized to the cytoplasm and the nucleus as well (Fig. 2.2 C). The cells were divided into soluble (cytoplasm) and insoluble (nuclei) fractions and examined by western blot anti-HA, which demonstrated that TbERK8 was present in both fractions (data not shown).

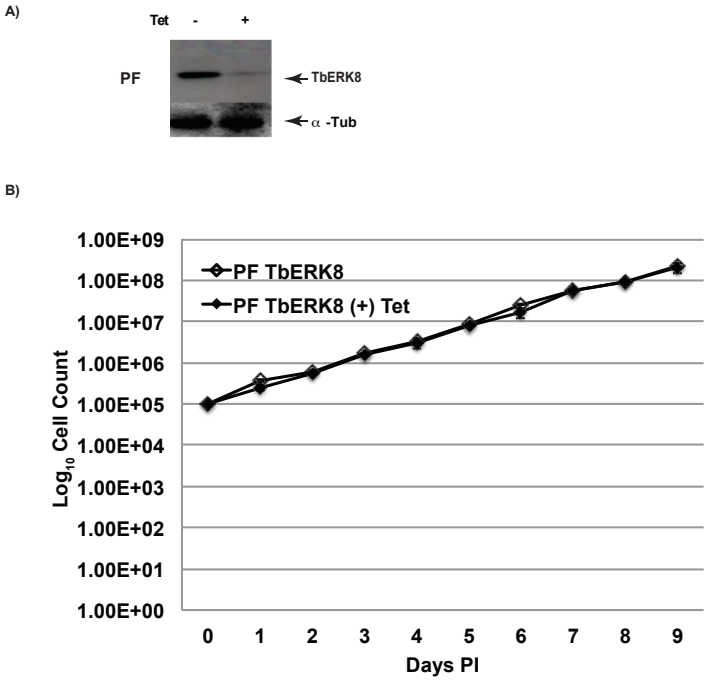

Figure 2.1 TbERK8 silencing in procyclic form does not result in a lethal phenotype. The TbERK8 RNAi construct was transfected into the parasites and resistant parasites where selected. The parasites were subcultutred at 1X10^^{5} per/ml and induced with 100 ng/ml of tetracycline. (A) Northern blot showing the TbERK8 mRNA levels of noninduced and induced RNAi (upper panel). Alpha-tubulin is used as a loading control (lower panel). (B) Graph showing the growth rate of procyclic form parasites during 9 days after silencing of TbERK8 being induced (+Tet), over three independent experiments.

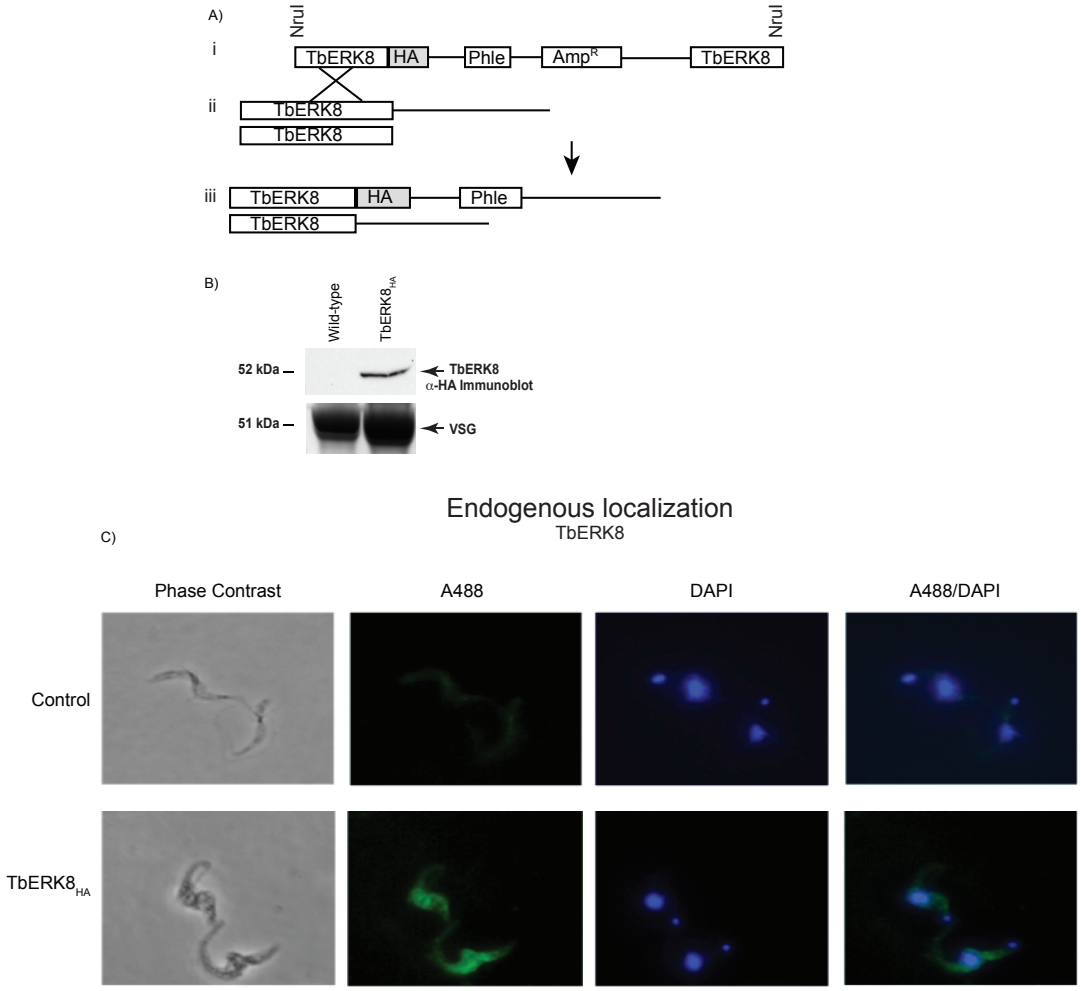

Figure 2.2 TbERK8 localizes to the cytoplasm and nucleus of *T. brucei*. (A) Scheme showing the procedure for endogenously tagging TbERK8. *(i)* NruI digestion of the vector containing TbERK8-HA. *(ii)* The plasmid is transfected into the parasites, the scheme shows how the homologous recombination occurs. *(iii)* Representative picture of the heterozygous TbERK8 locus. (B) Western blot analysis of the endogenous expression of the TbERK8-HA compared to a wild type TbERK8. VSG is used as a loading control. (C) The clones that expressed the TbERK8-HA were fixed with methanol and immunostaining with α-HA antibodies followed by Alexa Fluor® 488 anti-rabbit IgG. Representative parasites are shown with DAPI staining to observe the nuclei.

2.3.3 Silencing TbERK8 results in a decrease of EdU incorporation in bloodstream form *T. brucei*

EdU is a thymidine analog that gets incorporated into cells while they are undergoing DNA replication. We used EdU to follow DNA replication inside the parasite as we have previously described, and a control of nuclear staining with DAPI was used (Fig. 2.3 A) (81). In order to establish the best conditions for the experiment, we first followed the average rate of incorporation at 2 and 12 hours for uninduced cells. We moved forward adding EdU for 12 hours as it had a higher percentage of labeled nuclei that correlated to EdU incorporation, and in this a significant difference in EdU incorporation could be used to assess if TbERK8 silencing would affect DNA replication in any way (Fig. 2.3 B). We silenced TbERK8 by RNAi for 48 hours and confirmed the decrease of mRNA (Fig. 2.3 C). After 48 hours, EdU was added to the media for 12 hours. The cells were fixed with paraformaldehyde and the EdU labeled by click chemistry with Alexa Fluor® 488 Azide (83). The labeled nuclei were counted and compared to all the nuclei in the field of view. BSF cells that were expressing normal levels of TbERK8 incorporated 52% EdU in their nuclei after 48 hours, while when TbERK8 was absent there was only 7% incorporation, confirming that TbERK8 silencing has an effect on DNA replication.

2.3.4 Mutations on the conserved residues of TbERK8

Lysine 42 (K42) is the conserved residue in kinases that is necessary for positioning the γ-phosphate of ATP in the active site and is also required for phosphor-transfer to the substrate together with the conserved aspartic acid (D153). Both of these residues have been studied and mutated in Human ERK8 resulting in kinase-dead mutants unable to autophosphorylate or phosphorylate a substrate (50,57,84). MAPKs have an activation loop with the motif TxY, where specific residues must be phosphorylated in order for the protein to become fully activated. Mutations in these two residues in Human ERK8 studies resulted in inhibition of autophosphorylation (50,84).

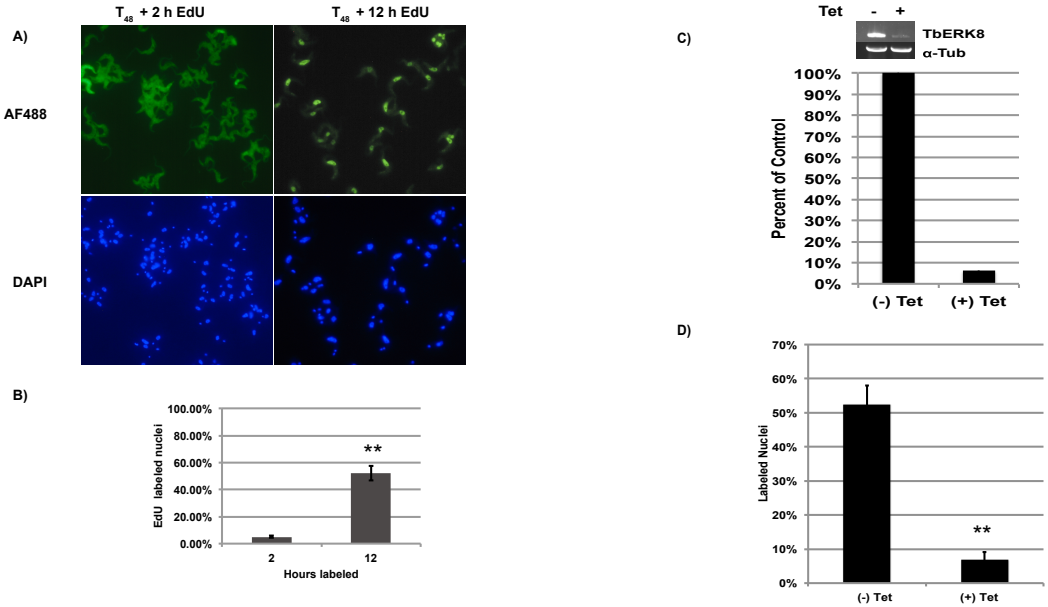

Figure 2.3 Effect of TbERK8 silencing in DNA replication in bloodstream form parasites. (A) Example picture of the labeling of BSF parasites after being treated with EdU for 2 hours or 12 hours (upper panel). DAPI stain to show nuclei localization is used as a control to show the localization of the nucleus and kinetoplast (bottom panel). (B) Graph bar showing the difference of EdU incorporation in BSF parasites after 2 h or 12 h of EdU present in the culture. (C) TbERK8 decrease in cells induced for RNAi silencing (+ Tet). Agarose gel showing the decrease of TbERK8 mRNA (upper panel) and alpha-tubulin as a control (lower panel). The bar graph represents the percentage of TbERK8 mRNA decreased after a 48 h induction. (D) Bar graph showing the comparison of the percentage of incorporated EdU in induced and uninduced TbERK8 RNAi in BSF cells.

Table 2.1 Residues mutated inside the kinase domain

Residue	Mutation	Role
K42	Alanine	ATP binding/ Phosphoryl transfer
D154	Alanine	Phosphoryl transfer
T174	Alanine	Kinase activation loop
Y176	Alanine	Kinase activation loop
T174- Y176	Alanine	Kinase activation loop

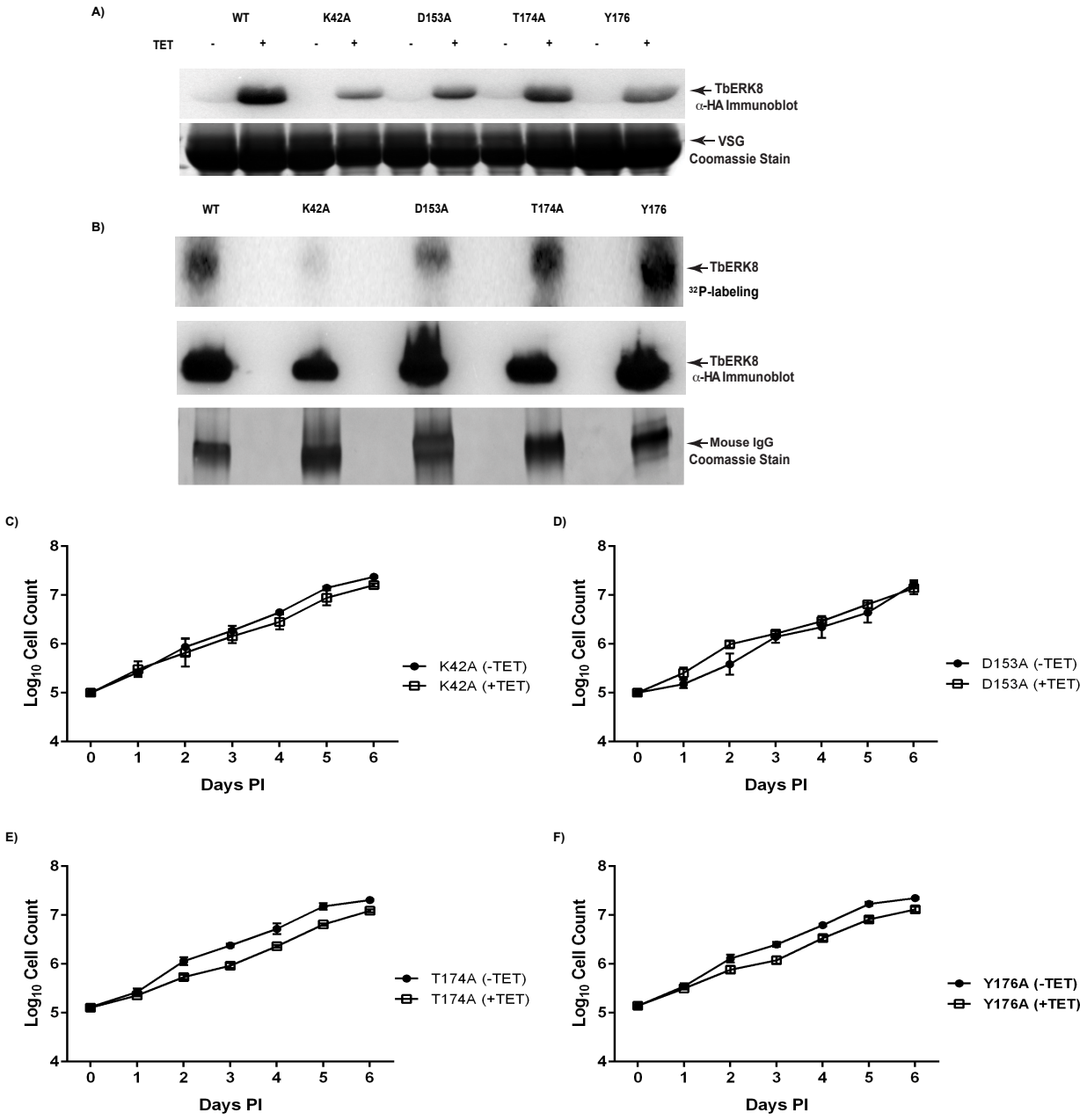

Figure 2.4 Overexpression of TbERK8 single mutants. (A) Immunoblot showing the expression of the TbERK8 mutants after being induced by the addition of tetracycline to the media for 48 h (Upper panel), VSG was used as a loading control (bottom panel). (B) Radiograph of the autophosphorylation of a TbERK8 Wild type control and the four TbERK8 single mutants (Upper panel). The TbERK8 was immunoprecipitated from the parasites on anti-HA beads. The western blot shows similar amounts of TbERK8s binding to the beads (middle panel). The Coomassie stain shows the mouse IgG heavy band as a loading control of similar amounts of beads that were loaded onto the gel (bottom panel). (C) Graphs showing the effect on parasite proliferation on the overexpressing TbERK8 mutants K42A, (D) D153A, (E) T174A and (F) Y176A.

We have made point mutations for each conserved residue (K42, D153, T174, Y176) in TbERK8 and overexpressed it in the parasites to observe if there is an effect on the parasite phenotype (Table 2.1). If one of these residues is critical for the biological function TbERK8, we should see a decrease in proliferation. We overexpressed each TbERK8 mutant in *T. brucei* and confirmed their expression. Western blot analysis of all the mutants and the wild type overexpressor shown by the 52 KDa bands (Fig. 2.4 A). We immunoprecipitated each of the mutants from parasites and checked their ability to autophosphorylate. Figure 2.4 B shows an autoradiograph of the autophosphorylation status of each mutant. As expected K42A was significantly decreased as well as D153A. The wild-type kinase and the active site mutants (T174A and Y176A) were still able to autophosphorylate. In order to identify changes in the phenotype, we monitored the proliferation of the parasites after 6 days of overexpression the mutants. In *T. cruzi*, overexpression of the wild type TcERK8 (TcMAPK2) arrested proliferation in epimastigotes (insect stage parasites) (85). In *T. brucei*, overexpression of TbERK8 did not cause an effect on the parasites. The K42A and D153A mutants did not show a significant decrease in proliferation (Fig. 2.4 C and 2.4 D), while parasites that overexpress the activation loop mutations show a slower growth rate for the first three days after induction, but grew similar to uninduced parasites during the last 3 three days. (Fig. 2.4 E and 2.4 F).

Fetal bovine serum is indispensable for the normal proliferation of bloodstream form *T. brucei* parasites. The absence of the normal 20% FBS in the media results in decrease in proliferation and death of the parasites. We titrated out the FBS to identify the IC_{50} for the TbERK8 overexpressor strains; ideally overexpression of the mutants would enhance the negative growth phenotype. The percentage of FBS starvation needed to inhibit proliferation in 50% was 0.9 % of FBS in the media (Fig. 2.5 A). None of the mutants developed a lethal phenotype in the serum-starved parasites. The K42A mutation did not show a significant decrease in proliferation when compared to the uninduced parasites under serum-starved conditions (Fig. 2.5 B). The D153A mutant showed a slight increase on the negative phenotype, while

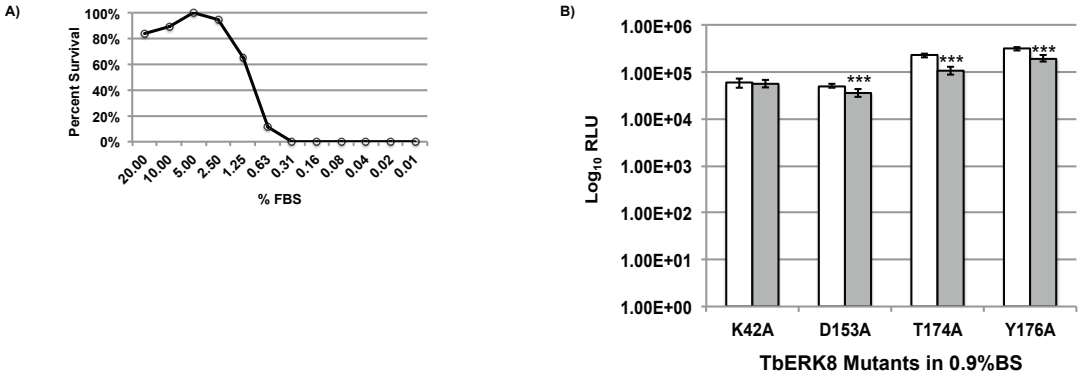

Figure 2.5 FBS starvation. (A) Graph depicts the effect that FBS starvation has on wild type parasites from 20% to 0% in order to identify the IC_{50} value. (B) The different TbERK8 single mutants on the kinase domain were grown at 0.9% FBS for 48 h and the proliferation was measured using Cell-Titer Glo®. The experiment was done by triplicate, the open bars represent the uninduced cells and the induced cells are represented by grey bars.

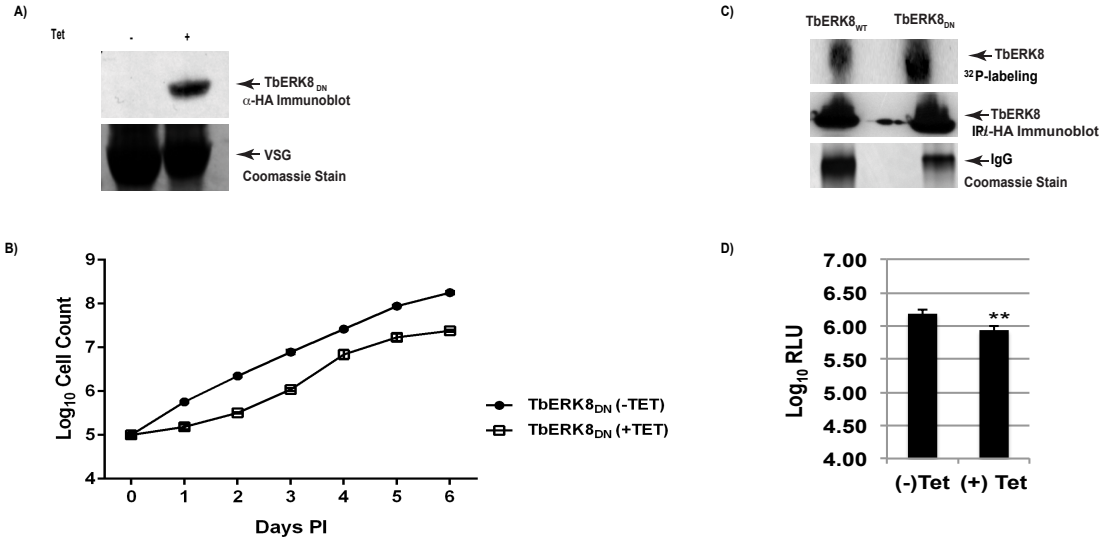

Figure 2.6 Dominant negative effect caused by a double mutation on T174 and Y176 to alanine. (A) Western blot showing the overexpression of the TbERK8 with the double mutation after inducing it with tetracycline (upper panel). Coomassie stain of the VSG on the parasite lysate was used as a loading control to compare the (bottom panel). (B) Graph depicting the parasite proliferation during 6 days of either $TbERK8_{DN}$ induced (+TET) or uninduced (-TET). (C) Radiograph showing that the $TbERK8_{DN}$ is able to autophosphorylate similar to the wild type TbERK8 (upper panel). Both iterations of TbERK8 were immunoprecipitated from the parasites using HA-affinity beads. The middle panel shows that a similar amount of protein was immunoprecipitated and checked for autophosphorylation. The IgG heavy chain was used as a loading control (lower panel). (D) Cells were starved of FBS and the effect on the proliferation was monitored on cells induced or un-induced to overexpress the $TbERK8_{DN}$. The bar graph shows the decrease on the parasite proliferation monitored by a luciferase assay that was measuring relative light units (RLU) showing a 5 fold reduction in parasite proliferation.

both of the activation loop mutations (T174A and Y176A) show a significant decrease in proliferation when compared to the uninduced parasites under serum-starve conditions (Fig. 2.5 B).

2.3.5 TbERK8 double mutations causes a dominant negative effect

Because we observed a decrease on proliferation when either activation loop residues had been mutated to alanine, we decided to make a (T174A, Y176A) double mutation on the activation loop of TbERK8 and examine its effect on proliferation. Figure 2.6 A shows the expression of TbERK8 mutant at the expected size of 52 KDa when induced with tetracycline for 24 hours. Proliferation in these parasites decreased dramatically during the first 3 days of overexpression, developing a dominant-negative effect. After day 4, the parasites then began to grow normally (Fig. 2.6 B). The double mutant was immunoprecipitated from the parasites to check if it was able to autophosphorylate. Since the active site residues were still conserved, the kinase was able to autophosphorylate, suggesting that there are residues in its polypeptide, besides the activation lip ones, that can be phosphorylated.

2.4 Discussion

We have observed that like most of the other reports on human ERK8 this protein localizes to the cytoplasm of the cells (55,82). It was also found in the nucleus, suggesting that like reported by Groehler *et al*. in human cells, there is a possibility TbERK8 is entering the nucleus.

We have found that the expression of TbERK8 is only essential in bloodstream form parasites and not in the insect stage, suggesting that TbERK8 is important for the infectious stage, making it an interesting drug target. Another group studied the effect of silencing TbERK8 and found that the cells were not able to complete cytokinesis resulting in multinucleated cells (49). Although we observed a decrease in EdU incorporation, we did not see the phenotype they reported. They used a different RNAi strategy which could explain the differences in phenotype. They are using a stem-loop RNAi induced silencing (86), while we are using a system with opposing T7 promoters that produces double stranded mRNA of the gene of interest (87). Nonetheless, in both cases, silencing TbERK8 induced a lethal phenotype, confirming our studies. Although other MAPK have been studied in *T. brucei*, TbERK8 is the first one shown to be essential for normal proliferation in the parasite. ERK4 was found to be important for differentiation from procyclic to bloodstream form (45,46), but the parasites are still able to proliferate. The ERK1/ERK2 have also been studied in *T. brucei,* but they are not essential for survival (49).

Overexpressing the activation loop double mutants generated a dominant negative effect in the parasite, which supports the idea that full activation of TbERK8 is indispensable for normal parasite proliferation. This confirms that altering key residues in TbERK8 affects the parasite and suggest that targeting this activation mechanism could be a good drug target strategy.

3. Deviating the level of proliferating cell nuclear antigen in *Trypanosoma brucei* elicits distinct mechanisms for inhibiting proliferation and cell cycle progression

This is an Accepted Manuscript of an article published in Cell Cycle online [February 20, 2015], available online: http://tandfonline.com/doi/full/10.4161/15384101.2014.987611

Ana L. Valenciano, Aaron C. Ramsey, and Zachary B. Mackey., "Deviating the level of proliferating cell nuclear antigen in *Trypanosoma brucei* elicits distinct mechanisms for inhibiting proliferation and cell cycle progression", Cell Cycle, 14:4, 674-688, Copyright (2015), with permission from Taylor & Francis

Author Contributions:

Ana Lisa Valenciano performed all the research except the experiments mentioned below and helped write the article.

Aaron C. Ramsey performed the experiments on the parasites overexpressing TbPCNA, the Hydroxyurea sensitivity assay and helped write the article.

Zachary B. Mackey oversaw and directed the research, and helped write the article.

Abstract

The DNA replication machinery is spatially and temporally coordinated in all cells to reproduce a single exact copy of the genome per division, but its regulation in the protozoan parasite *Trypanosoma brucei* is not well characterized. We characterized the effects of altering the levels of proliferating cell nuclear antigen, a key component of the DNA replication machinery, in bloodstream form *T. brucei.* This study demonstrated that tight regulation of TbPCNA levels was critical for normal proliferation and DNA replication in the parasite. Depleting TbPCNA mRNA reduced proliferation, severely diminished DNA replication, arrested the synthesis of new DNA and caused the parasites to accumulated in G2/M. Attenuating the parasite by downregulating TbPCNA caused it to become hypersensitive to hydroxyurea. Overexpressing TbPCNA in *T. brucei* arrested proliferation, inhibited DNA replication and prevented the parasite from exiting G2/M. These results indicate that distinct mechanisms of cell cycle arrest are associated with upregulating or downregulating TbPCNA. The findings of this study validate deregulating intra-parasite levels of TbPCNA as a potential strategy for therapeutically exploiting this target in bloodstream form *T. brucei*.

3.1 Introduction

Trypanosoma brucei is the protozoan parasite that causes African trypanosomiasis, also known as sleeping sickness. The bloodstream form of this vector-borne parasite proliferates in human blood and cerebrospinal fluid, where it causes a meningoencephalitic disease during late stage infections that is most often fatal if left untreated (10). DNA replication in *T. brucei,* as in all other organisms, is spatially and temporally coordinated to produce a single exact copy of the genome per cell division. In human cells, DNA replication is initiated at origins that become licensed by the components of the origin recognition complex: (Orc1-6), Ctd1, Cdc6, and the mini-chromosome maintenance proteins (Mcm 2-7) that form the pre-replication complex in G1 (88,89). The pre-replication complex in trypanosomatids consists of homologs for Orc1/Cdc6 proteins and a Cd45-Mcm2-7-GINS complex (71,90,91). Activation of replication origins occurs at S phase and involves formation of replication forks that become primed by the DNA polymerase α/primase complex. This allows the replication machinery to bind to activated forks and begin synthesis of new DNA.(92,93) At S phase, components of the DNA replication machinery localize into punctate foci in the nucleus that cover several replication forks or replicons (94).

Proliferating cell nuclear antigen (PCNA) is a central component of the replication machinery originally identified in patients with systemic lupus erythematosus (95). PCNA acts as a homotrimeric DNA sliding clamp that provides DNA polymerases δ and ε with the processivity necessary to duplicate the entire genome. It functions as a moving platform that complexes with many proteins to process signals important for directing DNA replication and repair pathways, which regulate cell cycle events (62,96,97). PCNA was also identified as a cyclin based on its cyclical pattern of expression in mammalian cells (98). Quaternary complexes in mammalian cells including CDKs, $p21^{WAF1/CIP1}$ and other cyclins can regulate the cell cycle by interacting with PCNA (99-101). Upregulation of PCNA occurs in cancerous cells allowing it to serve as a reliable diagnostic biomarker for predicting oncogenesis (102,103). Ligand-induced apoptosis is prevented by interactions between PCNA and negative regulators of growth such as

MyD118 and Gadd45 (96). This indicates that upregulating PCNA in mammalian cells may sequester negative regulators of growth that signal apoptosis or cell cycle check points (104).

A recent study used TbPCNA to establish the temporal and spatial patterns of DNA replication in *T. brucei* and reported differential regulation of TbPCNA during the cell cycle (73). We examined the consequences that deregulating intra-parasite TbPCNA levels had on proliferation and DNA replication in bloodstream form *T. brucei*. This study demonstrates that either depleting or overexpressing TbPCNA severely reduces proliferation and DNA replication in the parasite. The parasites were more sensitive to increased intra-parasite levels of TbPCNA than they were to depleted levels. Overexpressing human PCNA in *T. brucei* arrested its proliferation with similar efficiency as overexpressing TbPCNA. Finally, down regulation of TbPCNA hypersensitized *T. brucei* to the replication inhibitor hydroxyurea. These findings reveal the important roles that proper levels of TbPCNA play in maintaining proliferation and DNA replication in *T. brucei*. They also suggest that overexpressing TbPCNA arrests cell cycle progression by a different mechanism(s) than depleting it. This study also validates deregulating intra-parasite levels of TbPCNA as a viable strategy for therapeutic exploitation of *T. brucei*.

3.2 Results

3.2.1 Endogenous expression of TbPCNA in *T. brucei*

We subcloned the TbPCNA coding region into a modified version of the pLew111 expression vector (79,105) that included a hemagglutinin tag (HA). Figure 3.1A diagrams the strategy for generating clones that express HA-tagged TbPCNA at endogenous levels in the 221strain of wild type *T. brucei*. Selection with phleomycin identified six resistant transfectants. Immunoblot analysis was done to identify phleomycin-resistant transfectants that expressed HA-tagged TbPCNA ($TbPCNA_{HA}$). Expression of the endogenously tagged TbPCNA using this strategy was contingent on the plasmid being successfully integrated into one of the TbPCNA chromosomal loci by a homologous recombination event. Positive transfectants identified by immunoblot assays expressed a polypeptide with a predicted molecular mass of 35 kDa (32.3 kDa plus the 3 kDa HA-tag). Figure 3.1 B demonstrates a representative stable transfectant that expressed $TbPCNA_{HA}$ at endogenous levels.

T. brucei cell cycle stages can be estimated by the ratio of nuclei to kinetoplast, which are the DNA containing organelles in the parasite. G0/G1 parasites typically contain 1 nucleus and 1 kinetoplast (1N1K).

Parasites in late S phase typically have an elongated kinetoplast and 1 nucleus (1N1eK) (106,107). G2 parasites typically are 1N2K, and M phase parasites are 2N2K (108). Indirect immunofluorescence analysis demonstrated that HA-tagged PCNA localized to distinct spots in 1N1K parasites (Fig. 3.1 C). Distinct punctate nuclear spots were also detected in the nuclei of 1N1eK parasites (Fig. 3.1 D). Punctate spots in 1N2K parasites were detected, but to a lesser extent (Fig. 3.1 E). In 2N2K parasites, the anti-HA antibodies co-localized to the cytoplasm (Fig. 3.1 F). These immunofluorescent studies indicated that TbPCNA was primarily expressed in the nucleus during G1, S, and G2 phases, but entered the cytoplasm during M phase, which was the only observation that differed from the previous study.

PCNA is expressed throughout the cell cycle but is elevated during S phase in mammalian cells

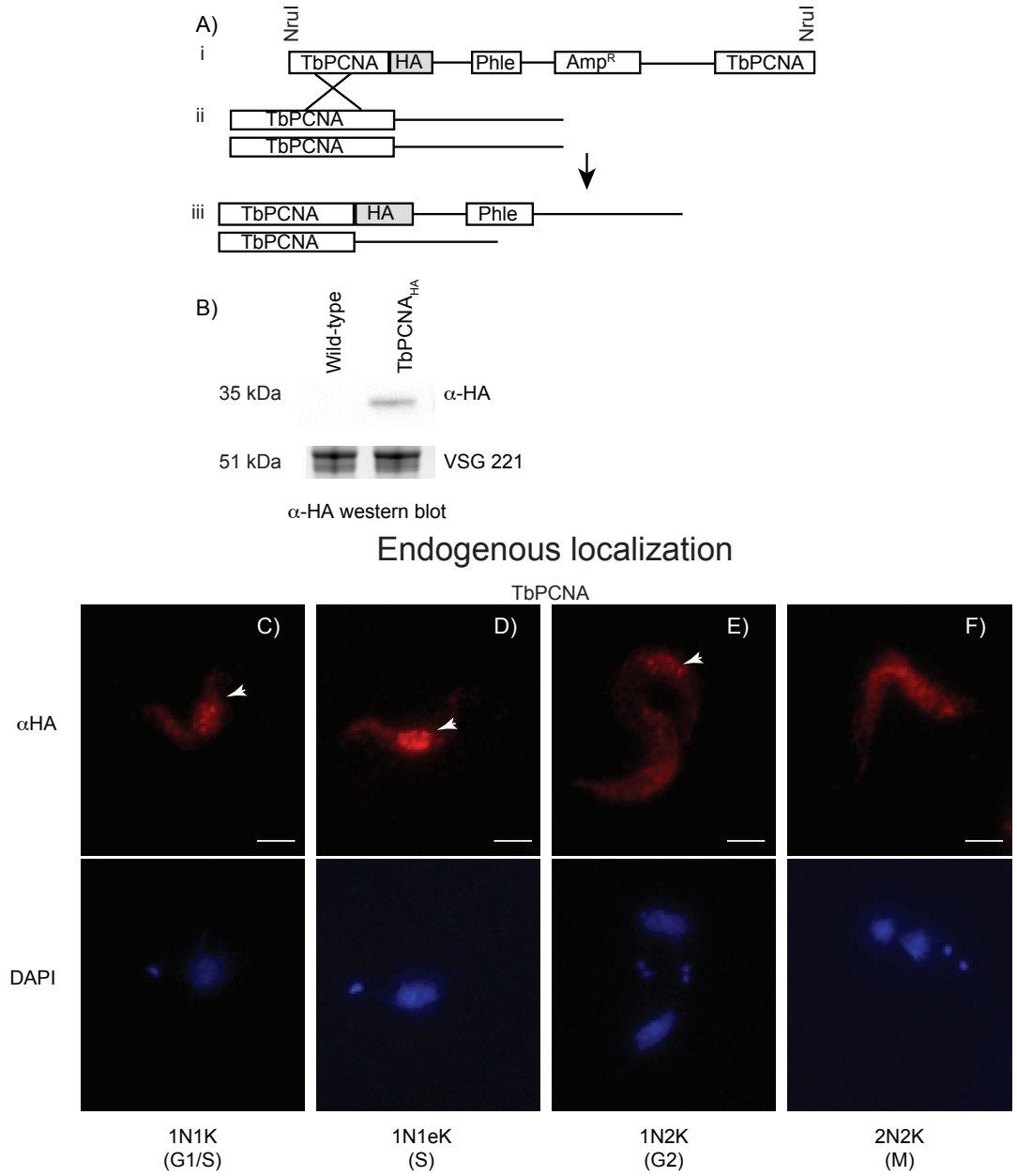

Figure 3.1 TbPCNA localizes to the nucleus and cytoplasm in bloodstream form *T. brucei*. (A) Scheme for endogenously tagging TbPCNA. *(i)* TbPCNA-HA vector linearized with NruI, which cuts at a unique site within the TbPCNA-HA cDNA. *(ii)* Linearized plasmid was stably transfected into *T. brucei* where a homologous recombination event occurred at the TbPCNA locus. *(iii)* Representation of the heterozygous TbPCNA locus in clones that express endogenously tagged $TbPCNA_{HA}$. (B) Immunoblot with antibodies against hemagglutinin (HA) detected clones that expressed endogenously tagged $TbPCNA_{HA}$. VSG 221 loading control was from Stain-Free™ gel. Positive clones were fixed in ice-cold methanol and stained with α-HA antibodies. Representative parasites from each stage of the cell cycle: (C) (G1/S) parasites (D) S phase parasites (E) G2 phase parasites and (F) M phase parasites were selected to show nuclear staining patterns of endogenously-tagged TbPCNA. Arrows point to punctate replication foci in the nucleus. K-kinetoplast, eK-elongated kinetoplast, N-nucleus, α-HA-anti-hemagglutinin antibodies, DAPI- 4',6-diamidino-2-phenylindole, dihydrochloride. Scale bars represent 5 µm.

(109,110). Similar expression patterns have been reported for PCNA homologs in yeast (111) and in the related kinetoplastid parasite, *Leishmania donovani* (112). TbPCNA was reported as being upregulated during S phase in procyclic stage *T. brucei* but not detectible in the G2/M phases (73). We synchronized the cultures with hydroxyurea as described by Forsythe *et al* (113). Nuclear and cytoplasmic fractions from *T. brucei* synchronized in S, G2 and M phases were prepared and examined by immunoblot analysis. TbPCNA expression was detected in the cytoplasmic and nuclear fractions of each synchronized population of *T. brucei.* This indicated that TbPCNA like other PCNA homologs was expressed throughout the cell cycle (Figure 3.S1). +

3.2.2 Depleting TbPCNA in *T. brucei* reduced proliferation and DNA replication

A 710-bp fragment from the TbPCNA cDNA was subcloned into pZJM (87) to examine the effects that depleting its mRNA by RNA interference (RNAi) would have on *T. brucei*. The pTbPCNA-RNAi plasmid was linearized with restriction endonuclease NotI and transfected into *T. brucei* (78). Stable transfectants were selected with phleomycin and used to express double stranded RNA under control of the pZJM tetracycline-inducible promoters (87).

To examine the effects that RNAi had on the steady-state levels of TbPCNA mRNA in *T. brucei*, stable transfectants were diluted to 10^5/ml and cultured in media without or with tetracycline for 48 h. Reverse transcriptase PCR (RT-PCR) analysis was done to examine the steady state levels in these stable transfectants. Semi-quantitative analysis by RT-PCR showed that depletion of TbPCNA mRNA occurred after induction with tetracycline for 48 h (Fig. 3.2 A and 3.S 2). Because TbPCNA mRNA was depleted in these stable transfectants upon tetracycline induction, we designated them as $TbPCNA_D$ clones. These clones were counted every 24 h and their cumulative numbers were graphed to analyse their growth patterns for 6 d. Continuously culturing $TbPCNA_D$ clones in media containing tetracycline clearly reduced their growth rate in comparison to culturing them in tetracycline-free media (Fig. 3.2 B). This indicated that depleting TbPCNA mRNA had a negative effect on *T. brucei* proliferation.

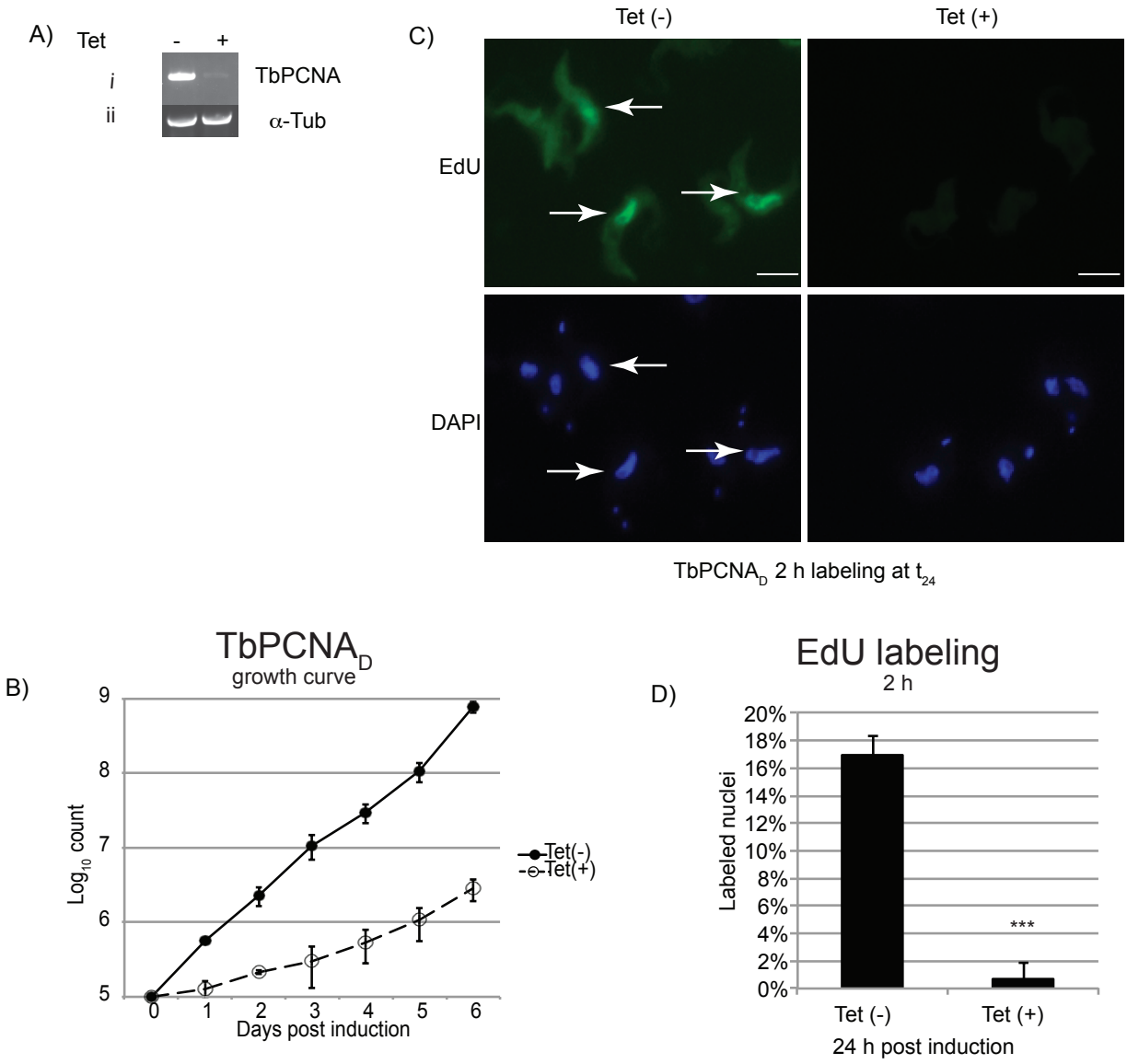

Figure 3. 2 TbPCNA mRNA depletion diminished proliferation and DNA replication. TbPCNA$_D$ clones were diluted to 1×10^5 per/ml and propagated in growth media without (Tet (-)) or with 1.0 µg/ml tetracycline (Tet (+)) for 48 h. The amount of 1.5 µg of total RNA was extracted from the parasites and used for RT-PCR amplification using primers to TbPCNA or aα tubulin (α-Tub). (A) 5 µl of RT-PCR reaction (after 23 of 35 cycles) was resolved on an agarose gel and stained with SYBR® Safe. Fluorescence intensity of the bands was quantified using a ChemiDoc™ MP. *(i)* RT-PCR product of TbPCNA after 23 cycles. *(ii)* RT-PCR product of α-Tub after 23 cycles used as a loading control for total RNA. (B) Growth curves representing the mean cumulative count over 6 d for TbPCNA$_D$ clones grown in media without (solid lines) or with (dashed lines) tetracycline. Graphs represent the mean counts with standard error from three independent clones repeated in triplicate. (C) Example of non-induced or induced TbPCNA$_D$ clones after labeling with EdU for 2 h. Arrows point to EdU-labeled nuclei and DAPI-stained nuclei in the same clones. (D) Bar graph representing the mean percent with standard error for EdU-labeled nuclei in control (Tet (-)) or induced (Tet (+)) clones. Results were obtained from experiments done in triplicate counting a minimum of 150 parasites per slide per condition. *** The difference between labeled and unlabeled nuclei had a p-value <0.05. Scale bars in graphs represent 5 µm.

Non-induced $TbPCNA_D$ clones were cultured in tetracycline-free medium that contained the nucleotide analogue EdU at a final concentration of 100 μM for 2 h to assess the baseline levels of DNA replication in *T. brucei.* EdU labeled parasites were fixed with paraformaldehyde and double-stained with Alexa Fluor® 488 azide, which specifically attaches to EdU by click chemistry (83), and with DAPI (Fig. 3.2 C). The percentages of EdU-positive nuclei in non-induced $TbPCNA_D$ clones were calculated by dividing the number of EdU-labeled nuclei by the number of DAPI-stained nuclei. Using this method, we detected labeling in 17% of control $TbPCNA_D$ clones after 24 h when the combined frequencies of S and G2/M of parasites were at their peak.

EdU labeling was performed again in $TbPCNA_D$ clones cultured in media containing tetracycline. After 24 h of TbPCNA mRNA depletion, we calculated that 0.7% of the $TbPCNA_D$ clones had EdU-positive nuclei after being labeled for 2 h (Fig. 3.2 D). Parasite viability was examined by trypan blue assay, which demonstrated that more than 98% of the parasites were still viable after TbPCNA had been depleted (data not shown). These results strongly suggested that depleting TbPCNA arrested DNA replication in *T. brucei* without initially killing the parasite.

3.2.3 Depleting TbPCNA prevented normal cell cycle progression in *T. brucei*

Cytometric analysis demonstrated that $TbPCNA_D$ clones cultured in tetracycline-free HMI-9 media underwent normal cell cycle progression. Tetracycline induction, which led to the depletion of TbPCNA in these clones, prevented *T. brucei* from undergoing normal cell cycle progression. The mean frequency of G0/G1 parasites dropped to 40% at T_{48} post-induction (Fig. 3.3 A), but S phase (Fig. 3.3 B) and G2/M phase (Fig. 3.3 C) parasites each accumulated to a frequency of 30% and at this time point.

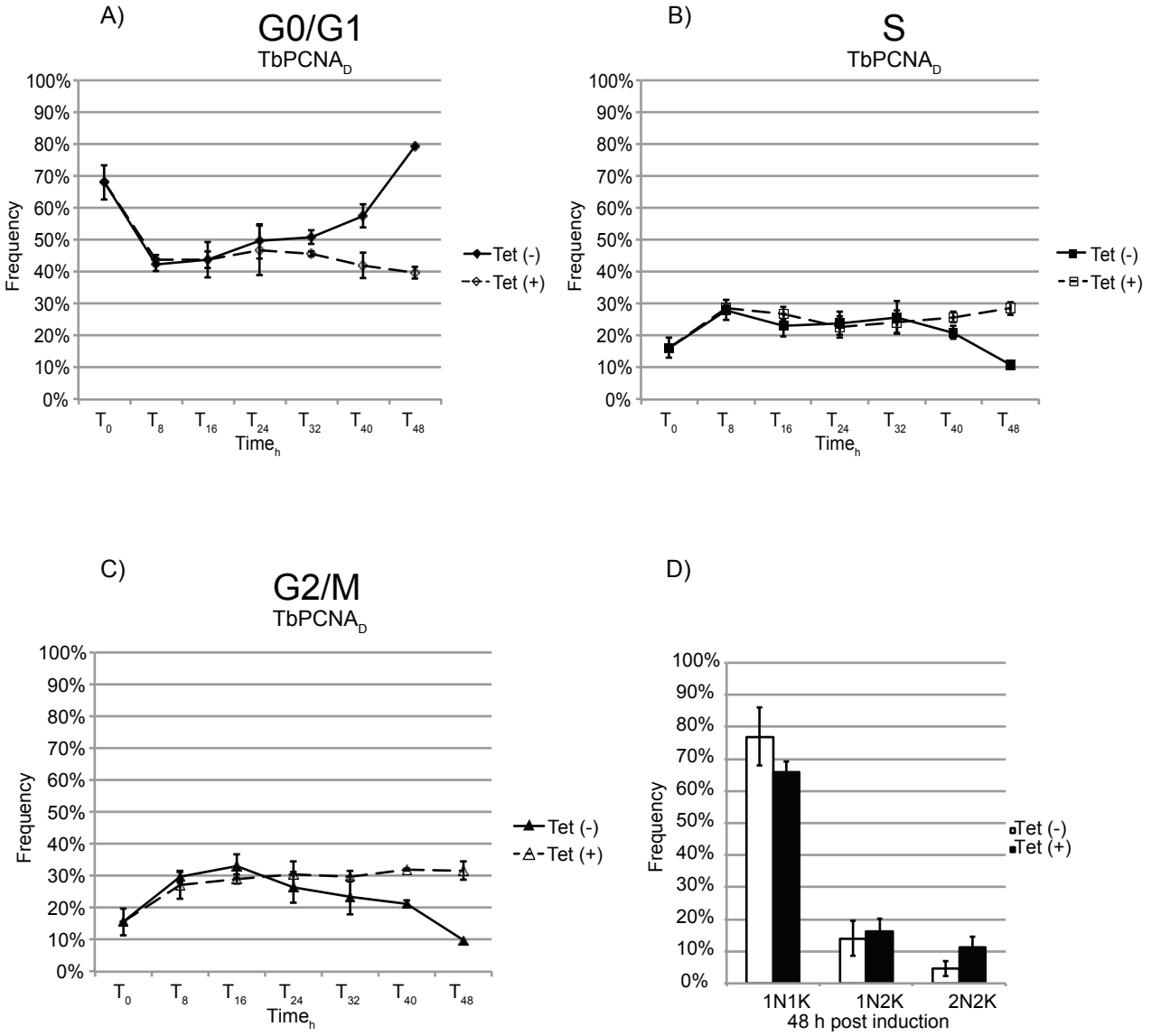

Figure 3. 3 Cell cycle progression ceased in $TbPCNA_D$ clones upon tetracycline induction. Asynchronous $TbPCNA_D$ clones were diluted to 1×10^5/ml to stimulate proliferation. Clones were cultured in media without (solid lines) or with (dashed lines) tetracycline at T_0 and allowed to grow for 48 h. Aliquots of the induced $TbPCNA_D$ clones were fixed and prepared for analysis by flow cytometry every 8 h, from T_0 to T_{48} and line graphs representing the mean frequencies of the cell cycle phases: (A) G0/G1, (B) S phase, or (C) G2/M obtained from cytometric histograms were plotted. Line graphs represent the mean frequencies with standard error obtained from histograms of 4 independent experiments. (D) Nuclei and kinetoplast were counted in the parasites 48 h post induction to estimate the frequency of 1N1K, 1N2K, 2N2K in $TbPCNA_D$ population. The bar graph represents the mean frequencies with standard error calculated from experiments done in triplicates counting a minimum of 150 parasites from each condition. These data indicate that depleting TbPCNA mRNA delayed or inhibited S and G2/M phase progression in these clones.

We stained the nuclei and kinetoplasts in non-induced or induced $TbPCNA_D$ clones with DAPI at T_{48} and counted them by fluorescent microscopy to visually estimate their cell cycle distribution. The frequency of 1N1K parasites decreased in tetracycline-induced clones at T_{48}, which correlated with the G0/G1 frequency drop observed by cytometric analysis. At this time point, the frequency of 1N2K and 2N2K parasites increased also (Fig. 3.3 D). These analyses together indicated that depletion of TbPCNA caused *T. brucei* to accumulate in G2 and M phases.

3.2.4 Overexpressing TbPCNA in *T. brucei* arrested proliferation

The TbPCNA-pLew111 expression vector was transfected into *T. brucei* after being linearized with NotI, which allowed for tetracycline inducible overexpression of TbPCNA in the parasite (79,105). Eight phleomycin-resistant transfectants were screened by immunoblot analysis to identify ones that expressed $TbPCNA_{HA}$ upon tetracycline induction. We designated tetracycline-inducible transfectants able to overexpress $TbPCNA_{HA}$ as $TbPCNA_{OE}$ clones. A representative immunoblot showed that basal levels of $TbPCNA_{HA}$ were detected in non-induced $TbPCNA_{OE}$ clones (Fig. 3.4 A). Such a result indicated that the promoter in this plasmid was not tightly regulated. Detection of high basal levels of $TbPCNA_{HA}$ in non-induced $TbPCNA_{OE}$ clones was consistent with the 20% read-through originally reported using the parental pLew82 plasmid (105), which is the backbone of pLew111. Several independent $TbPCNA_{OE}$ clones were diluted to 10^5/ml and cultured in HMI-9 media containing tetracycline at T_0 to test the effects that overproducing TbPCNA had on proliferation in *T. brucei*. Mean levels of proliferation were arrested in the $TbPCNA_{OE}$ clones as early as 24 h and lasted through day 6 post induction (Fig. 3.4 B). The luciferase assay provides a linear correlation between intra-parasite ATP concentrations and the amount of proliferation (114). This assay was used to measure proliferation in $TbPCNA_{OE}$ clones cultured for 48h in 96-well plates. Read-outs from the luciferase assay showed that proliferation in non-induced $TbPCNA_{OE}$ clones was more than 5 fold higher than it was in tetracycline-

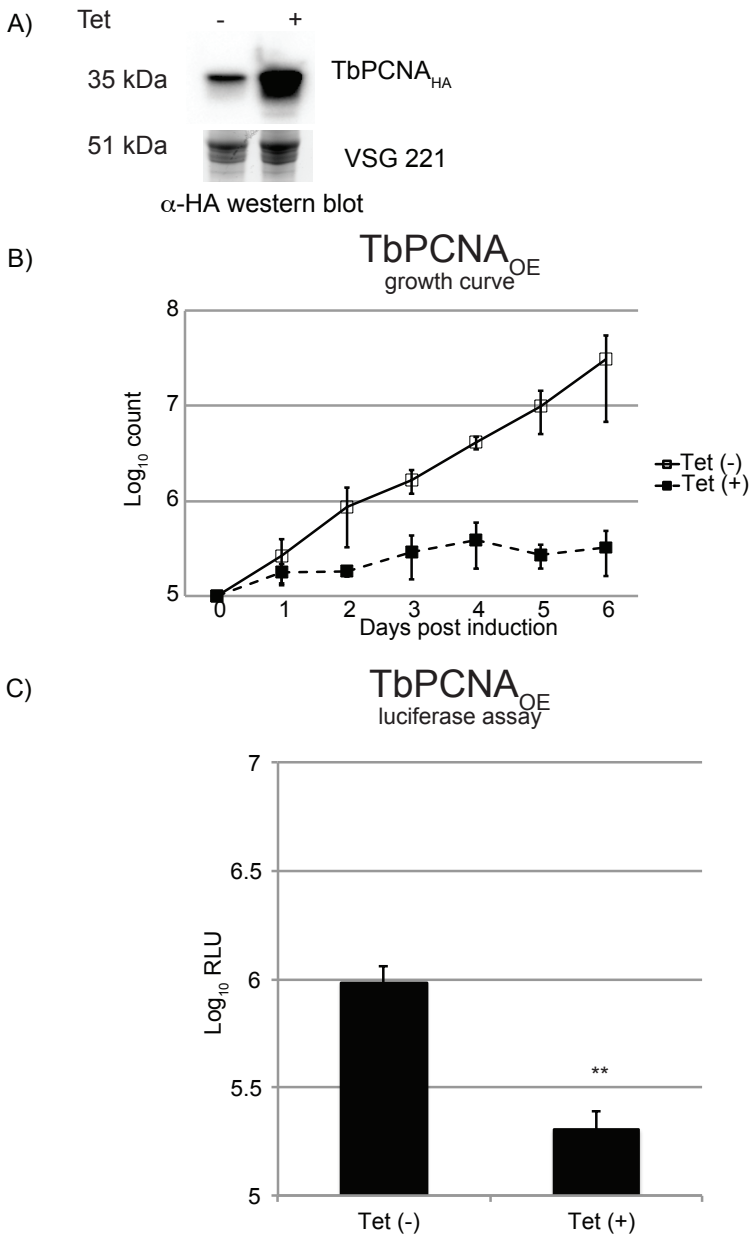

Figure 3. 4 Overexpression of TbPCNA arrests proliferation in bloodstream form *T. brucei*. A representative $TbPCNA_{OE}$ clone was grown in media without (Tet (-)) or tetracycline (Tet (+)). (A) Extracts prepared from about 2×10^6 parasites were resolved on a 10% SDS-PAGE gel and transferred to PVDF membrane for examination by immunoblot analysis using α-HA antibodies. Note basal levels of $TbPCNA_{HA}$ in control parasites (Tet (-) lane). VSG loading control represents Stain-Free™ image obtained from gel prior to transfer. (B) Three independent $TbPCNA_{OE}$ clones were cultured in growth media without (solid lines) or with (dashed lines) tetracycline and the mean count of these parasites was plotted as a line graph. Mean and standard deviation were calculated from these clones tested in 3 independent experiments. (C) $TbPCNA_{HA}$ transfectants were diluted to 10^5/ml and plated in 96-well plates. After 48 h of incubation, proliferation of control (Tet (-)) or induced (Tet (+)) clones was checked by luciferase assay, which returned values in relative light units (RLU). Bar graph represents the mean $\log_{10}$ RLUs with standard error for 3 independent clones replicated in triplicate experiments. ** Indicates that the difference in RLU values observed under each condition was significant with a *p*-value <0.05.

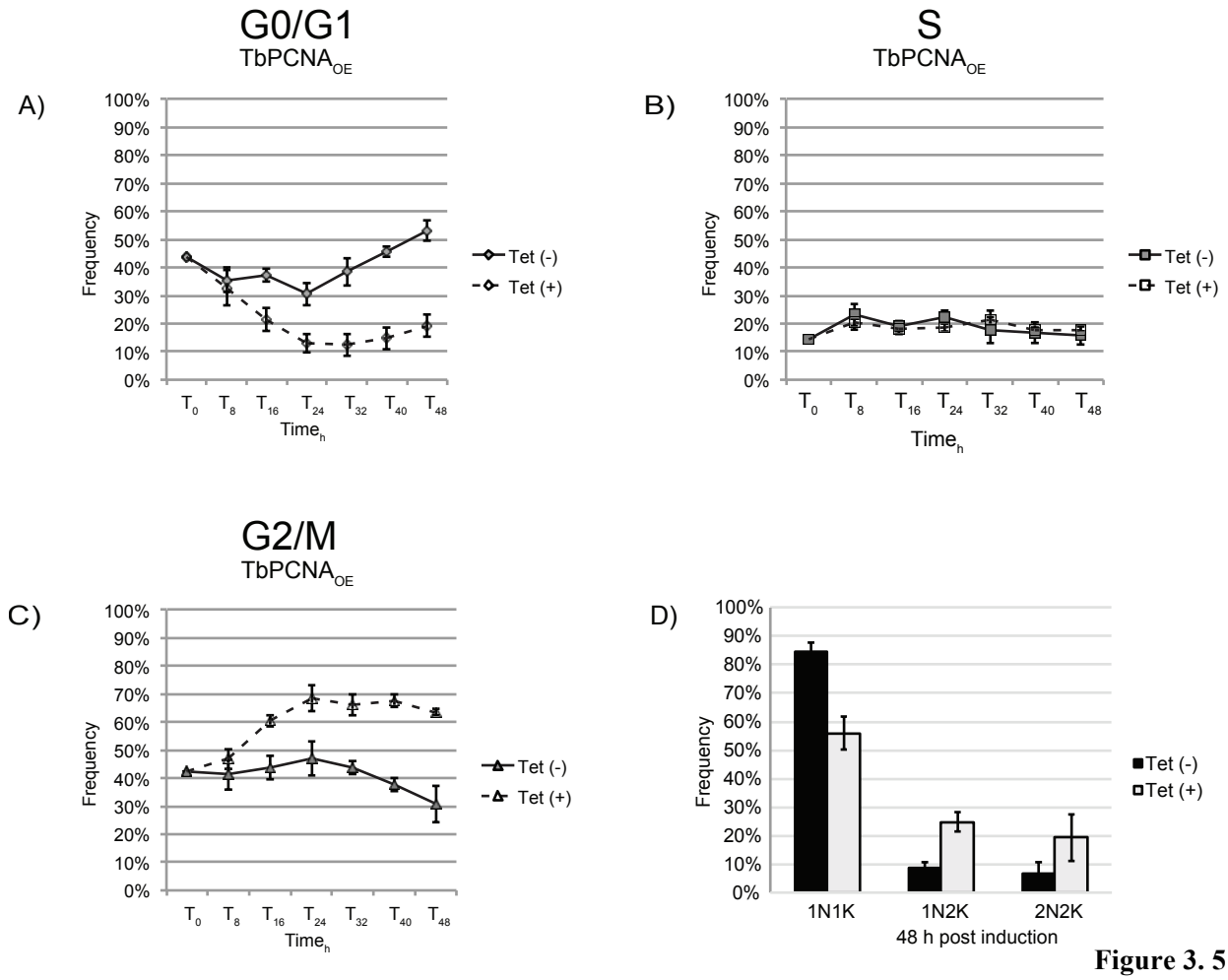

Figure 3. 5

Overexpressing TbPCNA arrested *T. brucei* in G2/M phase. Line graphs representing the cell cycle frequencies: (A) G0/G1; (B) S and (C) G2/M were plotted using data obtained from histograms generated from non-induced (Tet (-) solid lines) or induced (Tet (+) dashed lines) clones in 8 h intervals for 48 h. Each line graph represents the mean with standard error for 4 independent experiments. (D) TbPCNA$_{OE}$ clones were stained with DAPI to count their nuclei (N) and kinetoplasts (K) by fluorescence microscopy. Graphs were plotted showing changes in the frequencies of 1N1K, 1N2K or 2N2K clones in non-induced (black bars) or induced (grey bars) cultures after 48 h. Bar graphs show the mean frequency with standard error for 1N1K, 1N2K or 2N2K clones. Results were obtained from counting a minimum of 200 parasites per slide per condition tested.

induced clones (Fig. 3.4 C). Parasite viability was examined by trypan blue assay, which demonstrated that, similarly to $TbPCNA_D$ clones, greater than 98% of the parasite population remained viable after 48 h overexpression of TbPCNA (data not shown). These collective results clearly indicated that overexpressing TbPCNA arrested proliferation in *T. brucei.*

3.2.5 Overexpressing TbPCNA arrested *T. brucei* in G2/M

Cell cycle examination showed that the frequency of G0/G1 non-induced $TbPCNA_{OE}$ clones was about 40% at T_0 but increased to above 50% by T_{48}. Such a low frequency of G0/G1 parasites was consistent with the reduced growth rate observed in non-induced $TbPCNA_{OE}$ clones. Overexpression of TbPCNA in *T. brucei* for 48 h reduced the frequency of G0/G1 parasites in the population to about 19% (Fig. 3.5 A). It had little effect on the frequency of S phase *T. brucei,* which remained about 20% throughout the 48 h period of induction (Fig. 3.5 B). G2/M frequencies in non-induced clones remained about 40% until T_{32} and then declined, however the population of induced clones began shifting towards a G2/M majority at T_8. By T_{16} post-induction, the frequency of G2/M parasites was 60% and remained above that level until T_{48} (Fig. 3.5 C). These results indicate that overexpressing TbPCNA specifically arrested the parasites at G2/M. The representative histograms in Figure 3.S3 demonstrated the rapid onset of G2/M arrest that occurred upon induction of $TbPCNA_{OE}$ clones.

Frequencies for nuclei and kinetoplasts were 84% 1N1K, 9% 1N2K and 7% 2N2K for non-induced $TbPCNA_{OE}$ clones at T_{48}. These frequencies were typical for *T. brucei* cultures proliferating as asynchronous populations. Counts for nuclei and kinetoplasts of induced $TbPCNA_{OE}$ clones at T_{48} demonstrated that the frequencies of 1N1K: 1N2K: 2N2K parasites were 54%: 26%: 20% respectively (Fig. 3.5 D). These ratios were atypical in comparison to the rations in control parasites and further demonstrated that overexpressing TbPCNA in *T. brucei* cultures resulted in the accumulation of G2 and M phase parasites that were nearly 3 times the levels observed in control parasites.

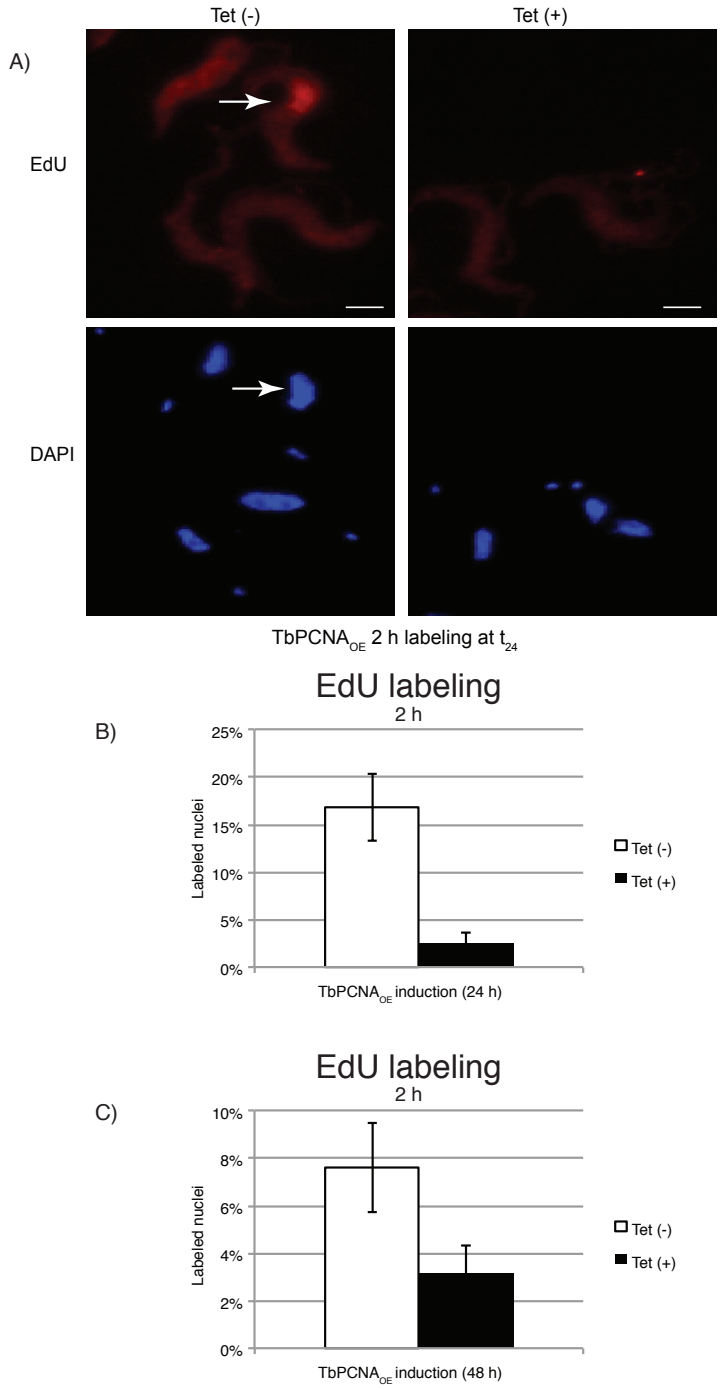

Figure 3. 6 Overexpressing TbPCNA inhibited DNA replication in *T. brucei*. TbPCNA$_{OE}$ clones were cultured in media without or with tetracycline for 24 or 48 h and then labeled for 2 h with EdU. The percent of clones undergoing DNA replication was quantified by fluorescence microscopy. (A) Representative micrograph of control (Tet (-) column) or induced (Tet (+) column) TbPCNA$_{OE}$ clones labeled with EdU after 24 h. Arrows point to EdU-labeled nuclei and to DAPI-stained nuclei of the same clone. (B) Bar graph representing the mean percent with standard error of EdU-labeled nuclei from control (Tet (-)) or induced (Tet (+)) clones at 24 h time points. (C) Bar graphs showing percent of nuclei labeled with EdU in control (Tet (-)) or induced (Tet (+)) clones at 48 h time points. Results for graphs were obtained from counting a minimum of 250 parasites per slide per condition. Scale bars represent 5 μm.

3.2.6 Overexpressing TbPCNA reduced *T. brucei* DNA replication without damaging DNA

Non-induced or induced $TbPCNA_{OE}$ clones were diluted at T_0 as described above and briefly labeled with EdU for 2 h during their log phase growth period (Fig.3.6 A). At T_{24}, about 17% of the non-induced clones had labeled nuclei after short EdU treatments. Inducing these clones for 24 h resulted in only 1% them having labeled nuclei after the 2 h EdU treatment period (Fig. 3.6 B). We observed that brief EdU incubations labeled less than 8% of nuclei in non-induced clones at T_{48}, as they approached stationary phase. Overproduction of TbPCNA in clones for 48 h led to about 3% of nuclei in the population being EdU-labeled (Fig. 3.6 C). This suggested that overproducing TbPCNA in *T. brucei* also reduced its ability to synthesize new DNA.

Phosphorylation of histone γH2A(X) has been used as a reliable marker for detecting DNA damage in mammalian cells (115). Recently, trypanosome histone γH2A(X) was identified and shown to function as a reliable marker for DNA strand breaks in *T. brucei* (116). We utilized antibodies raised against trypanosome histone γH2A(X) to examine if reducing DNA replication by upregulating TbPCNA caused accumulation of DNA stand breaks in the parasite. Quantitation by indirect immunofluorescence revealed that these antibodies stained about 5% of non-induced parasites, whereas they stained about 10% of $TbPCNA_{OE}$ clones after 24 h of induction (data not shown). These values were less than or equal to the baseline levels reported in control *T. brucei* (116), suggesting that overexpressing TbPCNA did not cause any appreciable accumulation of DNA strand breaks.

3.2.7 Overexpressing human PCNA arrested proliferation in *T. brucei*

TbPCNA was 35% identical to human PCNA and 36% identical to PCNAs of yeasts *Saccharomyces cerevisiae* and *Schizosaccharomyces pombe* based on Clustal W alignments. Alignment

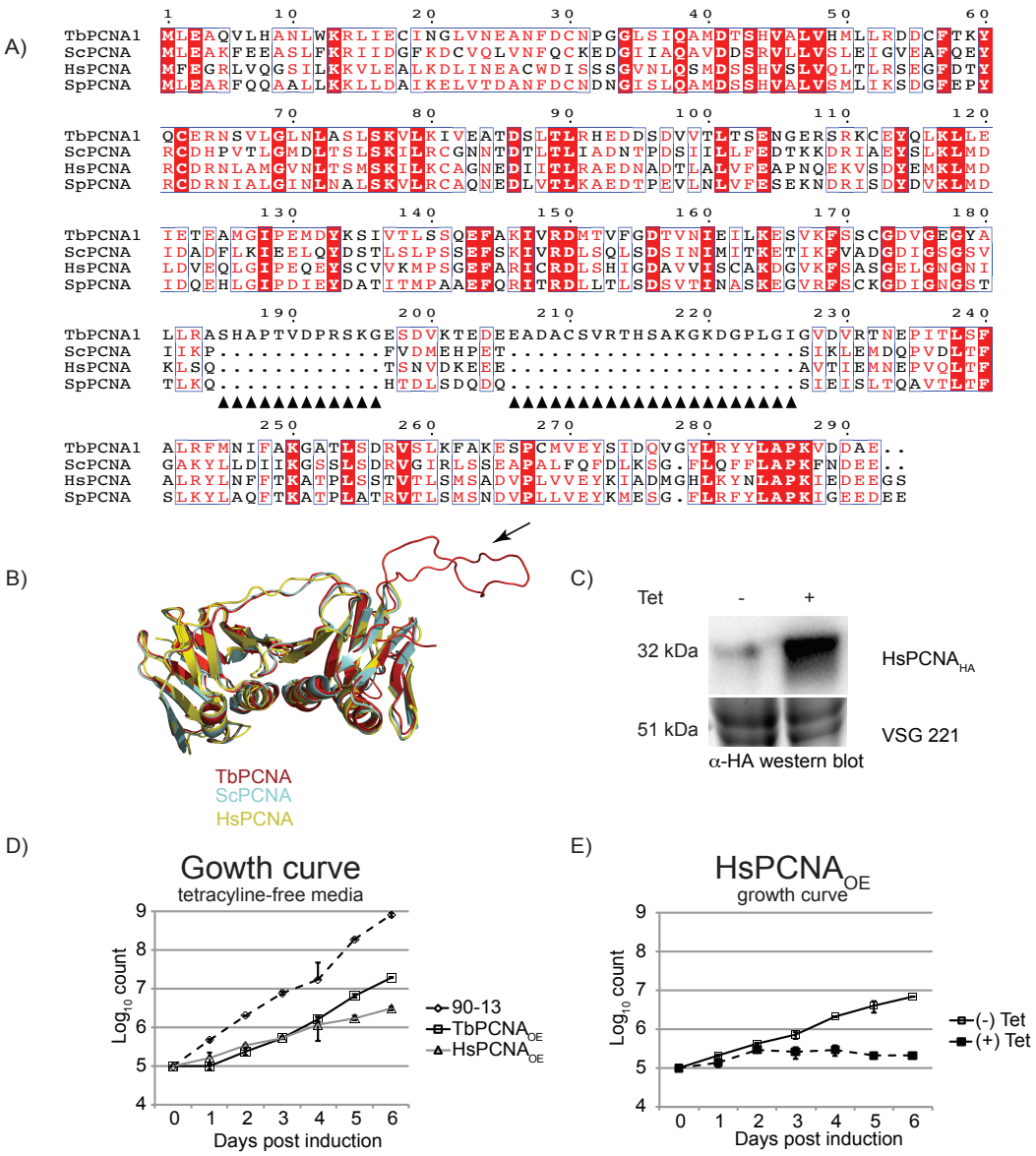

Figure 3. 7 Proliferation in *T. brucei* was arrested after being induced to overexpress human PCNA. (A) Clustal W alignment of PCNA homologs: *Trypanosoma brucei* (Tb), *Saccharomyces cerevisiae* (Sc), *Homo sapiens* (Hs), and *Schizosaccharomyces pombe* (Sp*)* were generated using the utility ESPript 3.0 to show their similarities. Red blocks indicate identical amino acids and white blocks indicate strongly similar amino acids. Black triangles represent sites where amino acid insertions occur in TbPCNA and other kinetoplastid parasites. (B) Homology model of *T. brucei*, yeast and human PCNA monomers with arrow pointing to unstructured loop in TbPCNA formed by the amino acid inserts. (C) Representative $HsPCNA_{OE}$ clone cultured in media without or with tetracycline were examined by immunoblot analysis to detect $HsPCNA_{HA}$ by α-HA antibodies. VSG loading control represents Stain-Free™ image obtained from gel prior to transfer. (D) Line graph comparing growth rates for 90-13 (dashed line), $TbPCNA_{OE}$ (black line) and $HsPCNA_{OE}$ (grey line) cultured in tetracycline-free media. (E) Graph comparing growth rates of $HsPCNA_{OE}$ clones cultured in non-induced (black line) or induced conditions (dashed line). Growth curves represent the mean value with standard deviations for experiments repeated 3 times using 3 independent clones.

of TbPCNA with these homologs demonstrated that TbPCNA contained amino acid insertions. The first insertion was located between residues 186 and 197 and the second was located between residues 206 and 226 (Fig. 3.7 A). Similar amino acid insertions were recognized in PCNA homologs from the related kinetoplastid parasite *Leishmania donovani (117).* As a member of the sliding clamp family, it is predicted that TbPCNA can assume a toroid structure similar to other PCNA homologs. The homology model for TbPCNA, based on monomer structures of yeast and human PCNAs (PDBs 3K4X and 3VKX respectively), predicted that it had 2 domains bridged by an interdomain-connecting loop (Fig. 3.7 B).

We subcloned the human HsPCNA cDNA into pLew111 for overexpression in *T. brucei* to test the notion that it would arrest growth in the parasite just as overproducing TbPCNA did. Phleomycin selection and immunoblot analysis were done as mentioned above to screen for stable transfectants that expressed HsPCNA upon tetracycline-induction. Based on the selection and screen, we identified 6 stable transfectants that expressed HsPCNA upon tetracycline induction that we designated as $HsPCNA_{OE}$ clones. Anti-HA antibodies detected a faint 32 kDa band in extracts from a non-induced representative $HsPCNA_{OE}$ clone, but a very prominent band was detected from the induced clone (Fig. 3.7 C). These observations were very consistent with those from $TbPCNA_{OE}$ clones.

The mean growth rates from several independent $HsPCNA_{OE}$ and $TbPCNA_{OE}$ clones cultured in tetracycline-free media were compared to that of parental 90-13 clones to determine the consequences of basal levels of expression from either PCNA homolog in the parasite. We observed that the doubling time for either $HsPCNA_{OE}$ or $TbPCNA_{OE}$ clones cultured in tetracycline-free media was about 24 h, whereas for 90-13 parasites it was about 7-9 hours (Fig. 3.7 D). The effects of overproducing HsPCNA in *T. brucei* were examined by comparing the mean growth rates of several independent clones cultured in media without or with tetracycline. This experiment clearly demonstrated that overexpressing HsPCNA in *T. brucei* arrested its proliferation (Fig. 3.7 E).

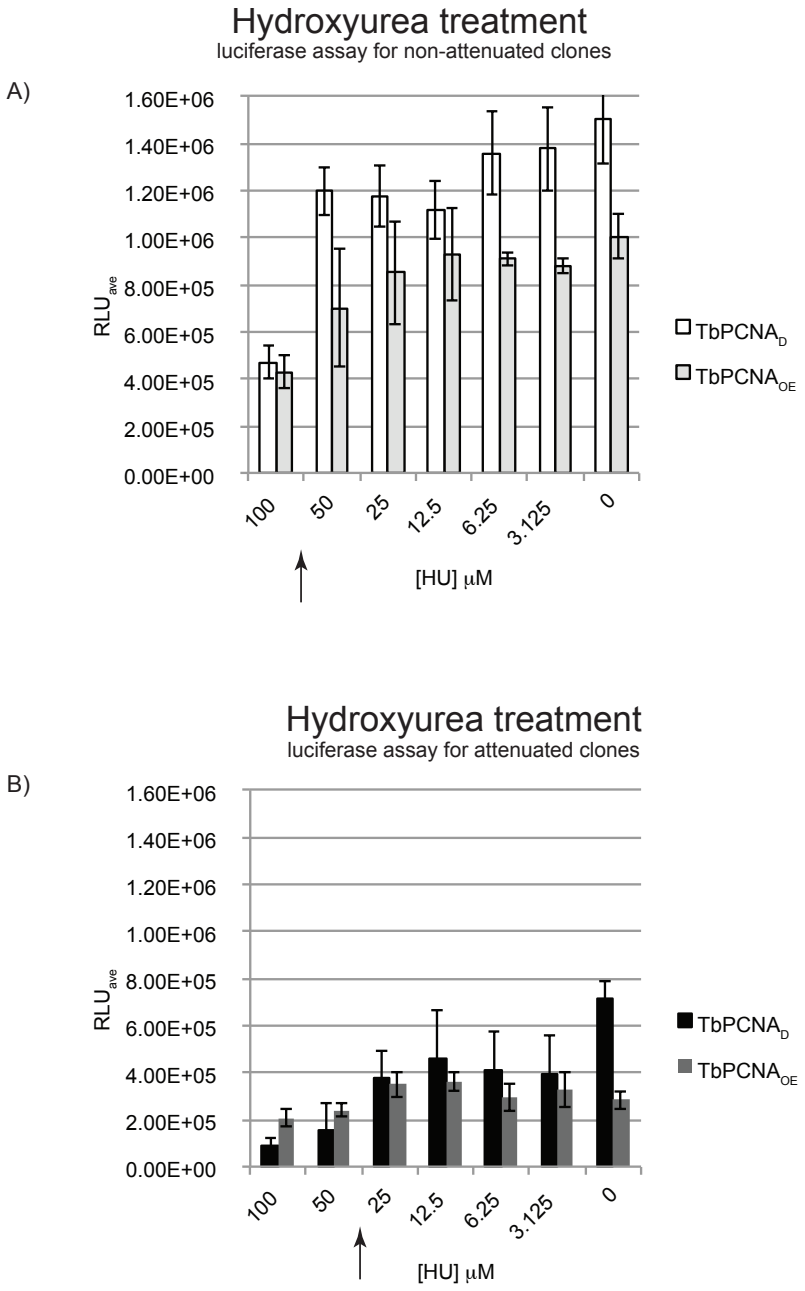

Figure 3. 8 Down-regulating TbPCNA hypersensitized *T. brucei* to hydroxyurea. Luciferase assays were used to measure proliferation in $TbPCNA_D$ or $TbPCNA_{OE}$ clones treated with hydroxyurea (HU) for 48 h. 10^4 parasites were grown in 96-well plates and treated with serial dilutions of HU followed by incubation at 37°C and 5% CO_2 for 48 h. The luciferase reagent (CellTiter-Glo®) was added to each plate to obtain relative light unit (RLU) readouts by luminometry. (A) Graph showing mean RLU values for non-attenuated clones of $TbPCNA_D$ (open bars) and $TbPCNA_{OE}$ (grey bars) treated with HU. Arrow is situated between HU concentrations in which the mean RLU values of non-attenuated clones were estimated to be 50% of the values for non-HU treated non-attenuated controls at 0 μM. (B) Graph that shows the mean RLU values for attenuated clones treated with HU. Arrow is situated between concentrations in which the mean RLU values for HU-treated attenuated $TbPCNA_D$ clones (black bars) were 50% of the values for non-HU treated attenuated controls at 0 μM concentration. RLU values represent the mean with standard deviations for 3 independent experiments.

3.2.8 Downregulating TbPCNA chemosensitized *T. brucei*

Luciferase assays were used to determine the IC_{50} of tetracycline for $TbPCNA_D$ or $TbPCNA_{OE}$ clones. The tetracycline IC_{50} was determined to be about 100 ng/ml for $TbPCNA_D$ clones and about 10 ng/ml for $TbPCNA_{OE}$ clones (data not shown). Inducing parasites with these concentrations of tetracycline was done to attenuate them without abrogating proliferation. Non-attenuated or attenuated clones were treated with serial dilutions of the DNA damaging agent H_2O_2 for 48 h to examine if they developed hypersensitivity. We expected hypersensitivity in attenuated clones to correlate with a decrease in their IC_{50} for H_2O_2 in comparison to the IC_{50} observed in non-attenuated clones. The IC_{50} of H_2O_2 remained constant in $TbPCNA_D$ or $TbPCNA_{OE}$ clones whether they were attenuated or not, which indicated that attenuating these clones did not make them hypersensitive to H_2O_2 (data not shown).

Treating non-attenuated $TbPCNA_{OE}$ or $TbPCNA_D$ clones with serial dilutions of the replication inhibitor hydroxyurea (HU) demonstrated that they had a similar IC_{50} for this agent, which was between 100 and 50 μM (Fig. 3.8 A). The IC_{50} of HU for attenuated $TbPCNA_{OE}$ clones also fell between 100 and 50 μM, which indicated that they were not hypersensitive to HU treatment. However in attenuated $TbPCNA_D$, the IC_{50} of HU was between 50 and 25 μM (Fig. 3.8 B). Such an IC_{50} reduction suggested that down-regulating TbPCNA and treating with HU had an adjuvant effect on proliferation in these clones, and indicated that attenuating $TbPCNA_D$ clones made them hypersensitive to HU treatment.

3.3 Discussion

Several components of the DNA replication machinery are highly regulated in the cell. The consequences of deleting or deregulating PCNA homologs in other model eukaryotic organism: yeast (111,118), mammals (119), and *Drosophila (120)* have been very well characterized demonstrating that the PCNA gene and its functional product are essential for cell survival. Gene products such as ERK8 and p21 can arrest cell cycle progression in human cells by reducing intracellular levels of PCNA (57,121). The $p21^{Cip1/Waf1}$ protein arrests DNA replication in human cells by sequestering PCNA, which prevents progression from G1 and G2 phases. Furthermore, several mechanisms of posttranslational modification: phosphorylation (67), ubiquitylation/sumoylation (122,123) and ADP ribosylation (124) are responsible for regulating the function and stability of PCNA in mammalian cells and yeasts.

Much less is known about how components of the DNA replication machinery are regulated or the consequences of deregulating their levels in *T. brucei.* We demonstrated that either upregulating or downregulating TbPCNA levels in *T. brucei* severely reduced proliferation by different mechanisms that remain uncharacterized. Abnormal growth phenotypes associated with depleting TbPCNA in this study were consistent with those predicted from the whole genome RNAi targeted screen of *T. brucei (48).* This study demonstrates that depleting TbPCNA by RNAi prevented G2 cell cycle progression in *T. brucei.* Such a phenotype is consistent with the S and G2/M phase arrest observed after PCNA was depleted in human cell by siRNA (125,126) and demonstrates an evolutionarily conserved function of PCNA.

Integration into the proper locus was essential for *T. brucei* clones to express endogenously tagged $TbPCNA_{HA}$. Stable clones that expressed endogenously tagged $TbPCNA_{HA}$ grew at similar rates as wild type parasites (data not shown). Therefore, we hypothesize that normal levels of TbPCNA were not perturbed in the endogenously tagged $TbPCNA_{HA}$ clones. It is possible that the increased cytoplasmic staining of TbPCNA observed during M phase with these clones was cause by misdirection from the HA-tag. Immunoblots of synchronized parasites demonstrated that TbPCNA expression was still present during both G2 and M stages of the parasites. This indicates that TbPCNA expression is present during

every stage of the cell cycle, which is the case in most other eukaryotic model organisms. The previous study followed TbPCNA expression in a single parasite and reported irregular patterns of TbPCNA expression in M phase parasites (73). Such irregular expression patterns in M phase parasites might explain why that TbPCNA was not detected in the nucleus of a single parasite. We examined multiple parasites per field of view and detected TbPCNA expression in the cytoplasm and nucleus of M phase parasites from endogenous and inducible TbPCNA clones. Further studies are needed to determine if cytoplasmic expression of TbPCNA plays a role in regulating the *T. brucei* cell cycle.

Upregulation of PCNA in mammalian cells is a hallmark of increased proliferation that serves as a predictable diagnostic marker for a broad range of cancers (102,103,127-129). In the related species *L. donovani,* upregulating LdPCNA was associated with clinical isolates of this parasite being resistant to antimonial compounds. Overexpressing LdPCNA laboratory strains protected it from such drugs (117). The phenotype observed after upregulating TbPCNA in *T. brucei* was in stark contrast to that reported for upregulating it in human cells or in *L. donovani*. Reduced proliferation in non-induced $TbPCNA_{OE}$ clones was correlated with marginal increases of intra-parasite TbPCNA levels caused by the lax plasmid promoter.

Observations from this study lead to the hypothesis that bloodstream form *T. brucei* has thresholds for its TbPCNA levels. This hypothesis is supported by the arrested proliferation in *T. brucei* observed after overexpressing either TbPCNA or HsPCNA. A similar outcome was reported after overexpressing pcn1, the PCNA homolog in the fission yeast *S. pombe* also supports this hypothesis. Upregulating pcn1 triggered a checkpoint that delayed the yeast from exiting G2/M, even when it was upregulated in checkpoint mutants of S. *pombe* (130). Overexpressing TbPCNA in bloodstream form *T. brucei* allowed the parasite to enter S phase but severely delayed progress beyond the G2/M phase. This is consistent with the notion that S phase in the kinetoplast was unaffected by overexpressing TbPCNA, whereas the nuclear S phase was inhibited or delayed. This represents a plausible explanation because in *T. brucei*, S phase in the kinetoplast precedes nuclear S phase (108). This would indicate that TbPCNA in the nucleus is regulated differently than it is in the kinetoplast, a matter that needs to be investigated

further. We concluded that the phenotype associated with overexpressing TbPCNA resulted from triggering an uncharacterized G2/M checkpoint in the parasite because both G2 and M phase parasites accumulated after overexpressing TbPCNA. Similar abnormal proliferation and cell cycle defects occurred when either human PCNA or TbPCNA were overexpressed in *T. brucei* (Figure 3.S4). Therefore, we conclude that overproducing either of these homologs may trigger the same mechanism that leads to G2/M arrest in the parasite. Two likely mechanisms for how overexpressing TbPCNA arrested proliferation in bloodstream form *T. brucei* were that excess TbPCNA triggered a checkpoint kinase or that it sequestered interacting proteins that regulate the cell cycle. The latter mechanism seems more plausible, because the function of PCNA is directed by its ability to form stable interactions with many proteins. Future studies to identify TbPCNA interacting proteins may help determine if upregulating TbPCNA sequesters critical cell cycle regulators in the parasite.

HU acts a replication inhibitor in eukaryotic cells and depleting TbPCNA associated with arrested DNA replication in *T. brucei.* We conclude that attenuating $TbPCNA_D$ clones and treating them with HU led to an additive or synergistic effect that made these parasites hypersensitivity to HU. Therefore, we interpret these observations to indicate that overexpressing or depleting TbPCNA mRNA in the parasite inhibited proliferation by separate mechanism.

Currently, mammalian cells and yeast are the predominant model system for characterizing PCNA. This has fundamentally restricted the types of studies for chemotherapeutic interventions of PCNA to human proliferative diseases such as cancer, arthritis and nephritis (126,131-134). The results of this study validate TbPCNA as a viable target for therapeutic intervention against African trypanosomiasis and broaden the categories of where PCNA therapeutics may be beneficial to infectious disease research. Future studies will elucidate mechanisms of TbPCNA regulation in *T. brucei*. Information gained from such studies can also reveal how deregulating TbPCNA triggers G2/M arrest. This information in combination with that obtained from several novel classes of PCNA inhibitors (126,134) may lead to the development of innovative therapies that target components of the *T. brucei* DNA replication machinery.

3.4 Materials and Methods

3.4.1 Cell culture

Bloodstream form *T. brucei* were incubated in 5% CO_2 at 37°C in HMI-9 medium modified to contain 20% fetal bovine serum (77). Parasites were cultured in media containing 100 U/ml penicillin and 100 µg/ml streptomycin. Selection medium contained 5 µg/ml hygromycin B, 2.5 µg/ml G418, and 2.5 µg/ml phleomycin. Parasites were induced by adding tetracycline to the medium at a final concentration of 1.0 µg/ml, unless further specified. The TbPCNA coding region was subcloned at the HindIII (http://www.thermoscientificbio.com/restriction-enzymes/hindiii/) and AflII (http://www.thermoscientificbio.com/restriction-enzymes/bspti-aflii/) restriction sites of the C-terminal HA-tagged modified version of pLEW111 (79). The restriction endonucleases NruI (https://www.neb.com/products/r0192-nrui) and NotI (https://www.neb.com/products/r0189-noti) were purchased from New England Biolabs.

3.4.2 Introduction of RNA interference (RNAi) transgenes into *T. brucei*

For electroporation, 10^7 parasites were pelleted by centrifugation and washed once with 10 ml of phosphate buffered saline (PBS) (4.3 mM Na_2HPO_4 137 mM NaCl, 2.7 mM KCl, 1.4 mM KH_2PO_4) pH 7.4. 1-to-10 µg of NotI (http://www.thermoscientificbio.com/restriction-enzymes/noti/) linearized plasmid was nucleofected into *T. brucei* using a Nucleofector™ Kit for Human T Cells (http://www.lonza.com/products-services/bio-research/transfection/nucleofector-kits-for-primary-cells/nucleofector-kits-for-primary-blood-cells/nucleofector-kits-for-human-t-cells.aspx). The parasites were pulsed using program X-001, transferred to 10 ml of modified HMI-9 media, and incubated overnight at 37°C with 5% CO_2. The next day, stable clones were selected and grown in media containing 5.0 µg/ml hygromycin B, 2.5 µg/ml G418, and 2.5 µg/ml of phleomycin.

3.4.3 RNA interference (RNAi) and quantification

RNAi was induced by supplementing selection media with tetracycline to a final concentration of 1 µg/ml. Parasites were counted using a Multisizer™ 3 Coulter Counter®Tetracycline-induced or non-

induced bloodstream form parasites were pelleted by centrifugation and resuspended in 1 ml of TRIzol® reagent (https://www.lifetechnologies.com/order/catalog/product/15596026). For all samples,1.5 μg of total RNA was used as a template for amplifying coding regions with the SuperScript® III One-Step RT-PCR kit (http://www.lifetechnologies.com/order/catalog/product/12574018) and gene-specific primers: (TbPCNA forward 5'-AAGCTTATGCTTGAGGCTCAGGTTCT-3' and reverse 5'-CTTAAGCTCGGCGTCGTCACCTTTG-3'). Primers for Tb-α tubulin (α-Tub forward 5'-ATGCGTGAGGCTATCTGCATCCACA-3' and α-Tub reverse 5'-AGGTTGCGGCGAGTCAAATCATAAAT-3') were used as internal controls to check for equal loading and integrity of *T. brucei* mRNA. Five microliters from cDNA samples were collected at 20, 23, and 25 PCR cycles to ensure that products were still in the linear range of amplification. PCR amplified cDNA products were resolved by agarose gel electrophoresis, stained with SYBR® Safe (https://www.lifetechnologies.com/us/en/home/life-science/dna-rna-purification-analysis/nucleic-acid-gel-electrophoresis/dna-stains/sybr-safe.html), and quantified by ChemiDoc™ MP.

3.4.4 Immunoblots

Expression of hemagglutinin-tagged TbPCNA expressed in *T. brucei* was examined by immunoblot as previously described (135). Stain-Free® gels used to resolve polypeptides for immunoblots were obtained from BioRad (http://www.bio-rad.com/en-es/product/mini-protean-precast-gels/mini-protean-tgx-stain-free-precast-gels). Histone γH2A(X) antibodies used in this study were a generous gift from David Horn (116).

3.4.5 Luciferase Assay

Parasites were diluted to 10^5/ml and a total of 10^4 were incubated in 96-well white opaque tissue culture plates in media with or without tetracycline at 1 μg/ml in biosafety cabinets for 48 h at 37°C with 5% CO_2. After the 48 h incubation period, 50 μl of CellTiter-Glo® reagent (https://www.promega.com/products/cell-health-and-metabolism/cell-viability-assays/celltiter_glo-luminescent-cell-viability-assay/) was added to each well and plates were placed on an orbital shaker at room temperature for 2 min to induce lysis. After a 10 minute incubation to stabilize the signal, the ATP

bioluminescence of each well was determined using a SpectraMax® L plate reader. Raw values measured in relative light units (RLU) were converted to $\log_{10}$ and percentage inhibition was calculated relative to the controls. Curve fitting was performed with Prism 4 software or Excel.

3.4.6 5-Ethynyl-2'deoxyuridine (EdU) labeling

At T_0 bloodstream form TbPCNA RNAi clones were subcultured at 1×10^5/ml in HMI-9 media without or with tetracycline to a final concentration of 1.0 µg/ml. After 48 h, EdU (https://www.lifetechnologies.com/order/catalog/product/A10044?ICID=search-product) was added in the culture media to final a concentration of 100 µM and labeling proceeded for 2 h. The parasites were pelleted by centrifugation, washed with 10 ml phosphate buffered saline (PBS) and fixed with 0.5% paraformaldehyde (https://www.emsdiasum.com/microscopy/products/chemicals/paraformaldehyde.aspx) for 30 min. The fixed parasites were resuspended in 100 µl of PBS, attached to poly-L-lysine coated slides and stained with Click-It® (https://www.lifetechnologies.com/order/catalog/product/C10337) and 4',6-diamidino-2-phenylindole (DAPI) (https://www.lifetechnologies.com/order/catalog/product/P36931). Visualization and quantification of labeled nuclei was done using indirect fluorescence microscopy Carl Zeiss and CellProfiler 2.0 (Massachusetts Institute of Technology).

3.4.7 Quantification of nuclei and kinetoplast

Parasites were visualized using an Axiovert A.1 microscope from Carl Zeiss and photographed using the Axiocam MRc camera system. The DAPI-stained Nuclei and kinetoplasts in *T. brucei* were photographed using a 63× or 100× objective. CellProfiler 2.0 and Zen software were used to count the nuclei and kinetoplasts from *T. brucei* images obtained by microscopy.

3.4.8 Flow cytometry analysis

T_0 parasites were subcultured to 1×10^5/ml and grown for 48 h in HMI-9 medium with or without tetracycline (https://www.goldbio.com/product/1896/tetracycline-hydrochloride). After 48 h (T_{48}), 1×10^6 cells were pelleted and washed 3×5 ml of PBS and fixed with 0.5 % paraformaldehyde (https://www.emsdiasum.com/microscopy/products/chemicals/paraformaldehyde.aspx) for 30 min, which

was then removed by washing with 5 ml of PBS. Washed parasites were RNAse A (http://www.amresco-inc.com/RNASE-A-SOLUTION-10MGML-E866.cmsx) treated and stained with propidium iodide (10µg/ml) (http://www.sigmaaldrich.com/catalog/product/fluka/81845?lang=en&region=US). Cytometric data was collected with an Accuri™ Flow Cytometer and analysed with FlowJo.

3.4.9 Indirect immunofluorescence microscopy

Parasites were washed once with PBS before attaching them to poly-L-lysine coated microscope slides. Attached parasites were then fixed with cold methanol for 5 minutes and allowed to air dry. The attached parasites were made permeable with 0.5% Triton X-100 for 5 minutes at room temperature and washed with PBS containing 0.5% BSA. Primary antibodies were diluted 1:200 in PBS containing 0.5% BSA and incubated on the prepared slides for 1 h in a humidified chamber at 37^{o}C. Slides were washed 3 times with 0.5% BSA in PBS. AlexaFluor® 488 or 594-conjugated secondary antibodies (488: http://www.lifetechnologies.com/order/catalog/product/A21206?CID=search-a21206 or 594: https://www.lifetechnologies.com/order/catalog/product/A21207?ICID=search-a21207) were diluted 1:1000 with PBS and incubated on the slides for 1 h at room temperature in a humidified chamber. The slides were washed 3 times with PBS and mounted with ProLong® Gold with DAPI (https://www.lifetechnologies.com/order/catalog/product/P10144?ICID=search-product). Micrographs were generated using an Axiovert A.1 and AxioCam MRc camera.

3.4.10 Genotoxic agents

Hydrogen peroxide (H_2O_2) (http://www.fishersci.com/ecomm/servlet/itemdetail?LBCID=81833512&storeId=10652&langId=-1&LBCID=81833512&catalogId=29104&productId=3017791&distype=0&fromSearch=0&hasPromo=1) was purchased from ThermoFisher. Hydroxyurea crystalline form (http://www.fishersci.com/ecomm/servlet/itemdetail?itemdetail=%27item%27&storeId=10652&productId=16609104&catalogId=29104&matchedCatNo=50525180&fromSearch=1&searchKey=50-525-180&highlightProductsItemsFlag=Y&endecaSearchQuery=%23store%3DRE_SC%23nav%3D0%23rpp%3D25%23offSet%3D0%23keyWord%3D50-525-

180%23searchType%3DPROD%23SWKeyList%3D%5B%5D&xrefPartType=From&savings=0.0&xrefEvent=1405969990000_0&searchType=PROD&hasPromo=0) was purchased from ThermoFisher.

3.4.11 Statistical analysis

The Student's *t*-test was used to compare numerical means obtained from non-induced or induced samples.

3.5 Acknowledgements

We thank Michael Klemba, Janet Webster and Ling Chen at Virginia Tech and Kenneth Kreuzer at Duke for reading and critical comments. This work was supported in part by Start-up fund NIFA139696, VT Drug Discovery Center VTCDD ##119286. ACR receives support from NSF S-STEM grant: DUE-0850198. ALV receives support from the Costa Rican Ministry of Science, Technology and Telecommunications (MICITT).

3.6 Supplementary Information

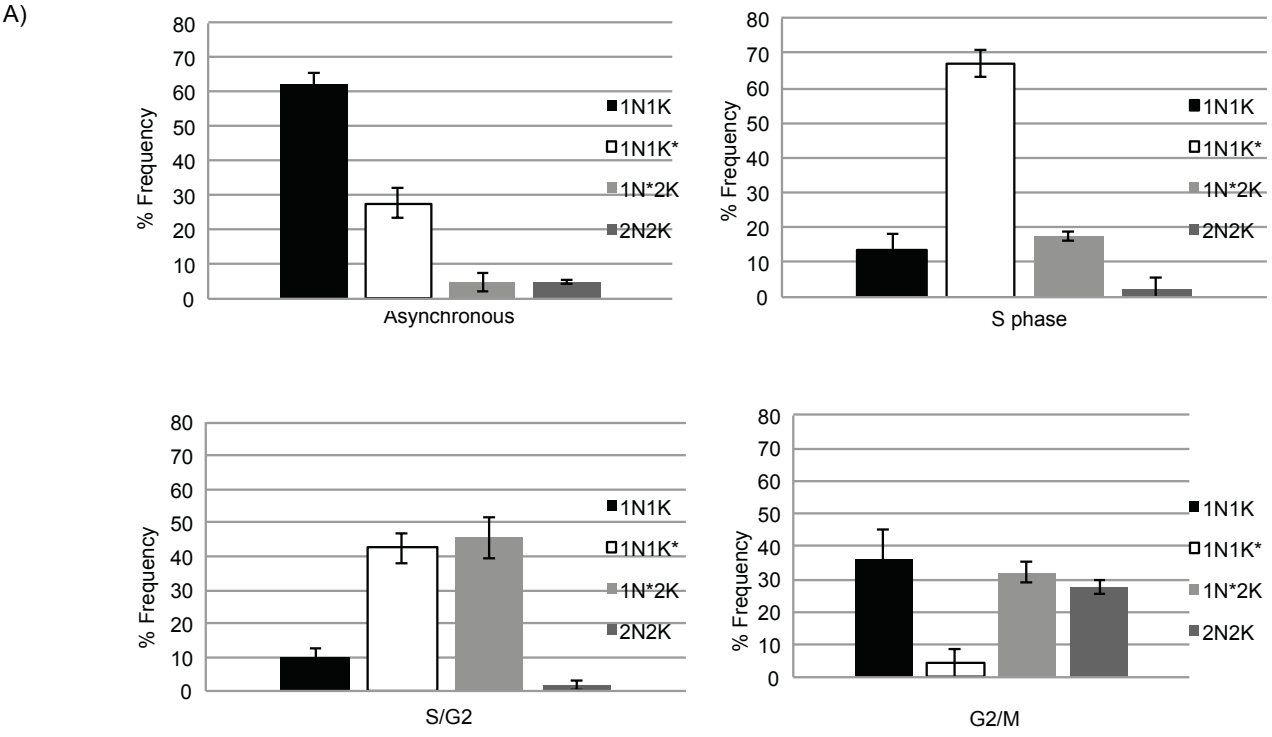

Figure 3.S1 Hydroxyurea synchronization of *T. brucei*. (Panel A) Asynchronous bloodstream form *T. brucei* were grown to ~1.10^6 and synchronized with hydroxyurea as described by Tan et al. (126) Briefly, parasites were treated with hydroxyurea for 6 h to synchronize them in S phase. After 6 h treatment, hydroxyurea was removed and the parasites were allowed to recover in fresh HMI-9 medium for 1 h to enrich the population in S/G2 phase. In parasites allowed to recover for 3 h, the population became enriched for G2/M phase parasites. Nuclei and kinetoplast were counted in the parasites after each time point to estimate the 1N1K, 1N2K, 2N2K frequency in Asynchronous parasites or after S phase, S/G2 or G2/M enrichments. Parasites estimated to be in late S phase with elongated kinetoplasts were indicated by 1N*1K and those estimated to be in late G2 phase with elongated nuclei were indicated by 1N*2K. The mean frequencies with standard error from each graph were calculated from experiments done in

triplicates counting a minimum of 150 parasites from each condition. (Panel B) *T. brucei* were lysed following the protocol of Forsythe et al. (113) Briefly, the parasites were lysed with NP-40 to obtain the NP-40 extractable cytoplasmic fraction. The insoluble pellet was washed 5 times with NP-40 lysis buffer and designated as insoluble nuclear fraction. The insoluble nuclear fraction was treated with DNAse I for 1 h at 37^{o} C to release any attached TbPCNA. Aliquots of fractions from these two conditions were boiled in SDS loading buffer and resolved by SDS polyacrylamide gel. The resultant gels were transferred to PVDF membrane and prepared for immunoblot analysis using anti-HA antibodies to detect $TbPCNA_{HA}$ in the cytoplasmic or nuclear fractions from each synchronized population of parasites. Sample loading was normalized by Stain Free® gel prior to transferring to PVDF membrane.

A)

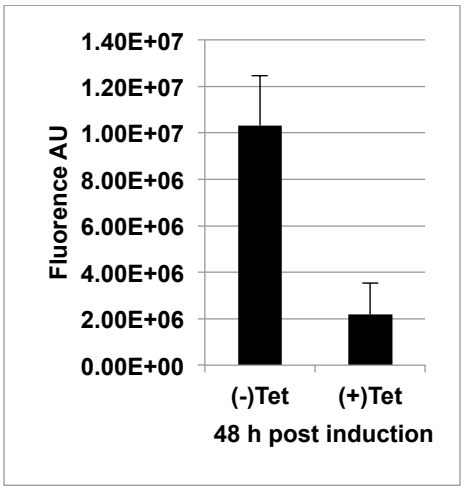

Figure 3.S2 Semi-quantative RTPCR analysis of TbPCNA. Total RNA preparation was done as described in methods section. RT-PCR primers and conditions were done as described in the methods section. Bar graph demonstrates reduction in the relative amount of TbPCNA mRNA amplified by RT-PCR after 48 h of RNAi depletion. Values are mean fluorescence in arbitrary units (AU) with standard deviations obtained from intensities of bands in agarose gels stained with SYBR Safe ®. ChemiDoc^{TM} system was used to quantify band fluorescence in the agarose gels. Values were obtained from experiments using as single clone repeated in triplicates.

S2

$TbPCNA_{OE}$ flow cytometry

(48 h) histograms

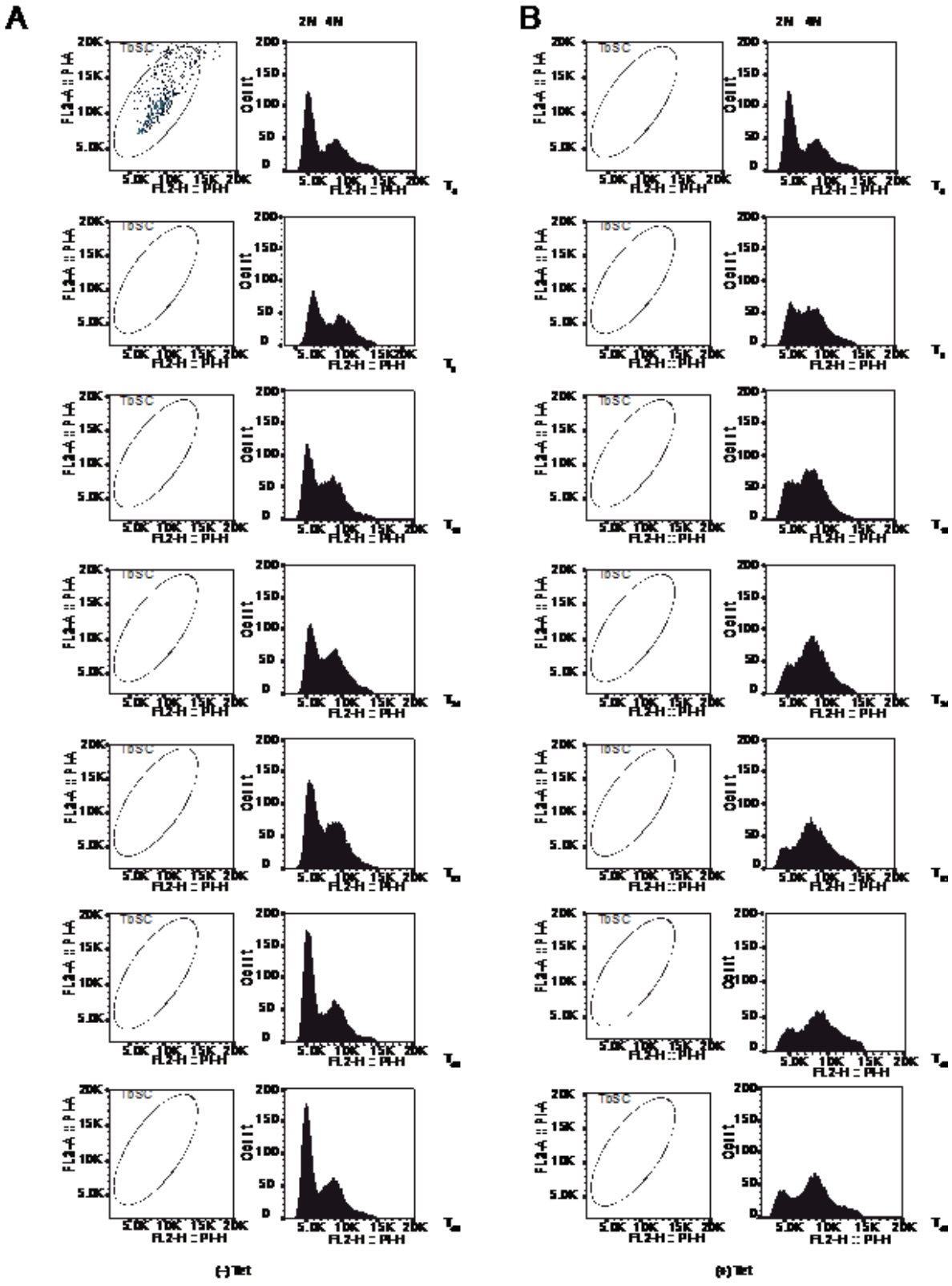

Figure 3.S3 Representative histogram for $TbPCNA_{OE}$ clones. Stationary phase $TbPCNA_{OE}$ clones were sub-cultured to $1x10^5$ parasites/ml at T_0 and allowed to grow for 48 h with or without overexpressing TbPCNA. In 8 h intervals from T_0 to T_{48}, 2.5×10^6 parasites were pelleted and washed 3 times with 5 ml of PBS and fixed with 0.5 % paraformaldehyde for 30 min, which was then removed by washing with 5 ml of PBS. Washed parasites were RNAseA treated and stained with propidium iodide (20µg/ml). Stained parasites were analysed using an Accuri Flow Cytometer. Histograms were prepared and analysed with FlowJo. Cultures were fixed with 0.5% paraformaldehyde and prepared for propidium iodide staining. Gated population of parasites analysed after each time point are displayed immediately to the left of each corresponding histogram. (A) Histograms of non-induced $TbPCNA_{OE}$ clones monitored from T_0 to T_{48}. (B) Histographs of tetracycline-induced $TbPCNA_{OE}$ clones monitored from T_0 to T_{48} showing the rapid shift of these induced clones to G2/M stage. The approximate mitotic index of *T. brucei* is represented at the top of the histogram as 2C and 4C, which corresponds to the mean value of nuclei at G0/G1 and G2/M respectively.

A)

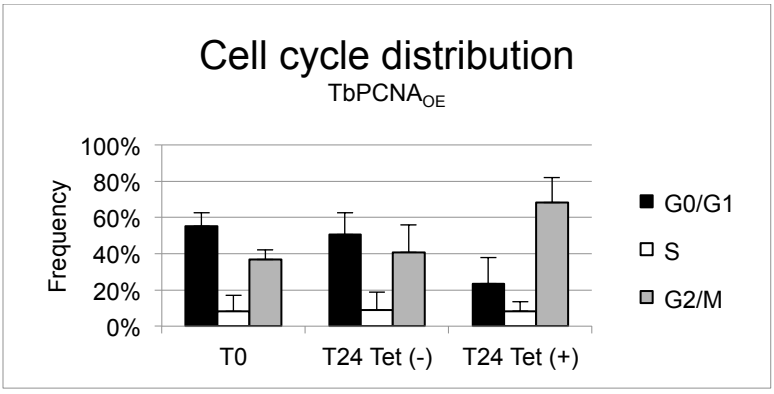

B)

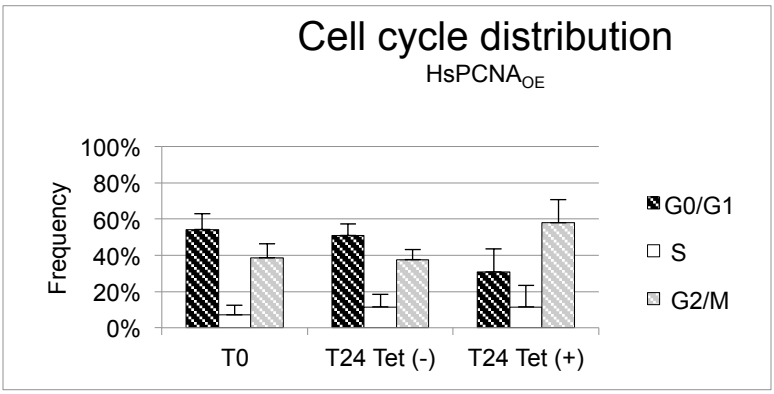

C)

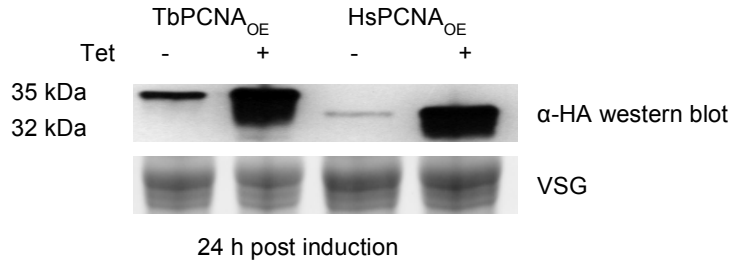

Figure 3.S4 Effects on cell cycle distribution after overexpressing TbPCNA or HsPCNA$_{OE}$ in *T. brucei.* Clones were prepared for cytometric analysis as described in Figure 3.S2 except parasites were collected at T_0 and T_{24}. Bar graphs comparing the cell cycle profiles of these two clones represent the mean cell cycle frequencies with standard error bars obtained form experiments done in triplicates for each parasite clone. (A) Cell cycle distributions for TbPCNA$_{OE}$ clones at and T_0 and T_{24} without (Tet (-)) or with (Tet (+)) tetracycline. (B) Cell cycle distributions for HsPCNA$_{OE}$ clones at and T_0 and T_{24} without (Tet (-)) or with (Tet (+)). (C) Immunoblot analysis using anti- HA antibodies to detect hemagglutinin-tagged TbPCNA or HsPCNA overproduced in representative clones.

4. Extracellular-signal regulated kinase 8 of *Trypanosoma brucei* uniquely phosphorylates the proliferating cell nuclear antigen homolog and reveals exploitable properties

Author contributions:

Ana L. Valenciano designed, performed and analyzed all the experiments except the experiments mentioned below; and helped write the article.

Giselle M. Knudsen performed, analysed and wrote the methods on the mass spectrometry experiments; and edited the article.

Zachary B. Mackey conceived, coordinated the study and helped write the paper.

Abstract

Tb927.10.5140 (TbERK8) is an essential mitogen-activated protein kinase (MAPK) expressed in bloodstream form *Trypanosoma brucei* that is homologous to the human extracellular-signal regulated kinase 8 (HsERK8). Among the MAPKs, ERK8 homologs represent atypical members that have long, divergent C-terminal extensions. These atypical members have dual specific activity and become fully activated through autophosphorylation rather than by upstream MAPK kinases. Here, we report that TbERK8 has a divergent C-terminal extension, is able to autophosphorylate, and has dual specific kinase activity. TbERK8 has a putative proliferating cell nuclear antigen (PCNA) interacting peptide (PIP-box) that is inefficient at forming a stable complex with TbPCNA, the PCNA homolog in *T. brucei*. The interaction between TbERK8 and TbPCNA resembles a transient enzyme and its substrate. Consistent with this notion, we have demonstrated that TbERK8, but not HsERK8, selectively phosphorylates TbPCNA *in vitro* and *in vivo.* We further identified an inhibitor that shows selectivity between the active sites of HsERK8 and TbERK8. These observations indicate that the biochemistry of TbERK8 has diverged in *T. brucei*, which might allow for the discovery of inhibitors that specifically target this atypical parasite MAPK.

4.1 Introduction

Trypanosoma brucei is the causative agent of Human African Trypanosomiasis or sleeping sickness, a meningoencephalitic disease that is most often fatal if left untreated (10). *T. brucei* possess a basic mitogen-activated protein kinase (MAPK) signaling network. Such networks are generally regulated by sequential phosphorylation of a three-tiered superfamily of serine/threonine protein kinases consisting of MAPK kinase kinases, MAPK kinases, and MAPKs (136-138). Once activated, MAPKs phosphorylate downstream effectors that include transcription factors, protein kinases, and phosphatases (61). In *T. brucei,* MAPKs have been shown to regulate differentiation, stress response, and transmission in both the insect and mammalian stage of this heteroxenous parasite (45,46,139,140). The important role that MAPKs have in regulating many critical processes in *T. brucei* makes them attractive targets for therapeutic exploitation.

We previously demonstrated that silencing the Tb927.10.5140 gene product in bloodstream form *T. brucei* arrests proliferation and leads to its death, revealing that its function is essential during this stage of the parasite (47). Tb927.10.5140 encodes a polypeptide that is homologous to the human extracellular signal-regulated kinase 8 (HsERK8) (47). HsERK8 is the first member of the ERK8 family. These members have characteristically long C-terminal extensions that are not conserved (61). HsERK8 is activated by autophosphorylation (50) and interacts with human proliferating cell nuclear antigen (HsPCNA) to form a stable complex, which protects HsPCNA from proteasome degradation (57). The HsERK8•PCNA interaction is mediated by a conserved PCNA interacting protein motif (PIP-box) located within the linker region between its two kinase domains (57). The canonical PIP-box is represented by the consensus sequence QxxΨxxϑϑ where Ψ= (hydrophobic residues) and ϑ= (aromatic residues) (74,93,141). TbERK8 contains a sequence that is similar to the PIP-box sequence of HsERK8, which is also located in its linker region. Here, we investigate the ability of this motif to interact with the *T. brucei* PCNA homolog (TbPCNA) and study the biochemical relationship between TbERK8 and TbPCNA *in vitro* and *in vivo*. We show that the biochemical properties of TbERK8 differ fundamentally from

HsERK8. These fundamental differences suggest that small molecules can be discovered and used to selectively inhibit TbERK8 biochemistry to kill *T. brucei.*

4.2 Materials and Methods

4.2.1 Culturing of *T. brucei*

Bloodstream form parasites were incubated in 5% CO_2 at 37 °C in complete HMI-9 medium purchased from Axenia Biologix (Dixon, CA.) using the formulation of Hirumi and Hirumi (77).

4.2.2 Primers for TbERK8 and TbPCNA constructs

The coding region for wild-type TbERK8 (wt-TbERK8) was amplified with the forward primer 5'-CGCGCCAAGCTTATGTCATCAGAAATAGAGCC-3' and the reverse primer 5'-CTTAAGTTTGTGCAACACACGAGAGGC-3'. The K42A point mutation (K42A-TbERK8) was made in TbERK8 cDNA using primers K42A forward 5'-GGTTGTAGCGTTAGCGAAGATATACGACGC-3 and reverse 5'-GCGTCGTATATCTTCGCTAACGCTACAACC-3' by the annealing overlapping PCR method (80).

The wild-type TbPCNA coding region (wt-TbPCNA) was amplified by PCR from *T. brucei* genomic DNA using the forward primer 5'-AAGCTTATGCTTGAGGCTCAGGTTCTG-3' and the reverse primer 5'-CTTAAGCTCGGCGTCGTCCACCTTTGG-3' Primers to generate the PIP-box from TbERK8 were 5'-CGATACTTAAGGGATCCATGTCCCCTATACTAGGT-3' and 5'-GCGAGAGTCGACTCAGTGGAAAGCCGCCACATACGG-3'. Primers to generate the PIP-box from TbAUK1 were 5'-GATCCCAGTTCCTTCTCAAGTATTATTATG-3' and 5'-TCGACATAATAATACTTGAGAAGGAACTGG-3'. Primers to generate the PIP-box from TbPFC19 were 5'-GATCCCAGGGCCACTTGTTTACCTACTACG-3' and 5'-TCGACGTAGTAGGTAAACAAGTGGCCCTGG-3'. These primers were annealed and subcloned into BamHI/SalI restriction sites of pGSTag (142).

4.2.3 Expression and Purification of Recombinant Proteins in *E. coli*

Wt-TbPCNA coding region was subcloned into the BamHI/HinDIII sites of pTrcHis A (Invitrogen, Grand Island, NY) and expressed with a 6×His tag in BL21-DE3. The recombinant protein was purified by nickel agarose affinity chromatography (Cat# 88222, Lot# PL208040, Thermo Scientific, Rockford, IL) as recommend by the manufacturer.

To express the TbERK8 kinase domain without the C-terminal extension, the nucleotides from 1-1019 of its coding region were subcloned into the BamHI/EcoRI sites of pGSTag to express it as a GST fusion protein in *E. coli*. The full-length version of TbERK8 (nucleotides 1-1329) was subcloned into BamHI/HindII of the pGSTag to express it as a GST fusion protein (GST-TbERK8). The pGEX-2T-HsERK8 expression plasmid was kindly provided by the laboratory of Deborah Lannigan, (Vanderbuilt University). *E. coli* expressing either GST-TbERK8, GST-TbERK8$_{KD}$, or GST-HsERK8 fusion protein were grown at 37 ºC until they reached an A_{600} of 1.0, then chilled on ice and induced with 0.2 mM IPTG at 16 ºC for 12 h. The *E. coli* were pelleted by centrifugation in at 7,000 rpm in a Beckman JLA 10.5 rotor at 10 ºC for 15 minutes. Pellets were lysed by sonication and clarified by centrifugation at 15,000 rpm using a Beckman JA 25.5 rotor at 4 °C. These GST fusion proteins were purified by GSTPrep FF 16/10 affinity chromatography (Cat# 28-9365-50, Lot# 10233091, GE Healthcare, Pittsburgh, PA) as recommended by the manufacturer.

4.2.4 Purification of TbERK8$_{BV}$ from SF9 Insect Cells

A recombinant baculovirus encoding the full coding region of TbERK8 was constructed by using the pFastBac1 baculovirus expression system (Life Technologies, Inc., Grand Island, NY). Sf9 insect cells (4 × 250 ml) were grown to a density of 2.0×10^6 cells/ml and then infected with the recombinant virus at a multiplicity of infection of 3-5. After rotation at 150 rpm for 72 h at 28°C, the cells were harvested by centrifugation, flash-frozen in liquid nitrogen, and stored at −80°C. The frozen pellet was thawed on ice and then resuspended in 200 ml of 50 mM Tris-HCl (pH 7.5), 75 mM NaCl, 0.1% Nonidet P-40, 1 mM EDTA, 0.5 mM dithiothreitol (DTT), 1 mM phenylmethanesulfonyl fluoride, 1 mM benzamidine-HCl, 1 μg/ml leupeptin, 2 μg/ml aprotinin, and 1 μg/ml pepstatin. After 30 min on ice, the lysate was cleared by centrifugation at 35,000 rpm for 30 min in a Beckman 45 Ti rotor at 4 °C. The clarified lysate was loaded on a carboxymethyl (CM) chromatography column (Cat# 17-0719-01, GE Healthcare, Pittsburgh, PA). Protein was eluted from the CM column with buffer A (150 mM NaCl in 20 mM Tris, pH7.4, 10% Glycerol and 1 mM EDTA). These fractions were pooled and loaded onto hydroxyapatite (HAP) chromatography resin (Cat# 130-0151, BioRad, Hercules, CA). TbERK8$_{BV}$ was

eluted from the HAP column in buffer B (HEPES, pH 7.4 10% glycerol, 75 mM NaCl, 75 mM phosphate ions). Fractions from the HAP column were pooled and loaded onto an S-Fast Flow column (Cat# 17-0511-01, GE Healthcare Life Sciences, Pittsburgh, PA) and eluted with buffer A containing 250 mM NaCl.

4.2.5 Autophosphorylation of recombinant TbERK8$_{BV}$ and GST-TbERK8$_{KD}$

We incubated 0.1μg of purified TbERK8$_{BV}$ or GST-TbERK8$_{KD}$ protein in 30 μl of buffer K (30 mM Tris pH7.4, 10 mM $MgCl_2$, 1 mM DTT, 5% glycerol, 1mM ATP and 0.1 mg/ml bovine serum albumin). Ten μCi of ^{32}P-γ-ATP were added and the reactions incubated at 30 ºC for 30 min. SDS loading buffer was added to the reaction mixtures and boiled for 1 min to stop the reaction. TbERK8 autophosphorylation by this method was detected by SDS-PAGE and autoradiograpy. Alternatively, TbERK8 autophosphorylation was done using 1 mM of cold ATP. In this case, TbERK8 autophosphorylation was detected by immunoblot analysis using the anti-phosphotyrosine antibody PY20 (Cat# GTX10321, Lot# 33072, GeneTex Inc. Irvine, CA) at 1/500. PY20 was recognized by a horseradish peroxidase-conjugated secondary antibody to the mouse IgG2b (Cat# GTX77294, Lot# 821600258, GeneTex Inc. Irvine, CA).

4.2.6 Kinase Activity Assays

Recombinant full-length TbERK8 purified from Sf9 insect cells (200 nmol) was incubated with 100 μmol TbPCNA$_{6H}$. Ten μCi of ^{32}P-γ- ATP (Cat# BLU502H250UC, Perkin Elmer, Boston, MA) were used in a 30 μL reaction using buffer K. The samples were incubated for 5 min at 30°C and stopped as described above. Reactions were resolved in an SDS-PAGE gel, and bands were visualized by autoradiograpy. TbPCNA phosphorylation was quantified with a Typhoon FLA 7000 phosphorimager (GE Healthcare, Pittsburgh, PA). To determine the K_m of TbERK8$_{BV}$ for TbPCNA$_{6H}$, kinase assays were performed as above with varying concentrations of purified recombinant TbPCNA$_{6H}$ ranging from 10 nM to 5 μM. Steady-state kinetics of TbERK8 were calculated by fitting data to the Michaelis-Menten curve using Prism Graphpad 5.0.

4.2.7 Expression of Hemagglutinin tagged (HA-tagged) recombinant proteins in *T. brucei*

pLEW11-3HA was generated by modifying the plasmid pLEW111 (79), which allows for tetracycline inducible protein expression, to include a C-terminal hemagglutinin tag (HA-tag). The coding region for wt-TbERK8, K42A-TbERK8, and wt-TbPCNA were subcloned into the HindIII and AflII restriction sites of pLEW11-3HA. Nucleofections were carried out with 1 μg to 10 μg DNA using the Lonza Nucleofector II™ program X-001 and the Nucleofector™ kit for Human T cell transfection (Cat# VPA-1002, Lonza Pharma&Biotech, Walkersville, MD). Stable transfectants were selected based on their resistance to phleomycin. HA-tagged recombinant proteins wt-TbERK8$_{HA}$, K42A-TbERK8$_{HA}$, and wt-TbPCNA$_{HA}$ were induced with tetracycline and expressed in the *T. brucei* 90-13 strain as described by Wirtz *et al* (78). The expression of recombinant proteins was confirmed by immunodetection with rabbit anti-HA (Cat# H6908, Lot# 083M4837V, Sigma, St. Louis, MO) antibody and by mass spectrometry.

4.2.8 pHAR construct

The TbERK8 RNAi construct from pZJM (87) was digested with BamHI and KpnI and subcloned into the modified pLEW11-3HA plasmid containing wt-TbPCNA. We named the resulting plasmid pHAR because of its ability to express HA tagged TbPCNA and TbERK8 RNAi cassette simultaneously. The plasmid pHAR was linearized with the restriction enzyme BsaBI, which has a unique site in the TbPCNA coding region, and nucleofected into the Tb90-13 to produce a stably-transfected *T. brucei* strain that expressed endogenous levels of HA-tagged TbPCNA and the tetracycline inducible TbERK8 RNAi cassette. TbPCNA protein levels in these parasites were monitored by immunoblot as described below.

4.2.9 Immunoblot Analysis of HA-tagged Proteins

Parasites from cultured bloodstream form *T. brucei* stage were harvested at 2×10^6 per/ml, lysed with Tb lysis buffer (1.0% Triton X-100, 10 mM Tris pH 7.5, 25 mM KCl, 150 mM NaCl, 1 mM $MgCl_2$, 0.2 mM EDTA, 1 mM dithiothreitol, 20% glycerol), and incubated on ice for 30 min, followed by ultracentrifugation at 15,000 rpm for 5min to produce a clarified lysate. For immunoblotting, 25 μg of

clarified lysate was resolved by SDS-PAGE and transferred to polyvinylidene difluoride membrane (PVDF). After transferring and blocking, the membrane was incubated with rabbit anti-HA (1:2,000 dilution) for 1 h and washed three times for 5 min with TBST (10 mM Tris, pH 7.4, 150 mM NaCl, 0.4% Tween 20). After the third wash, horseradish peroxidase-conjugated donkey anti-rabbit IgG (1:1,000 dilution) (Cat# 32460, Lot# PI207724 Thermo-Scientific, Rockford, IL) was added to the blots for 1 h. The blots were then washed again 3 times for 5 min each and examined by enhanced chemiluminescence (ECL) (GE Healthcare Life Sciences, Pittsburg, PA).

4.2.10 TbPCNA Pull down with GST-PIP-box fusion constructs

The three GST-PIP-box fusion proteins: TbERK8 PIP-box (GSTtbE8-PIP), TbAUK1 PIP-box (GSTtbAUK1-PIP), and TbPFC19 PIP-box (GSTtbPFC-PIP) were overexpressed in *E. coli* and captured on glutathione agarose beads (Cat# G-250-10, Gold Bio Inc., St. Louis, MO) following the protocol suggested by the manufacturer. Briefly, the pellets from 250 ml cultures were lysed using 10 mL of buffer 4 (50 mM Tris, 1% DOC, 0.3 M urea, pH 8, 1 mM phenylmethanesulfonyl fluoride, 1 mM benzamidine-HCL) as described by Danilevich *et al* and clarified by centrifugation (4 °C at 15,000 rpm) using a Beckman JA 25.5 rotor. GST beads (200 μl) were added to the clarified lysate and incubated overnight at 4 °C rotating to saturate the beads. The saturated beads were washed 5 times with PBS. The washed GST agarose beads were incubated with lysates from *T. brucei* that overexpressed wt-TbPCNA$_{HA}$ for two hours at 4 °C. Beads were washed 5 times with PBS, boiled in 5X SDS loading buffer, and resolved by polyacrylamide gel electrophoresis. The loading controls were visualized by Coommassie stain or by StainFree®, (Cat# 456-8035, BioRad, Walnut Creek, CA), which contains a trihalo compound that produces a fluorescent product when covalently crosslinked to protein tryptophan residues. These gels reduced the need to stain gels and allowed bands to be visualized with a ChemDoc MP (BioRad, Walnut Creek, CA). TbPCNA bands were detected by immunoblots using anti-HA or anti-His antibodies (Cat# MA1211315, Thermo Scientific, Rockford, IL).

4.2.11 Immunoprecipitation of HA tagged proteins

Stable *T. brucei* transfectants that expressed either HA-tagged TbERK8 or TbPCNA were induced with tetracycline to a final concentration of 1 μg/ml for 24 hours. Extracts from induced parasites were pelleted by centrifugation and lysed with 1 ml of immunoprecipitation (IP) lysis buffer on ice for 30 min (1% Triton X-100, 10 mM Tris pH 7.9, 25 mM KCl, 150 mM NaCl, 1 mM $MgCl_2$, 0.2 mM EDTA, 1 mM dithiothreitol (DTT), 10% glycerol, and 1× complete protease inhibitor mix (Cat# 11873580001, Roche, Indianapolis, IN). Lysates were incubated with 30μl anti-HA immuno-affinity beads from (Cat# 26181, Thermo Scientific, Rockford, IL) and rotated overnight at 4°C. The beads were washed 5 times with 1 ml of IP lysis buffer.

4.2.12 $TbPCNA_{6H}$ Pull down with full length $TbERK8_{HA}$

Wt-$TbERK8_{HA}$ prepared from *T. brucei* lysates was adsorbed onto 30 μl of immuno-affinity beads and washed 5 times in 1 ml of immunoprecipitation lysis buffer. Ten microliters of the anti-HA immunoaffinity beads with wt-$TbERK8_{HA}$ were incubated with a final concentration of 15 ng/μl of $TbPCNA_{H6}$ in 300 μl reactions with rotating at 4 °C for two hours. Beads were washed 5 times with 1 ml of PBS, resolved by SDS-PAGE, followed by anti-His tag immunoblotting for detection of bound $TbPCNA_{6H}$.

4.2.13 Autophosphorylation and Kinase Activity Analysis with in vivo Expressed TbERK8

Ten microliters of the HA-immuno-affinity beads with either wt-$TbERK8_{HA}$ or the K42A-$TbERK8_{HA}$ mutant bound were tested for autophosphorylation as described above. To test the substrate specificity of the *in vivo* expressed proteins, we preincubated ten microliters of the immuno-affinity beads with 10 μCi of ^{32}P-γ-ATP in 30 μl of buffer K. Subsequently, 100 μmol of either $TbPCNA_{6H}$ or the generic kinase substrate myelin basic protein (MBP) (Cat# 13-110, Millipore, Darmstadt, Germany) were added, and the reactions incubated at 30 ºC for 30 min. Reactions were stopped by adding 5X SDS-PAGE loading buffer and boiling for 1 minute. Ten microliters of the kinase IP reaction were resolved by SDS-

PAGE and examined by autoradiography. Bands identified by Phosphorimager were quantified as described above. We used a mock reaction (no substrate) for each set of experiments as well as affinity beads incubated in lysates from the non-transfected *T. brucei* 221 wild type strain as negative controls to detect background labeling.

4.2.14 Peptide Sequencing by Mass Spectrometry

Peptide sequencing and protein identification was performed using liquid chromatography-tandem mass spectrometry (LC-MS/MS). For protein identification, peptide samples were prepared from gel bands that were excised from SDS-PAGE gels and subjected to in-gel trypsin digestion (143).

Sequencing was performed using either an LTQ-Orbitrap XL or an LTQ-Orbitrap Velos mass spectrometers (Thermo Scientific, Rockford, IL), each equipped with a 10,000 psi system nanoACUITY (Waters, City State) UPLC instrument and EZ-Spray source (Thermo Scientific, Rockford, IL). Reversed phase liquid chromatography was performed using an EZ-Spray C18 column (Thermo, ES800, PepMap, 3 μm bead size, 75 μm x 15 cm). The LC was operated at 600 nL/min flow rate for loading and 300 nL/min for peptide separation over a linear gradient for 60 min from 2% to 30% acetonitrile in 0.1% formic acid. Tandem mass spectrometry experiments using the LTQ OrbitrapXL and the LTQ Orbitrap Velos instruments both used survey scans recorded over a 350-1500 m/z range. The LTQ Orbitrap XL was operated in collision induced dissociation (CID) mode, and MS/MS CID scans were performed on the six most intense precursor ions, with the following parameters: a minimum of 1,000 counts precursor, isolation width 2.0 amu, and 35% normalized collision energy. The LTQ Orbitrap Velos was operated in higher energy collision dissociation (HCD) mode, and MS/MS HCD scans were performed on the six most intense precursor ions with the following parameters: 3,000 count threshold, isolation width 2.0 amu, and 30% normalized collision energy. Internal recalibration to a polydimethylcyclosiloxane (PCM) ion with m/z = 445.120025 was used for both MS and MS/MS scans on both instruments (144).

Mass spectrometry centroid peak lists were generated using in-house software called PAVA, and data were searched using Protein Prospector software v. 5.10.17 (145). For protein identification, searches

were performed against the curated *T. brucei* 972 genome in the TriTrypDB database v 8.0 (http://tritrypdb.org/tritrypdb/, June, 2014) containing 30,295 entries. This database was concatenated with a fully randomized set of 30,295 entries for estimation of false discovery rate (146). Data were also searched against the SwissProt database (downloaded January 11, 2012) for identification of common contaminant proteins. Peptide sequences were matched as tryptic peptides with up to 2 missed cleavages, and carbamidomethylated cysteines as a fixed modification. Variable modifications included: oxidation of methionine, N-terminal pyroglutamate from glutamine, start methionine processing, protein N-terminal acetylation, and Ser/Thr phosphorylation. Mass accuracy tolerance was set to 20 ppm for parent and 0.6 Da fragment for CID experiments, and 20 ppm for parent and 30 ppm for fragment mass error for HCD experiments.

For reporting of protein identifications from this database search, score thresholds were selected that resulted in a protein false discovery rate of less than 1%. The specific Protein Prospector parameters were: minimum protein score of 22, minimum peptide score of 15, and maximum expectation values of 0.02 for protein and 0.05 for peptide matches. Site Localization In Peptide (SLIP) scoring (147) was used to score the site assignment for phosphorylation sites, with manual validation of all reported phosphorylation spectra.

4.3. Results

4.3.1 TbERK8 Phylogenetic Analysis

The amino acid sequence Tb927.10.5140 was analyzed with the BLAST on Orthologous groups tool (148) to retrieve a non-biased group of orthologous sequences. Redundant sequences were filtered out of the group while TbMAPK1 (Tb927.10.7780) and TbMAPK3 (Tb927.8.3550) were added in to optimize the ClustalW alignment among the orthologous groups. Table 4.1 lists the genes identified from the search that were used to build a phylogenetic tree (Fig. 4.1 A). Human sarcoma (SRC) tyrosine kinase was used as the out-group because tyrosine kinases are not encoded in the *T. brucei* genome (40,149). Based on the phylogenetic tree, we found that Tb927.10.5140 was located in the clade with HsERK8, whereas TbMAPK1 and TbMAPK3 were more distantly related (Fig. 1A). ClustalW alignment of Tb927.10.5140 with the open reading frame of HsERK8 demonstrated that these two kinases were about 36% identical at the amino acid level. The kinase domains of these two proteins from divergent species are about 51% identical at the amino acid level based on ClustalW alignment. Tb927.10.5140 also has a long C-terminus that extends 100 amino acids beyond the kinase domain that is not conserved, which is a defining characteristic of the ERK8 family members (Fig. 4.1 B) (50). We adopted the nomenclature of TbERK8 for Tb927.10.5140 because its coding region encodes a protein that was most closely related to HsERK8 (47,50).

4.3.2 TbERK8 Auto-phosphorylates with dual-specific kinase activity, independently of its C-terminal extension

A long, non-conserved C-terminal extension is a unique characteristic of ERK8 homologs. In HsERK8, the long C-terminal extension is required for its auto-phosphorylation and full activation (50,51,61,150). It also contains a series of P-X-X-X-P repeats that form a chromatin-binding region. The C-terminal extension of TbERK8 is 100 amino acid residues shorter than that of HsERK8 and doesn't contain the P-X-X-X-P repeats.

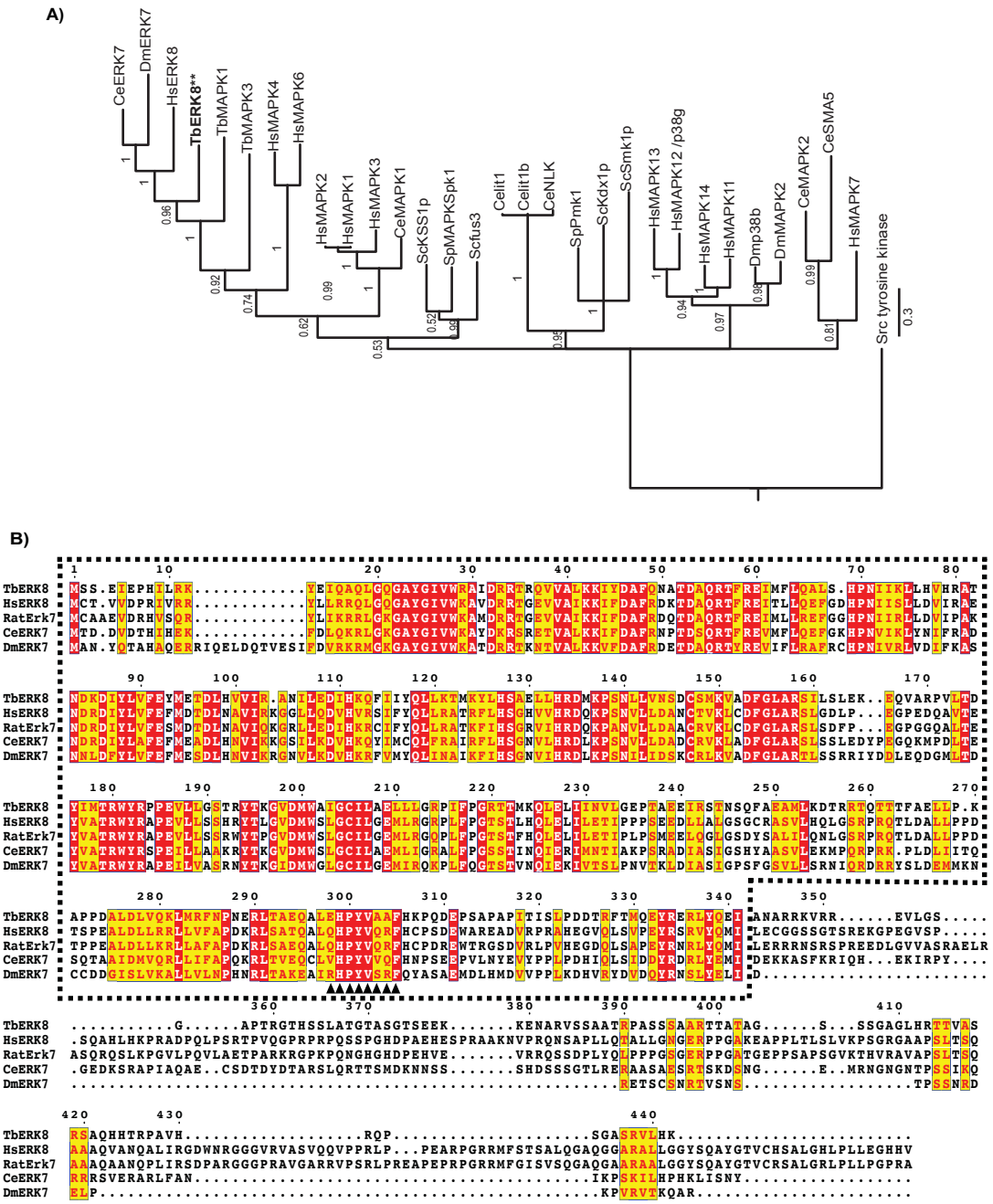

Figure 4.1 Phylogenetic tree and amino acid sequence alignment of ERK8-related kinases. (A) Phylogenetic relationship of the sequences and the credibility weight of the groupings were inferred using MrBayes after running 100,000 generations. Relationships with confidence values greater than 0.5 are shown at the branch points of the phylogenetic tree. The tree shown is derived from alignment with the ends trimmed to remove regions that were represented by only a few sequences. A separate analysis was done using the entire alignment and the tree topology was nearly identical to the tree shown here. (B) ClustalW alignment of ERK8 homologs. Polypeptide sequences obtained from TbERK8 BLAST on Orthologous groups were aligned using ClustalW with gap opening penalty of 5 and gap extension penalty of 0.05. The kinase domain is shown inside the box and the triangles (▲) highlight the PIP-box sequences. Tb: *Trypanosoma brucei,* Hs: *Homo sapiens,* Ce: *Caenorhabditis elegans,* Dm: *Drosophila melanogaster,* Sp: *schizosaccharomyces pombe,* Sc: *saccharomyces cerevisiae,* Rat: *Rattus rattus.*

Table 4.1 ERK8 orthologs. The Tb927.10.5140 ORF was searched using the BLASTO on Orthologous group tool to retrieve the unbiased group of related eukaryotic MAPKs listed below.

Kinase	Accession Number
Tb ERK8*	Tb927.10.5140
Ce ERK7	Q11179
Dm ERK7	AAF46481
Hs ERK8/MAPK15	NP_620590
Sp MAPK Spk1	NP_594009
Hs MAPK3	NP_002737
Sc MAPK1/3 fus3	NP_009537
Hs MAPK7	NP_002740
Ce MAPK-1	CE24971
Hs MAPK2	Hs20986529
Hs MAPK1	NP_620407
Hs MAPK13	NP_002745
Dm p38b	NP_477361
Dm MAPK2	NP_477163
Sp Pmk1	NP_595289
Hs MAPK14	AAP36304
Hs MAPK11	NP_002742
Hs MAPK12/p38gamma	AAB40118
Sc KSS1p	NP_011554
Sc Kdx1p	NP_012761
Hs MAPK4	CAA42411
Hs MAPK6	NP_002739
Sc Smk1p	NP_015379
Ce Protein SMA-5, isoform a	NP_741909
Ce NLK Isoform c	NP_001022807
Ce lit-1	NP_001022806
Ce lit-1_b	NP_001022805
Tb MAPK3	Tb927.8.3550
Tb MAPK1	Tb927.10.7780
SRC_tyrosine_kinase	NP_033297

Tb: *Trypanosoma brucei,* Ce: *Caenorhabditis elegans,* Dm: *Drosophila melanogaster,* Sp: *schizosaccharomyces pombe,* Sc: *saccharomyces cerevisiae,* Hs: *Homo sapiens.*

We tested full-length TbERK8 purified from baculovirus ($TbERK8_{BV}$) for its ability to autophosphorylate by incubating it in kinase buffer that contained ^{32}P-γ-ATP. Its ability to incorporate ^{32}P indicates that TbERK8 is able to autophosphorylate despite its shorter C-terminal extension and its lack of P-X-X-X-P repeats (Fig. 4.2 A). We also designed a C-terminal truncated form of TbERK8 that expressed only the kinase domain (GST-$TbERK8_{KD}$, residues 1-343) and re-tested its ability to autophosphorylate. The $TbERK8_{KD}$ also incorporated ^{32}P when incubated in kinase buffer with ^{32}P-γ-ATP substrate, indicating that it was able to autophosphorylate (Fig. 4.2 B). Typical ERKs are fully activated by upstream dual-specific MAPK-kinases that phosphorylate a conserved TxY motif in the activation loop Typical ERKs are fully activated by upstream dual-specific MAPK-kinases that phosphorylate a conserved TxY motif in the activation loop. HsERK8 is atypical because its full activation is catalyzed by autophosphorylation instead of an upstream MAPK; thus, it has dual-specific activity (50,51,61,150). We demonstrated that TbERK8 could autophosphorylate tyrosine residues by using the PY20 antibody (Fig. 4.2 C) and further investigated this using mass spectrometry. Peptide sequencing by LC-MS/MS of trypsin-digested recombinant $TbERK8_{BV}$ revealed phosphorylation at both the Thr174 and Tyr176 residues, which correspond to its activation loop motif (Figure 4.2 D). Based on these observations, we conclude that TbERK8 is able to autophosphorylate independently of its C-terminal extension and, like HsERK8, has dual-specific activity that allows it to phosphorylate the tyrosine residue within its activation loop.

4.3.2 Examination of the putative TbERK8 PIP-box

One of the proposed functions of human ERK8 is to interact with PCNA and form a stabile complex that prevents it from being degraded by the proteasome (57). Like many other proteins, HsERK8 interacts with human PCNA through a conserved PIP-box motif (57) (Fig. 4.1 B arrows, and 4.3 A). The corresponding sequence in TbERK8 has a sequence that is 75% identical to the functional PIP-box of human ERK8 but its ability to interact with TbPCNA is not known. We generated the GST-TbERK8PIP-box fusion protein (GSTtbE8-PIP) to test the ability of this putative PIP-box to interact with TbPCNA (Fig. 4.3 B). Figure 4.3 C shows a representative immunoblot of lysates from tetracycline-induced *T.*

brucei expressing $TbPCNA_{HA}$. Pull-down assays were done by incubating *T. brucei* lysates from tetracycline-induced parasites with GST control (GST-Ctrl) or with GSTtbE8-PIP beads. The GSTtbE8-PIP beads pulled down about 5 times more TbPCNA than the GST-Ctrl beads (Figs. 4.3 D and 4.3 E). To assess if the TbERK8 PIP-box was fully accessible when fused to the end of GST, we did orthogonal pull down experiments using two canonical PIP-box motifs from unrelated proteins: (1) *T. brucei* aurora kinase 1 (TbAUK1) and (2) paraflagellar complex (TbPFC19) (Tb927.11.8220 and Tb927.10.10140, respectively). The PIP-box of either TbAUK1 or TbPFC19 was similarly fused with GST and immobilized on GST beads. We found that these PIP-box motifs were about 10 fold and 6 fold more efficient at pulling down $TbPCNA_{6H}$ than the TbERK8 PIP-box motif, respectively (Fig. 4.3 F and 4.3 G). This indicates that the PIP-box motifs were exposed in GST-fusion proteins. We also immobilized full-length $TbERK8_{HA}$ to immuno-affinity beads for use in pull down assays to express its putative PIP-box in the native conformation. The full-length TbERK8 did not pull down $TbPCNA_{6H}$ (data not shown). The interaction between the TbERK8 PIP-box and TbPCNA contrasted with the stable complex formation between HsERK8 PIP-box and HsPCNA reported by Groehler *et al* (57). We conclude that the putative PIP-box of TbERK8 is very poor at forming a stable complex with TbPCNA in comparison with functional canonical PIP-box motifs from other *T. brucei* proteins.

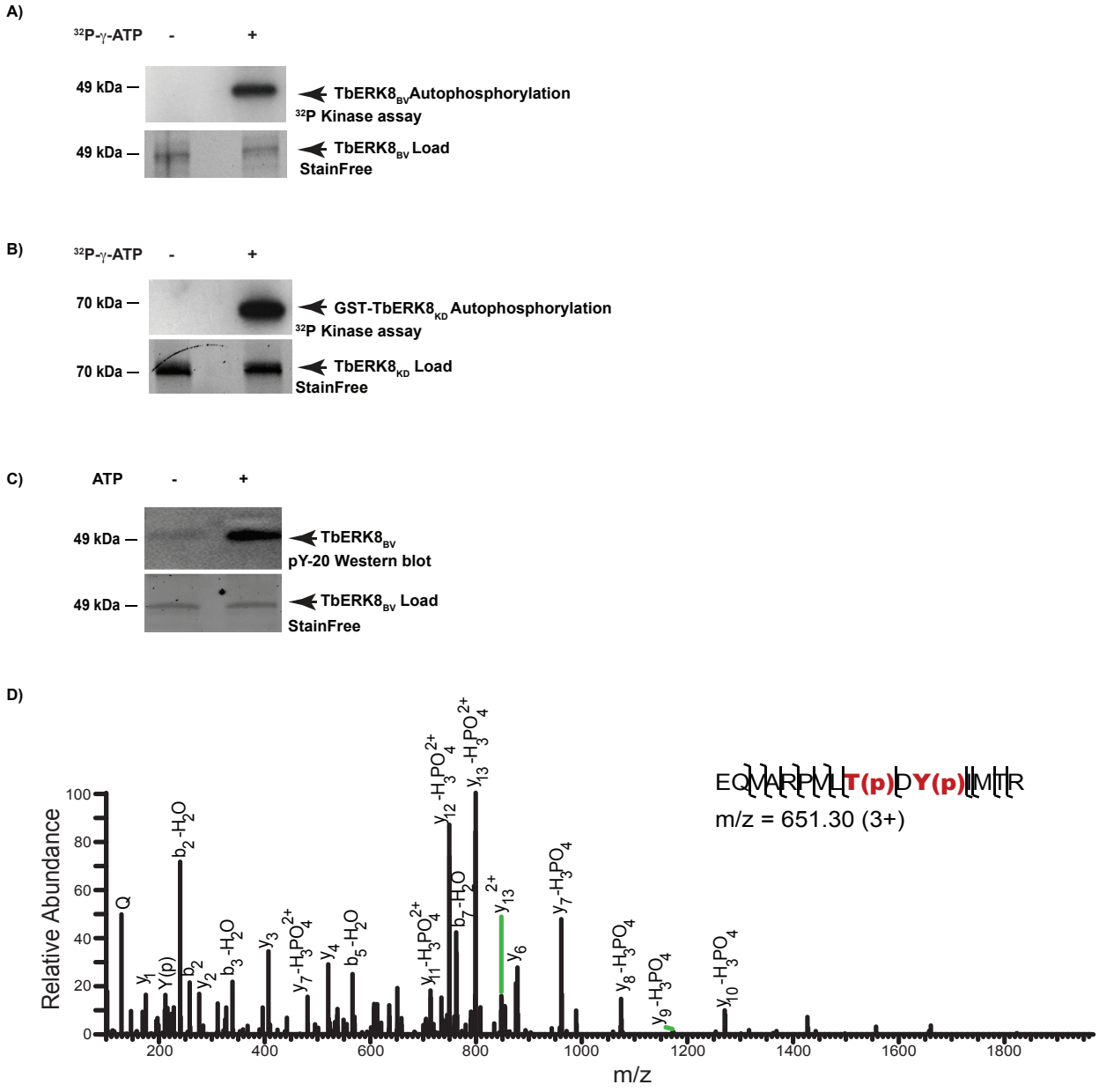

Figure 4.2 Autophosphorylation of TbERK8. Top panels: (A) Autoradiograph of purified recombinant $TbERK8_{BV}$ incubated in kinase reaction buffer without (-) or with (+) 10 µCi ^{32}P-γ-ATP; (B) Autoradiograph showing the autophosphorylation of the GST-TbERK8 kinase domain (GST-$TbERK8_{KD}$) that lacks the C-terminus. GST-$TbERK8_{KD}$ was tested for autophosphorylation in a kinase reaction without (-) or with (+) 10 µCi ^{32}P-γ-ATP; (C) Immunoblot using PY20 antibodies to detect phosphotyrosine residues associated with autophosphorylation of $TbERK8_{BV}$. Bottom panels are StainFree® gels showing the loading controls for TbERK8 samples. (D). LC-MS/MS mass spectrum of $_{166}$EQVARPVLT(phospho)DY(phospho)IMTR$_{180}$ peptide from TbERK8 containing the phosphorylated Thr174 and Tyr176 residues, with m/z = 651.30 (3+), 0.52 ppm error.

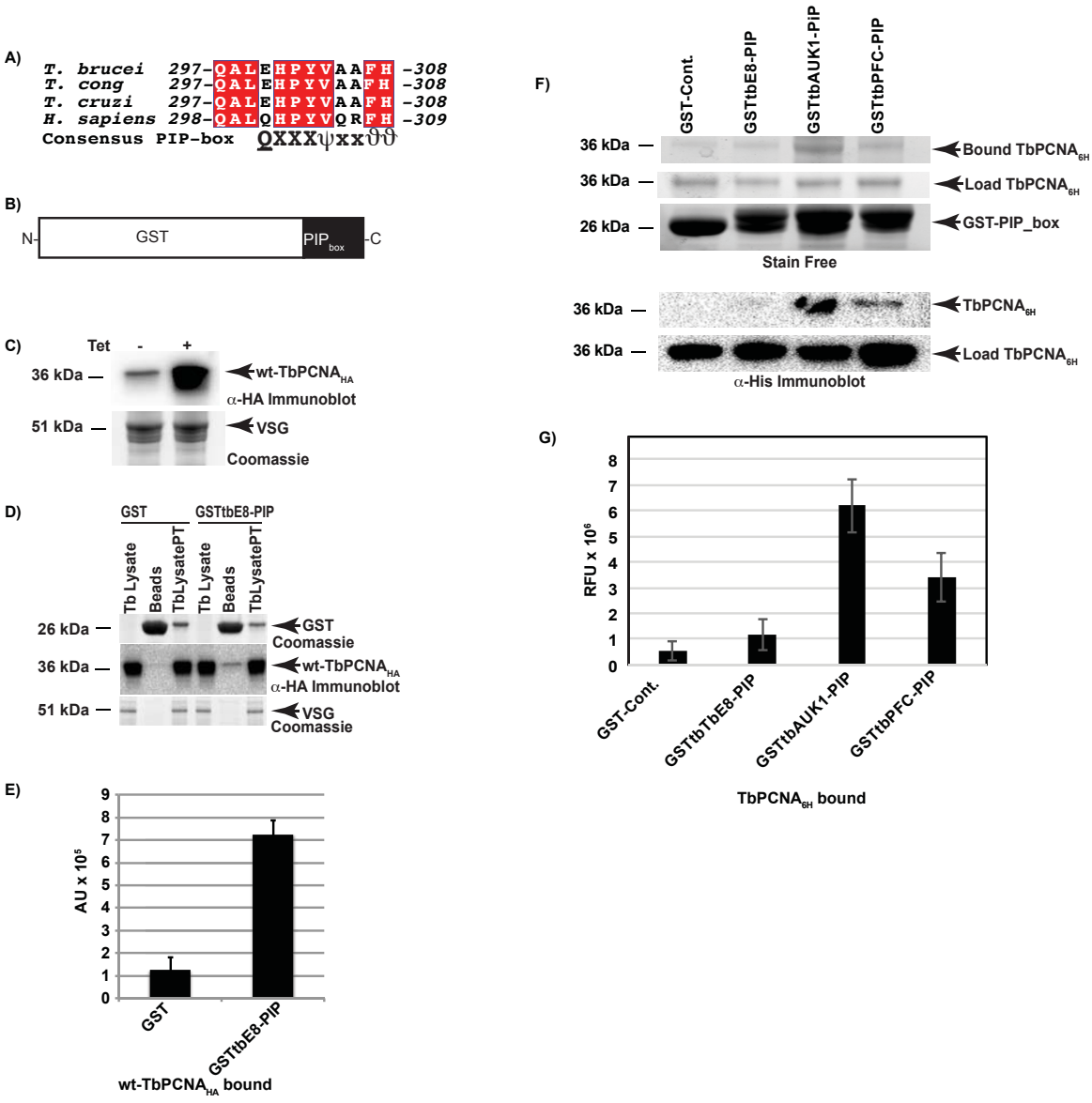

Figure 4.3 TbERK8-PIP-box inefficiently pulls down TbPCNA. (A) Alignment of putative PIP-box motifs from ERK8 homologs of *T. brucei, T. congolense* (*T. cong*), *T. cruzi,* and *H. sapiens*. The PIP-box motifs are 100% identical in related trypanosome species and are 75% identical to the PIP-box of HsERK8. (B) Schematic presentation of GST-*T. brucei* PIP-box fusion proteins. The PIP_{box} in the schematic represents the putative TbERK8 PIP-box or the canonical PIP-box from TbAUK1 or TbPFC19. Note, construct is not to scale. (C) Immunoblot analysis of wt-$TbPCNA_{HA}$ in control (Tet -) or tetracycline-induced (Tet +) bloodstream form *T. brucei* with antisera to hemagglutinin (α-HA). Bottom panel shows Coomassie-stained gel image of variant surface antigen (VSG) loading control. (D) Examination of wt-$TbPCNA_{HA}$ pulled down by GST-control (GST-Ctrl) or GST-TbERK8-PIP-box (GSTtbE8PIP-box) glutathione agarose beads. Top panel shows the Coomassie-stained gel image of GST fusion proteins, middle panel shows the immunoblot analysis using α-HA antibodies to detect wt-$TbPCNA_{HA}$, and lower panel shows Coomassie-stained gel image of VSG loading control. (E) Quantitation of wt-$TbPCNA_{HA}$ pull down. Bar graph showing results from densitometry trace comparing the amount of TbPCNA pulled down by GST-Ctrl beads to that pulled down by GST-tbERK8-PIP beads. Values are mean arbitrary units (AU) with standard deviation for three independent experiments. (F) Pull down of recombinant $TbPCNA_{6H}$ by GST-bound TbERK8 PIP-box (GSTtbE8-PIP) and GST-bound

canonical PIP-boxes from TbAUK1 (GSTtbAUK1-PIP) and TbPFC19 (GSTtbPFC-PIP). The top two StainFree® gel images show $TbPCNA_{6H}$ bound to the beads in comparison to the loading controls. The third StainFree® gel shows all the GST-PIP-boxes used. The bottom two panels show the immunoblot analysis of $TbPCNA_{6H}$ bound to the beads in comparison to the loading controls. (G) Relative quantity of $TbPCNA_{6H}$ pulled down by various GST-PIP-boxes. (Relative Fluorescent Units, RFU), (Arbitrary Units, AU).

Table 4.2 Summary of phosphorylated residues identified on TbPCNA immunoprecipitated from *T. brucei*.

	pThr202	pSer211	pSer216
O/E-TbPCNAHA	+	-	+
EL-TbPCNAHA	+	-	+
pHAR-TbPCNAHA	-	-	-

Overexpressed (O/E), Endogenous Levels (EL), after TbERK8 depletion (pHAR)

4.3.4 TbERK8 Phosphorylates TbPCNA

To determine if TbERK8 was able to phosphorylate TbPCNA, we mixed recombinant $TbERK8_{BV}$ and $TbPCNA_{6H}$ in kinase buffer containing ^{32}P-γ-ATP. Autoradiography of the kinase reactions revealed that both $TbERK8_{BV}$ and the 36-kDa $TbPCNA_{6H}$ were phosphorylated (Fig. 4.3A). We repeated the kinase reactions in buffer containing cold ATP and resolved the phosphorylated TbPCNA by SDS-PAGE to identify phosphorylated residues by LC-MS/MS analysis. More than 96% of the TbPCNA sequence was covered by the peptides detected by LC-MS/MS, including two peptides that were phosphorylated at residues Ser_{211} (Fig. 4.4 B) and S_{216} (Fig. 4.4 C). We further examined $TbERK8_{BV}$ by steady-state kinetics analysis and calculated the K_M for TbPCNA to be 0.22 ± 0.05 μM (Fig. 4.4D). The calculated k_{cat}/K_M (2.6×10^5 Sec^{-1} M^{-1}) indicates that phosphorylation of TbPCNA was efficiently catalyzed *in vitro* by recombinant TbERK8.

4.3.5 *In vivo* Expressed TbERK8 Preferentially Phosphorylates TbPCNA Over MBP *in vitro*

Lysine 42 (K42) of TbERK8 is a conserved residue in other kinases. It is essential for positioning the γ-phosphate of ATP in the active site making it essential for phosphotransfer to kinase substrates (151,152). We mutated this predicted catalytic lysine to an alanine in TbERK8 and expressed the K42A-$TbERK8_{HA}$ mutant in bloodstream form *T. brucei.* Anti-HA antibodies confirmed the expression of both wt-$TbERK8_{HA}$ and K42A-$TbERK8_{HA}$ in tetracycline-induced parasites. Both HA-tagged proteins migrated at 52 kDa, as expected for TbERK8 (49-kDa) plus the 3-HA tag (3 kDa) (Fig. 4.5 A). To test for the autophosphorylation activity of the *in vivo* expressed proteins, either wt-$TbERK8_{HA}$ or K42A-$TbERK8_{HA}$ was immunoprecipitated from *T. brucei* with α-HA affinity beads and incubated with kinase buffer containing ^{32}P-γ-ATP. Autoradiography detected a labeled polypeptide of 52 kDa for wt-$TbERK8_{HA}$ and a faintly labeled polypeptide of the same size for the K42A-$TbERK8_{HA}$ mutant (Fig. 4.5 B). The bar graph in Figure 4.5 C shows that the level of autophosphorylation in the

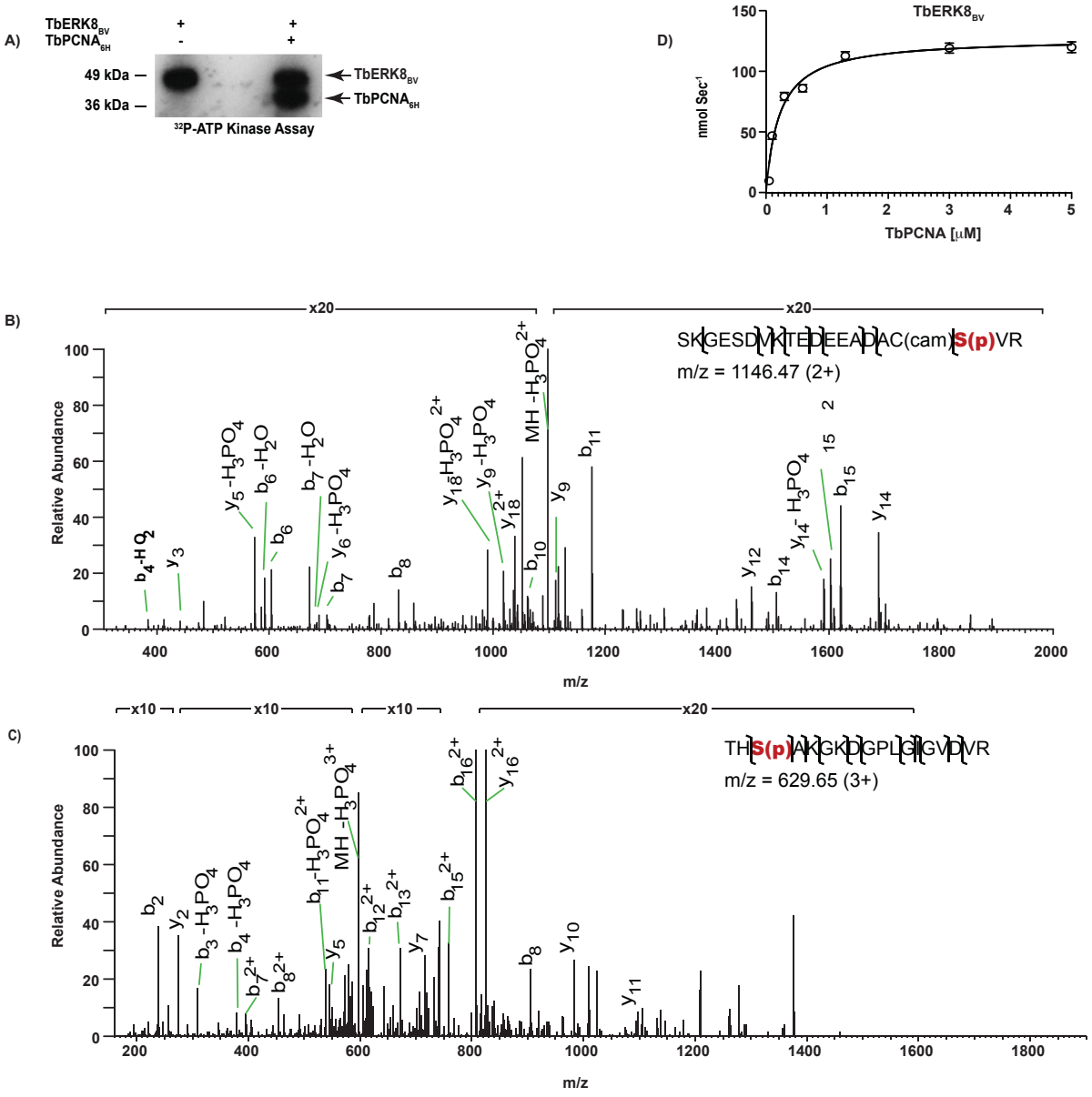

Figure 4.4 Recombinant TbERK8$_{BV}$ phosphorylates TbPCNA$_{6H}$ *in vitro*. (A) Autoradiograph showing the phosphorylation of TbPCNA$_{6H}$ by TbERK8$_{BV}$. (B) LC-MS/MS mass spectrum of $_{194}$SKGESDVKTEDEEADACS(phospho)VR$_{213}$ peptide from TbPCNA containing a phosphorylated Ser$_{211}$ residue, with m/z = 1146.47 (2+), 5.1 ppm error. (C) LC-MS/MS mass spectrum of $_{214}$THS(phospho)AKGKDGPLGIGVDVR$_{231}$ peptide from TbPCNA containing a phosphorylated Ser$_{216}$ residue, with m/z = 629.65 (2+), 1.9 ppm error. (D) Steady-state kinetic curve of TbERK8$_{BV}$ using varying concentrations of purified recombinant TbPCNA$_{6H}$. The plot represents the mean data with standard deviation from 3 experiments.

defective K42A-TbERK8$_{HA}$ mutant was about 8 fold less than that of the wild type enzyme when corrected for loading and background. This observation is consistent with the predicted critical role of K42 in the kinase activity of TbERK8. We conclude that the ^{32}P-incorporated into TbERK8 resulted from its autophosphorylation rather than from non-specific kinase activity that might have been captured on the affinity beads.

To test the *in vitro* substrate specificity of recombinant TbERK8, we compared its activity using the generic kinase substrate myelin basic protein (MBP) and recombinant TbPCNA$_{6H}$ purified from *E. coli* as substrates. Purified recombinant TbERK8$_{BV}$ from insect cells phosphorylated both MBP and TbPCNA$_{6H}$ efficiently *in vitro* (Fig. 4.5 D). By comparison, wt-TbERK8$_{HA}$ immunoprecipitated from *T. brucei* showed more efficient *in vitro* phosphorylation activity toward TbPCNA$_{6H}$ than MBP (Fig. 4.5 E). Mock control beads incubated in lysates from non-transgenic *T. brucei* 221 showed only background labeling for both MBP and TbPCNA. When immunoprecipitated K42A-TbERK8$_{HA}$ was used in kinase reactions, only background levels of phosphorylation similar to those of the mock control were observed. These results confirmed that the labeling of TbPCNA$_{6H}$ was directly linked to TbERK8 activity captured on the immunoaffinity beads, ruling out non-specific kinase activity that might have co-precipitated on the beads. We conclude that TbERK8 expressed in *T. brucei* preferred recombinant TbPCNA as a substrate over MBP. Mass spectrometry analysis of TbPCNA$_{6H}$ phosphorylated by immunoprecipated wt-TbERK8$_{HA}$ detected phosphorylation at residues Thr$_{202}$ and Ser$_{211}$ (Fig. 4.5 H). These phosphorylated residues were found within the unique backside loop of TbPCNA.

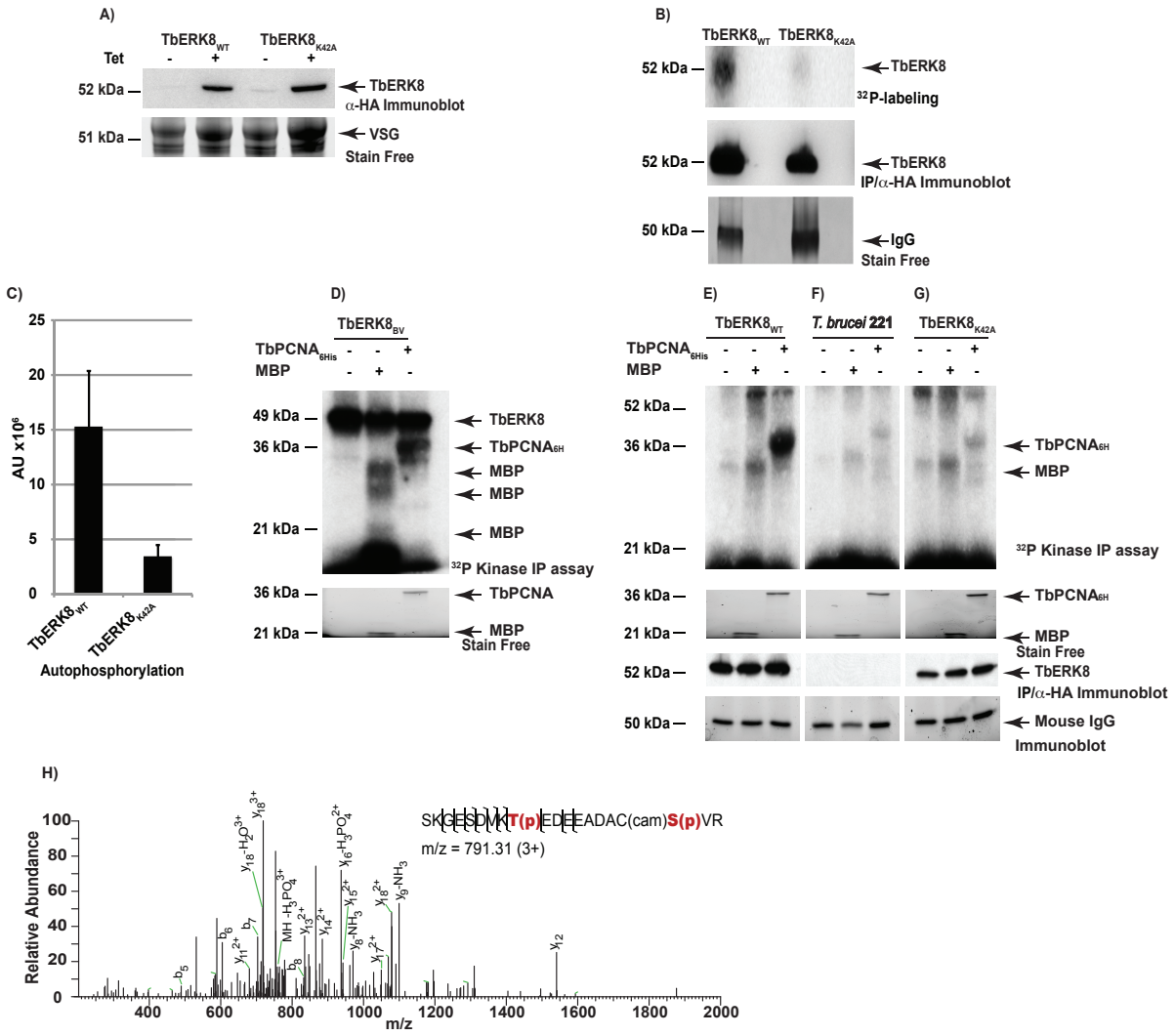

Figure 4.5 *In vitro* substrate specificity of recombinant TbERK8. (A) Immunoblot verifying the expression of wt-TbERK8$_{HA}$ and K42A-TbERK8$_{HA}$ in the parasite after tetracycline induction (+). Arrow points to the 52-kDa HA-tagged TbERK8 band recognized by α-HA antibodies. *T. brucei* variant surface antigen (VSG arrow) was used for the loading control. (B) Autophosphorylation of wt-TbERK8$_{HA}$ or K42A-TbERK8$_{HA}$ immunoprecipitated from parasites as detected by autoradiography (top panel). wt-TbERK8$_{HA}$ or K42A-TbERK8$_{HA}$ bound to the immuno-affinity beads was detected using immunoblot (middle panel). StainFree® loading control (lower panel). (C) Quantitation of autophosphorylation using Phosphorimager analysis to measure the arbitrary units (AU). Bar graphs represent the mean percentage with standard deviation for an experiment done in triplicate. (D) Recombinant TbERK8$_{BV}$ purified from insect Sf9 cells efficiently phosphorylates both MBP and TbPCNA$_{6H}$. Top panel shows the autoradiograph of the kinase reactions. First lane is a kinase reaction with no substrate added, the second lane is with 100 μ mol MBP, and the third lane is with 100 μmol of TbPCNA$_{6H}$. The bottom panel is a StainFree® gel showing the loading of MBP and TbPCNA$_{6H}$. (E) Recombinant wt-TbERK8$_{HA}$ expressed in the parasite phosphorylates TbPCNA$_{6H}$ efficiently. Top panel shows the autoradiograph of kinase immunoprecipitation assays done with immuno-affinity beads pre-adsorbed with (wt-TbERK8$_{HA}$), with (*T. brucei 221* lysate) and with (K42A-TbERK8$_{HA}$). Each of the three sets of beads were tested with either no substrate (first lane of each experiment in the top row), 100 μmol of MBP (second lane of each top panel), or 100 μmol of TbPCNA (third lane of each panel). The second panel shows the StainFree® loading controls for MPB and TbPCNA$_{6H}$. The third panel shows the α-HA immunoblot detecting the

HA-tagged TbERK8 bound to the immuno-affinity beads (absent in beads pre-incubated with *T. brucei 221* lysates). The bottom panel is a α-IgG immuno-blot as a loading control for the affinity beads. (F) LC-MS/MS mass spectrum of $_{194}$SKGESDVKT(phospho)EEDEEADAC(cam)S(phosphor)VR$_{213}$ peptide from TbPCNA containing phosphorylated Thr$_{202}$ and Ser$_{211}$ residues, with m/z = 791.31.65 (3+), 1.9 ppm error.

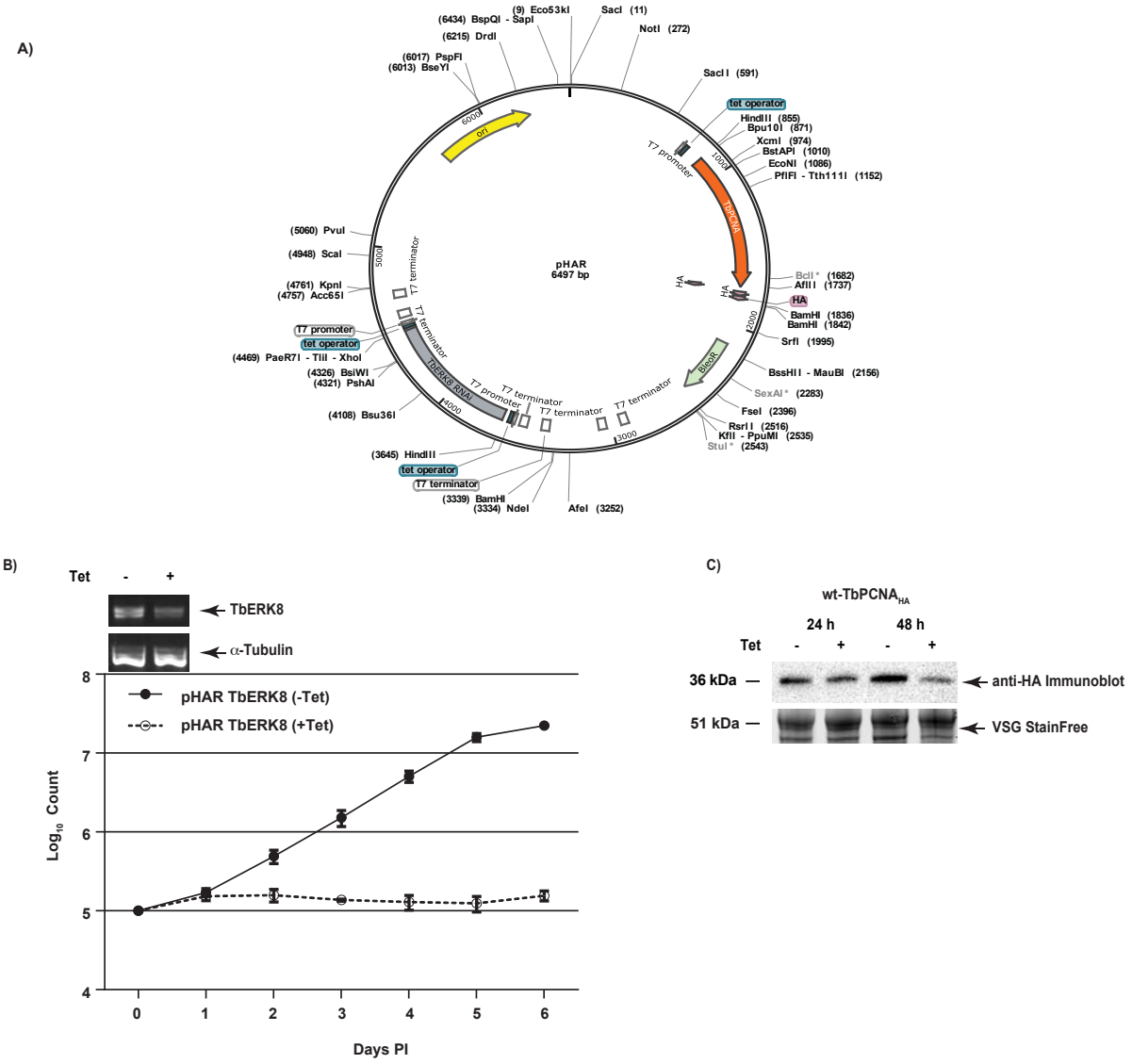

Figure 4.6 TbPCNA phosphorylation *in vivo*. (A) Map of the plasmid pHAR. The plasmid has an HA-tag for endogenous expression of TbPCNA and an RNAi construct for TbERK8 silencing. (B) Decreased proliferation in pHAR stable parasites with tetracycline induction to reduce TbERK8 mRNA levels. Sybersafe gels at the top show the reduction of TbERK8 mRNA levels as detected by RT-PCR after 48 h of induction (upper panel). α-tubulin was used as a control (bottom panel). The bottom graph shows the growth curve for pHAR stable parasites with (+Tet) (◯) or without (-Tet) (●) tetracycline induction for TbERK8 silencing. The growth curve represents parasite proliferation monitored during 6 days in three replicates. (C) Reduction in TbPCNA levels in pHAR stable parasites after tetracycline induction to reduce TbERK8 mRNA levels. Western blot shows the levels of expression of TbPCNA after 48 h of tetracycline induction (upper). The StainFree® gel shows VSG as a loading control (bottom).

4.3.6 *In vivo* phosphorylation of TbPCNA by TbERK8

Previous studies in normal human breast cell lines demonstrated that depleting HsERK8 correlated to a reduction in intracellular HsPCNA levels (57). We, therefore, examined the effect of TbERK8 depletion on TbPCNA levels in *T. brucei*. A single plasmid, pHAR (Fig. 4.6 A), was generated and transfected into *T. brucei* to simultaneously allow expression of HA-tagged TbPCNA under the control of the endogenous TbPCNA allele and tetracycline-inducible RNAi expression against TbERK8 mRNA. Tetracycline induction of *T. brucei* stably expressing pHAR resulted in a decrease in TbERK8 mRNA levels as well as decreased proliferation (Fig. 4.6 B). This result was consistent with our previous study of depleting TbERK8 in bloodstream form *T. brucei* (47). We also observed a marked decrease in the abundance of endogenously tagged TbPCNA after 48 h of TbERK8 depletion (Fig. 4.6 C). This result is similar to that reported in normal human breast cell lines upon siRNA depletion of HsERK8 (57). We conclude that TbERK8 is important for the stability of TbPCNA.

To examine the *in vivo* phosphorylation status of TbPCNA, we immunoprecipitated TbPCNA from stably transfected *T. brucei* strains that express wt-TbPCNA$_{HA}$ at endogenous or overexpressed levels and subjected it to LC-MS/MS analysis. Identical phosphorylation patterns at residues Thr$_{202}$ and Ser$_{216}$ were detected on the immunoprecipitated TbPCNA, whether it was expressed at endogenous or overexpressed levels (summarized in Table 4.2). In contrast, no phosphorylation of TbPCNA was detected after TbERK8 was depleted in the pHAR parasites (Table 4.2). We conclude that TbERK8 phosphorylates TbPCNA *in vivo*.

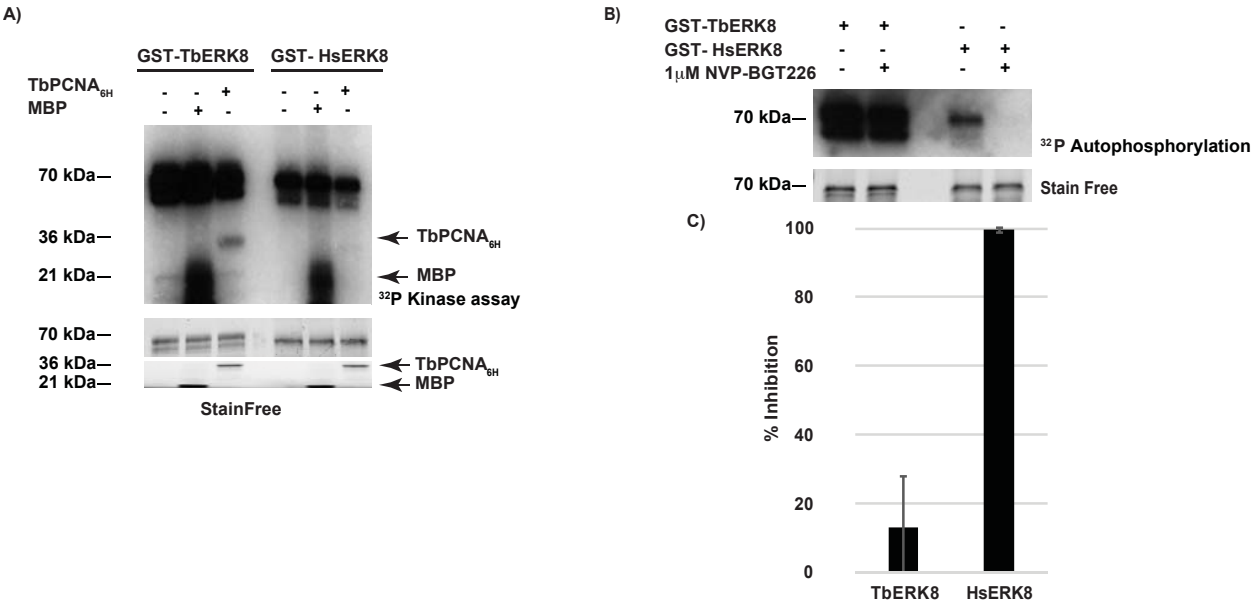

Figure 4.7 HsERK8 and TbERK8 have different kinase activity profiles. (A) The phosphorylation of PCNA by ERK8 is specific to the parasites. Top panel shows the autoradiograph of kinase reactions conducted with GST-bound TbERK8 (GST-TbERK8) and HsERK8 (GST-HsERK8). The first lane in each set of the kinase reactions contains no substrate, the second lane contains 100 μmol MBP, and the third lane contains 100 μmol TbPCNA. The middle panel shows StainFree® loading control of GST-TbERK8 and GST-HsERK8. The bottom panel shows StainFree® loading control for MBP and $TbPCNA_{6H}$. (B) Autophosphorylation of HsERK8, but not TbERK8, is inhibited by NVP-BGT226. Top panel is the autoradiograph showing the autophosphorylation of either TbERK8 or HsERK8 without or with 1 μM of NVP-BGT226. Bottom panel is the StainFree® gel showing the loading controls for TbERK8 and HsERK8. (C) Quantitation of the autophosphorylation inhibition. Bar graph shows the mean inhibition of autophosphorylation at 1 μM of NVP-BGT226 with standard error from duplicate experiments.

4.3.7 TbERK8 and HsERK8 have differential substrate and inhibitor preferences

TbERK8 and HsERK8 were tested for their ability to phosphorylate PCNA homologs from both species using a ^{32}P-kinase assay. This assay was done to probe the active site of each ERK8 homolog for selectivity to PCNA substrates. TbPCNA was the only substrate that was ^{32}P-labeled in the kinase assays, but this only occurred when TbERK8 was used. Figure 4.7 A shows the results of GST-TbERK8 and GST-HsERK8 kinase assays that were tested against either MBP or TbPCNA. This demonstrated that the active sites of these two kinases could discriminate between PCNA substrates from distantly related species. To further explore the specificity of these ERK8 active sites, we screened the Selleckchem library of 274 kinase inhibitors against *T. brucei* at 1 μM to identify 10 compounds with bioactivity to *T. brucei*. When these bioactive compounds were tested at 1 μM against both recombinant ERK8 homologs, the ATP-competitive inhibitor NVP-BGT226 was shown to selectively prevent recombinant HsERK8 from autophosphorylating in the ^{32}P kinase assay (Fig. 4.7 B At this concentration, TbERK8 activity was not inhibited but that of HsERK8 was inhibited by more than 99% (Fig. 4.7 C). This differential inhibition by NVP-BGT226 clearly demonstrates that small molecule probes can be used to distinguish the active site of TbERK8 and HsERK8.

4.4 Discussion

We conclude from this study that TbERK8 belongs to the MAPK15/ERK8 family based on its sequence similarity and conserved biochemical activity. Like HsERK8, the founding member of the ERK8 family, TbERK8 has dual-specific kinase specificity and is able to autophosphorylate the TxY motif in its activation loop autophosphorylation (50,84). However, the biological properties of TbERK8 appear to have diverged from HsERK8. For example but knocking down TbERK8 mRNA in *T. brucei* is lethal to the parasite (47), whereas depletion of HsERK8 mRNA in human cells does not result in a lethal phenotype (54,55,57,153). We hypothesize that TbERK8 possesses distinct biochemical properties that distinguishes it from HsERK8 and allows it to function as a key switch in the biology of *T. brucei*. Here, we reveal that TbERK8 uniquely phosphorylates TbPCNA in *T. brucei*. Such an enzyme/substrate relationship is not observed in the human homologs.

TbERK8 contains a putative PIP-box, which is inefficient in forming a stable complex with TbPCNA. In contrast, the non-canonical PIP-box motif of HsERK8 is sufficient to pull down HsPCNA from cellular extracts region (57). The stable complex formation between HsERK8 and HsPCNA protects HsPCNA from proteasome degradation. We speculate that the weak interaction between TbERK8 and TbPCNA might be fundamental to its ability to maintain the biochemistry of their enzyme/substrate relationship.

TbERK8 demonstrated an unusual biochemistry in that it phosphorylated TbPCNA at serine and threonine residues within an extended backside loop region (Fig. 4.8 A). This study advances our knowledge of TbERK8 biochemistry by demonstrating that it phosphorylates TbPCNA *in vitro* and in the parasite. Furthermore, *T. brucei* now provides the first example in which a PCNA homolog is phosphorylated on serine or threonine residues and by an ERK family member. In general, ERKs are proline-directed serine/threonine ((S/T)P) kinases and such activity has been demonstrated in HsERK8 (50,84). However, the presence of a Pro at the +1 position is not an absolute substrate requirement for ERKs and other MAPKs (154,155). None of the phosphorylated residues in TbPCNA had a proline at the

+1 position. We have identified only one potential site with a ((S/T)P) motif within TbPCNA ($_{263}$AEKSP$_{267}$), but the phosphorylation of Ser266 is not detected by our mass spectrometry analysis *in vitro* or *in vivo*.

The ability to phosphorylate residues in the unique TbPCNA backside loop was an exclusive activity of TbERK8 that did not exist in HsERK8. Demonstration of this unique TbERK8 activity reveals a potential preference that its active site has for loop structures. We observed differential phosphorylation of TbPCNA at serine and threonine residues within the unique backside loop by TbERK8 purified from Sf9 cells or parasites. TbERK8 purified from Sf9 cells or parasites also displayed differential preference in phosphorylating the generic kinase substrate MBP versus recombinant TbPCNA. Such differences could be caused by post-translational modification of the TbERK8 active site in the parasite, or a result of regulation by another factor that co-purifies with TbERK8 during immunoprecipitation. Further studies are necessary to distinguish between these hypotheses and additional structural studies can provide better information for how the unique loop of TbPCNA fits into the active site of TbERK8.

In contrast to TbERK8, HsERK8 does not phosphorylate HsPCNA as demonstrated in this study and in a previous study by Groehler *et al* (57). The only known cellular substrate of HsERK8 to date is the RNA binding protein HuR (58), but the exact residues that are phosphorylated on HuR by HsERK8 remain unknown. HuR is encoded by *ELAVL1* and binds the 3'UTR of the PDC4 tumour suppressor to protect it from miRNA 21 mediated gene silencing (156-158). Three *ELAVL* isoforms have been identified in *T. brucei* (159). It is not known which, if any, of these isoforms can be phosphorylated by TbERK8. HsPCNA phosphorylation has only been reported on tyrosine residues (67,160,161), but not on serine/threonine residues like TbPCNA. HsPCNA is phosphorylated by tyrosine kinases such as epidermal growth factor receptor (EGFR) (67,161) and the Recepteur d'Origine Nantais (RON)/c-ABL pathway (69,70). Receptor tyrosine kinase-mediated phosphorylation of HsPCNA occurs at Y211 and correlates with aggressive cancer either by increased DNA synthesis activity (67) or inhibition of mismatch repair (68). Such tyrosine kinase-mediated mechanisms of phosphorylation are not possible in

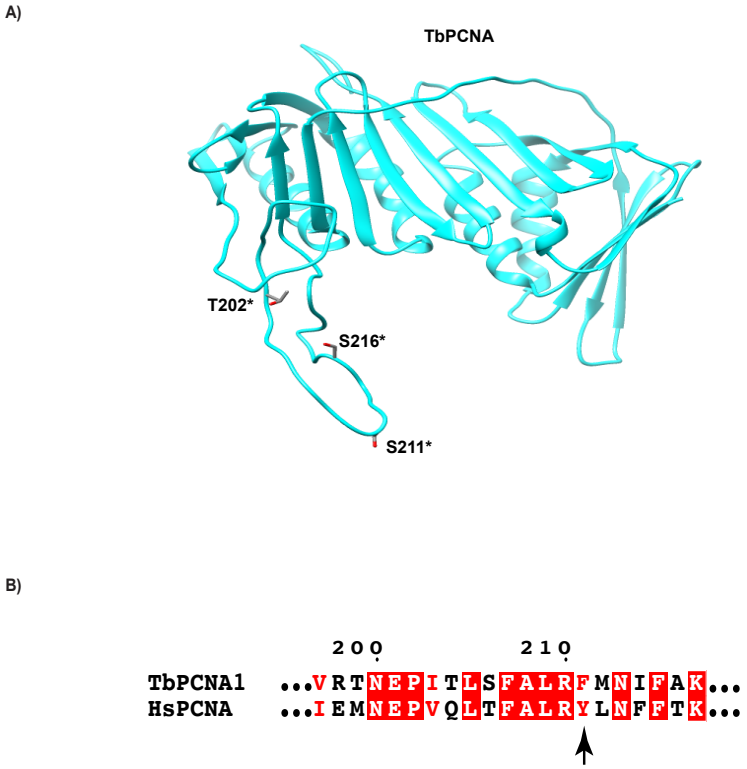

Figure 4.8 Models of phosphorylation for TbPCNA. (A) TbPCNA model showing the phosphorylated *T_{202}, *S_{211} and *S_{216} are situated in the unstructured loop whereas the other potential phosphorylation sites S/T residues are located within the domains of TbPCNA. (B) ClustalW alignment of TbPCNA and human PCNA with black arrow showing tyrosine 211, which is phosphorylated by receptor tyrosine kinases. Note that TbPCNA has a phenylalanine residue at the corresponding position. *denotes phospho-serine residues.

T. brucei because the parasite lacks any gene for tyrosine kinases (40,149) and because TbPCNA has a phenylalanine residue at the position that corresponds to Y211 in HsPCNA (Fig. 4.8 A).

Such biological and biochemical differences between the two ERK8 homologs implicate TbERK8 as an attractive target that can be therapeutically exploited. We initially tested SCYX5070 to probe the active site of TbERK8. This 2,4-diaminopyrimidine was a logical first choice because it kills *T. brucei* at submicromolar concentrations and TbERK8 (formerly Tb10.70.2070) was one of the many kinases that its immobilized version pulled down from parasite lysates (162). At 1 μM this compound neither inhibited TbERK8 nor HsERK8 homolog and had no selectivity for TbERK8 (data not shown).

After screening a library of kinase inhibitors for bioactivity against *T. brucei*, we have identified NVP-BGT226 that selectively inhibited HsERK8. NVP-BGT226 has been quite a useful tool for examining the role of PI3K and mTOR in several cancer cell lines (163-165). Like many other kinase inhibitors, NVP-BGT226 is a promiscuous molecule that also inhibits several other human protein kinases (166). The ability of this promiscuous inhibitor to inhibit HsERK8 but not TbERK8 demonstrated the basic principle that the active sites of HsERK8 and TbERK8 can be selectively inhibited. This creates opportunities to further our studies to discover and develop small molecules that can selectively inhibit TbERK8 to kill *T. brucei* or be useful for chemically mapping out its biological functions.

4.5 Acknowledgements

This work was supported in part by Start-up fund NIFA139696, VT Drug Discovery Center VTCDD ##119286. We would like to thank Zhijian Jake Tu[1] in the Virginia Tech Department of Biochemistry for technical expertise with phylogenetic analyses. Janet Webster and Ling Chen in the Fralin Life Science Institute for critical reading. MS analysis was performed in the Bio-Organic Biomedical Mass Spectrometry Resource at UCSF (A.L. Burlingame, Director) supported by GM103481. ALV receives support from the Costa Rican Ministry of Science, Technology and Telecommunications (MICITT). NO receives support from a NIH F31.

4.6 Supplementary Information

Table 4.S1 Purification scheme for TbERK8. Clarified lysates of baculovirus-infected SF9 insect cells that expressed TbERK8 were purified through column chromatography. After each chromatography step, the TbERK8 active sites were quantified using ActivX^{TM} Desthiobiotin-ATP Probe (Thermo Scientific Rockford, IL) as recommended by the manufacturer.

	Concentration	**Total Amount**	**Specific Activity**	**Total Activity**	**Percent Yield**	**Fold Purification**
Crude lysate	11.4 mg/ml	2280 mg	3.7×10^2 AU/mg	8.4×10^5 AU	100%	1.0
CM cellulose	0.6 mg/ml	44.6 mg	7.3×10^3 AU/mg	3.2×10^5 AU	39%	20.0
Hydroxy Apatite	0.4mg/ml	3.0 mg	8.8×10^4 AU/mg	2.6×10^5 AU	31%	237.0
S Sepharose	0.4mg/ml	2.0 mg	1.2×10^5 AU/mg	2.4×10^5 AU	29%	324.0

5. High-throughput screening of a kinase inhibitor library identified AZ960 as a compound that inhibits TbERK8 and kills *Trypanosoma brucei*

Author Contributions:

Ana L. Valenciano designed, performed and analysed all the experiments except the experiments mentioned below; and wrote the article.

Aaron Ramsey did the duplicates on the High-throughput screening in the parasites

Zachary B. Mackey oversaw and directed the research, and helped write the paper.

Abstract

Human African Trypanosomiasis (HAT) is a vector borne disease caused by *Trypanosoma brucei* species. The approved treatments for HAT cause toxic side effects and are ineffective against the parasite, consequently new treatments that can specifically target the parasite with fewer side-effects are needed. We screened a library of 273 kinase inhibitors to test for small molecules that can kill *T. brucei* and inhibit the extracellular-signal regulated kinase 8 homolog (TbERK8), which is essential for normal proliferation in the parasite. Six compounds were identified from this screen that were able to inhibit growth in *T. brucei* and inhibit TbERK8 activity *in vitro*. One of the compounds, AZ960 had an IC_{50} value that was lower for TbERK8 than it was for HsERK8. The ability of AZ960 to kill the parasite, and inhibit TbERK8 with a lower IC_{50} than HsERK8, makes it a promising candidate to develop increased potency and selectivity against TbERK8.

5.1 Introduction

Human African Trypanosomiasis (HAT), more commonly known as sleeping sickness, is a neuropathogenic disease caused by the vector-borne parasite *Trypanosoma brucei.* Infection with this parasite is usually fatal when left untreated (10). The approved treatments for this disease cause toxic side effects associated with their use that range from hair loss to patient mortality (5,25). There is a clear need for new treatments to be developed that do not have toxic side effects, are more affordable, and can be orally administered to improve the treatment access to patients in endemic areas.

Kinases are one of the largest class of drug targets use to produce treatments for several types of cancer, immunological, and cardiovascular diseases. In parasites, there are unique kinases that have not been identified in mammals. Other kinases have been identified as important due to their role on regulating essential pathways, and their structural differences compared to human kinases, making them good drug targets to develop new treatments (42). Imidazopyrazines have been found to be lipid kinase inhibitors that target phosphatidylinositol-4-OH kinase (PI(4)K), which is essential in all stages of the plasmodium life cycle. The efficacy of these drugs has been recently confirmed with success in rodent models. This is one of many examples that confirms kinases as good drug targets in treating parasitic diseases (167).

Several kinase inhibitors that kill the parasites are actively being studied. Identified through high throughput screenings, they show real promise as potential treatments (168-170). The family of mitogen activated protein kinases (MAPK) are activated by external stimuli. This results in the activation of a three-tiered kinase cascade that regulates essential processes including signal transduction, gene regulation, cell cycle control, and apoptosis. Extracellular-signal regulated kinase (ERK) one of the groups belonging to MAPK family, they are proteins that regulate how the cells respond to signals from the external environment. TbERK8 belongs to the ERK8 group and is essential for normal proliferation in bloodstream form parasites (47). Additionally, knocking down TbERK8 does not present a lethal phenotype in human cells, and we have shown previously that the mechanism of TbERK8 differs from its

human homolog (Chapter 4). In our most recent studies, we are chemically validating TbERK8 as a drugabble target.

Here we share the results of a phenotypic screen where we monitored parasite proliferation with a small kinase inhibitors library containing 273 small molecules. We identified 10 compounds that were previously uncharacterized against *T. brucei* and observed that 6 were able to inhibit TbERK8. One compound (AZ-960) had a lower IC_{50} for TbERK8 than for HsERK8.

5.2 Materials and Methods

5.2.1 Cell Culture

The bloodstream form parasite strain WT-221, used for the screening, was maintained in HMI-9 media (Axenia Biologix) that follows the Hirumi-Hirumi recipe (77), with 10% FBS, 10% serum plus, 100 U/ml penicillin, 100 µg/ml streptomycin, and 5% CO_2 at 37°C.

5.2.2 Plasmids and Constructs

The coding sequence of the TbERK8 kinase domain was amplified using fwd primer 5'-ATGTCATCAGAAATAGAGCCACATATC-3' and rev primer 5'-AATTTCTTGGTATAGCCGCTC-3' and subcloned into pGSTag using BamHI and EcoRI restriction sites. HsERK8 in pGEX-2T was kindly provided by Dr. Deborah Lannigan.

5.2.3 Recombinant Protein Purification

The recombinant proteins were expressed as GST tag fusion proteins as previously reported. Briefly, the cells were grown to an A_{600} of 1.0 and induced with 0.2 mM IPTG at 16°C overnight. Cells were collected, resuspended in lysis buffer (25mM Tris, 75 mM Nacl, 0.5% Triton-X and 0.5% Nonidet P-40, 1 mM phenylmethanesulfonyl fluoride, 1 mM benzamidine-HCl) and passed through the microfluidizer to homogenize the cells. The lysates were centrifuged at 35000 RPMS for 30 minutes, filtered and loaded onto a 16/10 GST column from GE following the recommendations from the manufacturer. The column was equilibrated using PBS and the proteins were eluted in PBS with 10 mM reduced glutathione.

5.2.4 Screening of a kinase inhibitor library

We used a kinase inhibitor library obtained from Selleck, catalog number L1200 (partnership with Pfizer), to see all the compounds visit the company website (http://www.selleckchem.com/screening/kinase-inhibitor-library.html). It was kindly provided to us by the Virginia Tech Center for Drug Discovery (VTCDD). The 273 compounds were provided lyophilized in 96 well format.

5.2.5 *Trypanosoma brucei* proliferation/viability Screen

To monitor the proliferation of the parasites we used a luciferase based assay as previously described (114). Briefly, parasites were cultured at $1X10^5$ in the conditions previously mentioned and plated in sterile 96-well flat white bottom plates (Greiner) using the automatic Matrix Tech WellMate microplate dispenser (Thermo Scientific). The lyophilized compounds were diluted to 20 uM in PBS with 20% DMSO and added to the parasites at a final assay concentration of 1 uM in 1% DMSO using a multichannel micropipette. After 48 hours, CellTiter-Glo® was used following the recommendations of the manufacturer, the cells were lysed and shaken for 2 min at room temperature. Finally, the luminescence was measured using a SpectraMax® L microplate reader. The screen was performed two times on different days to obtain accurate results for each hit. The quality of the screen was measured by calculating the Z_{prime} and Z_{factor} as previously reported (47). The positive hits were selected as the ones that presented statistical difference in both assays compared to the controls (Z_{score}: >1.96, $p < 0.5$). The IC_{50}s of the positive hits were found by doing 2 fold dilutions of the compounds, starting at a concentration of 2 uM and ending at 0.0156 uM. The different concentrations of the compounds were tested in the parasites as described above.

5.2.6 Recombinant protein inhibition

The hits obtained from the whole cell screen that had not been studied in *T. brucei* before where tested for its ability to inhibit recombinant TbERK8 and HsERK8. The proteins where tested at 125 ng of either TbERK8 or HsERK8 in a 30uL reaction with Buffer K (30 mM Tris pH 7.4, 10 mM $MgCl_2$, 1 mM DTT, 5% glycerol, 1 mM ATP and 0.1 mg/ml BSA), 10uCi of ^{32}P-γ-ATP and 2.5 ug of MBP. The reactions where incubated at 30°C for 30 minutes, stopped using SDS-PAGE loading dye, boiled for one minute and resolved in a SDS-PAGE gel. The gel was dried and exposed to film. We performed an IC_{50} of AZ 960 inhibitor by testing several dilutions in the same conditions mentioned above. To obtain the IC_{50} curve, quantification was performed using a Storm 820 PhosphorImager (GE Life Sciences).

5.3 Results

5.3.1 Novel *T. brucei* bioactive compounds revealed by screening a Kinase Inhibitor Library.

We screened a Selleckchem focused library which contained 273 kinase inhibitors to identify compounds that were able to inhibit TbERK8 and kill cultured *T. brucei.* Each of the compounds were assigned unique identification numbers from the Virginia Tech Center for Drug Discovery (VTCDD). The compounds were initially screened in a phenotypic assay at 1 μM final concentration in 96-well plate format, where the proliferation of the parasites was being measured. The phenotypic screen was done in duplicate on separated days. As the negative control we used untreated parasites in 1% DMSO, because the library was also diluted and prepared in DMSO. And as a positive control we used 100 μM H_2O_2, the parasites are highly sensitive.

The Z-factor for the entire screen was about 0.8 which indicates that it was of good quality overall. Figure 5.1 A shows the plot of relative light units (RLU) for each well in the duplicated screen. We use a Z-score of 1.96 which corresponds to a *p-value* >0.05. Base on this cut off, thirteen compounds were identified that significantly reduced the mean RLU valued which correlates to a negative effect on parasite proliferation. EC_{50} values for 9 compounds that had not been previously tested in the *T. brucei* were calculated (Fig 5.1 B). We observed that most of these compounds inhibit the parasites with an EC_{50} at a nanomolar range. Table 5.2 shows a detailed list of the compounds that we obtained EC_{50} for, as well as the structures of the molecules and what are the specific targets that are known to be inhibited by this compounds. From the compounds studied here, all of them have known drug targets, but not all of the reported targets are present in the parasites, such as JAK, which are tyrosine kinases and these ones are not encoded in the parasites.

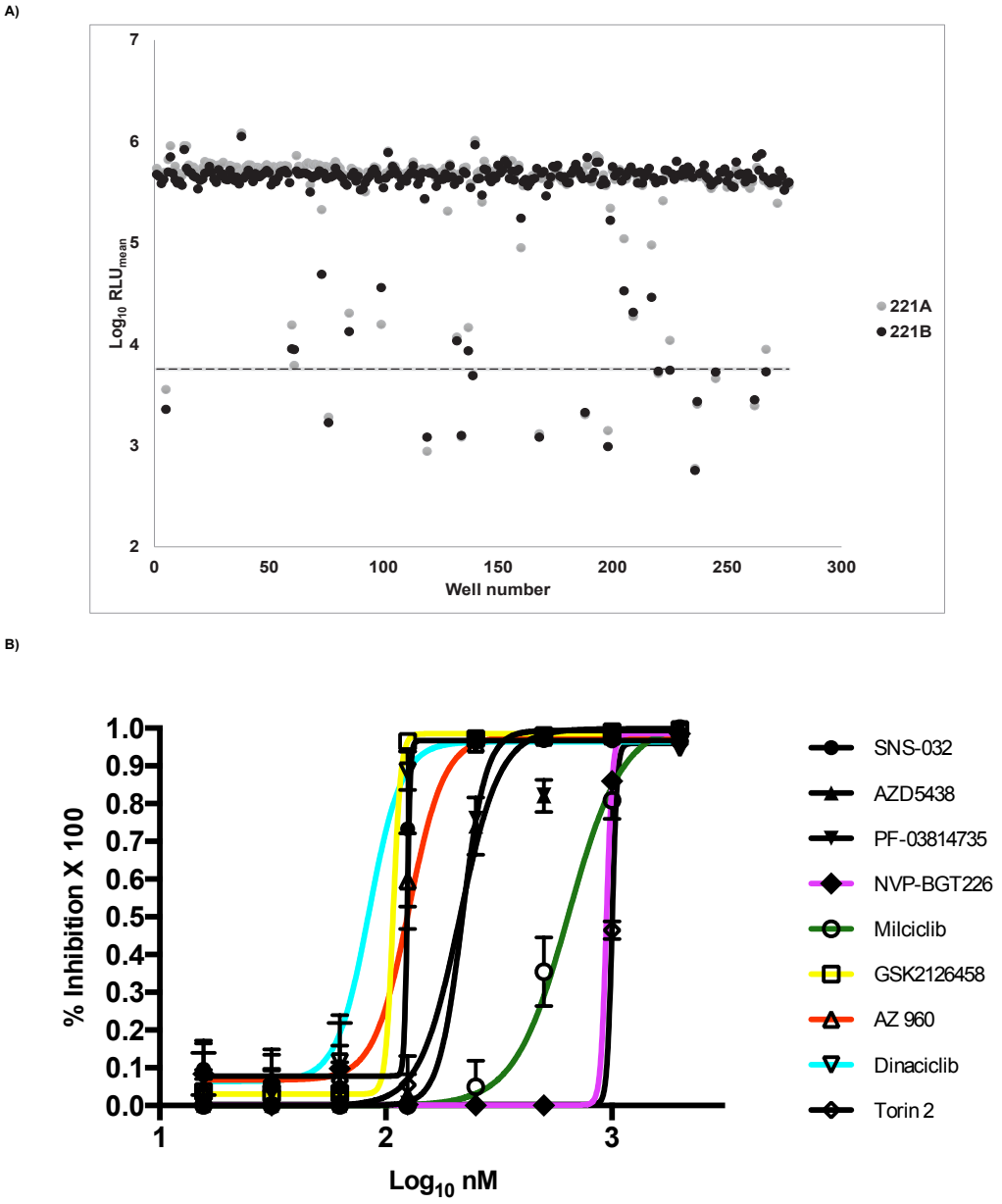

Figure 5.1 Whole cell kinase inhibitor screen. (A) Dot graph showing the duplicate of the 273 compounds screened in the parasites at 1 µM for 48 h. Hits were selected as the ones where the readout in both screens shifted from the mean of the average on the plate. (B) Trypanosomal EC_{50}. Graph showing the IC_{50} values for the 10 hits that have not been tested in *T. brucei* before. Drugs were tested by serial dilution starting at 2 µM for 48 hours and the changes in proliferation were monitored in a Spectra Max L microplate reader after adding CellTiter-Glo®.

Table 5.1 EC_{50} values of the novel *T. brucei* kinase inhibitors

Lane	Drug Name	Targets	EC_{50} (μM)	Bioactivity described against parasites	Smiles
1	SNS-032 (BMS-387032)	CDK9,7,2 (CDK2/Cyc A, CDK7/CycH	0.12	This study	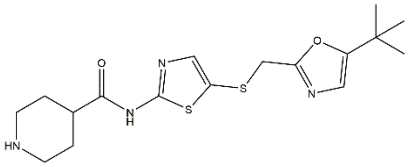
2	SP600125	JNK1,2,3	-	Studied in T. cruzi and P. falciparum.	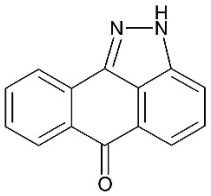
3	AZD5438	CDK1,2,9	0.21	This study	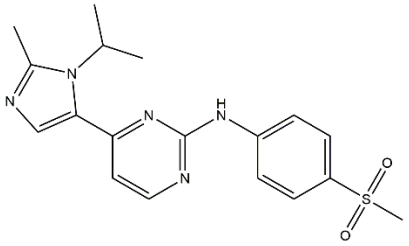
4	PF-03814735	Aurora KinaseA/B	0.26	This study	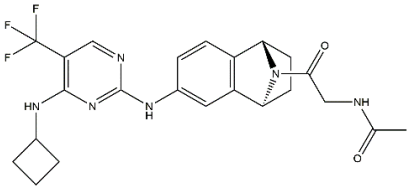
5	NVP-BGT226	PI3K/mTOR	0.95	This study	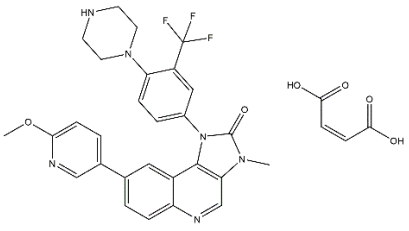
6	Milciclib (PHA-848125)	CDK2/CycA	0.61	This study	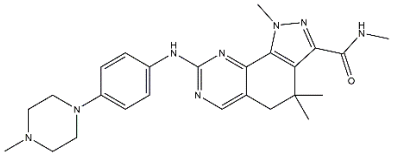

7	GSK2126458	PI3K, mTOR	0.11	This study	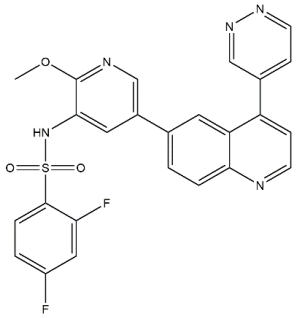
8	AZ 960	JAK2	0.12	This study	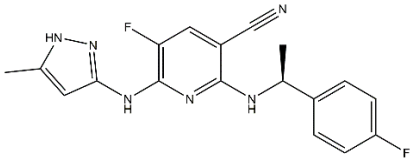
9	Dinaciclib (SCH727965)	CDK2,5,1,9	0.08	This study	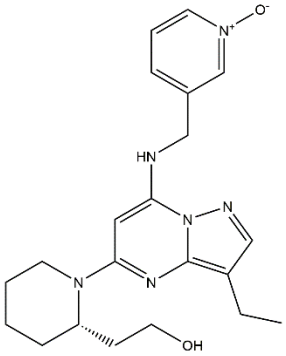
10	Torin 2	mTOR	1	Antimalarials	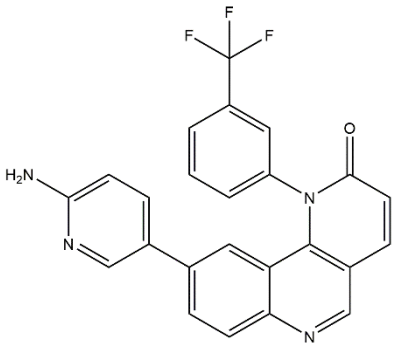

5.3.2 Kinase Inhibitor hits tested on recombinant protein

We have previously validated TbERK8 as a target because it is essential for normal proliferation in the parasite. In order to chemically validate this kinase as a drug target, 10 compounds that were bioactive against *T. brucei* were tested against recombinant TbERK8 to identify small molecules that could selectively inhibit the TbERK8 over HsERK8.

We established that recombinant TbERK8 and HsERK8 both had kinase activity based on their ability to autophosphorylate or phosphorylate MBP in the absence of inhibitor (Fig. 5.2 A). The 10 inhibitors were tested at 1 μM. From what we could see on Figure 5.2 A (Table 5.2), two of the compounds were not able to inhibit either the parasite or the human ERK8 homolog. Four of them were able to inhibit both HsERK8 and TbERK8. These 6 compounds were not promising since they do not resulted in any preference towards either of the ERK8 homologs.

Three of the inhibitors (SNS-032 (BMS-387032)), NVP-BGT226 and Dinaciclib (SCH727965) specifically inhibited HsERK8 (Fig. 5.2 A), compounds 1, 5 and 9 respectively (Table 5.2). This indicates that there were differences in the kinase domain of these proteins that could be detected by these small molecules, confirming the idea that there are differences in the kinase domain of these proteins that can be exploited for drug discovery.

Compound AZ960 (8) killed the parasite at 0.12 μM (Table 5.1) in the phenotypic assay and inhibited TbERK8. We pursued this compounds because its dosage curve for TbERK8 was different from that of HsERK8, it showed more preference over TbERK8 and a slightly lower IC_{50},with 0.44 μM for TbERK8 and 0.64 μM for HsERK8 (Fig. 5.2 B and Table 5.2). This was the most promising compound, showing a slight preference for TbERK8 and also being able to kill the parasite at nanomolar range, putting it as a compound that should be further studied.

Table 5.2 Inhibitory effect of the hits obtained from the phenotypic screen on the kinase activity of HsERK8 and TbERK8.

Lane	Drug Name	Targets	HsERK8	TbERK8
1	SNS-032 (BMS-387032)	CDK9,7,2 (CDK2/CycA, CDK7/CycH	+	-
2	SP600125	JNK1,2,3	+	+
3	AZD5438	CDK1,2,9	+	+
4	PF-03814735	Aurora KinaseA/B	+	+
5	NVP-BGT226	PI3K/mTOR	+	-
6	Milciclib (PHA-848125)	CDK2/CycA	+	+
7	GSK2126458	PI3K, mTOR	-	-
8	AZ 960	JAK2	-/+	+
9	Dinaciclib (SCH727965)	CDK2,5,1,9	+	-
10	Torin 2	mTOR	-	-

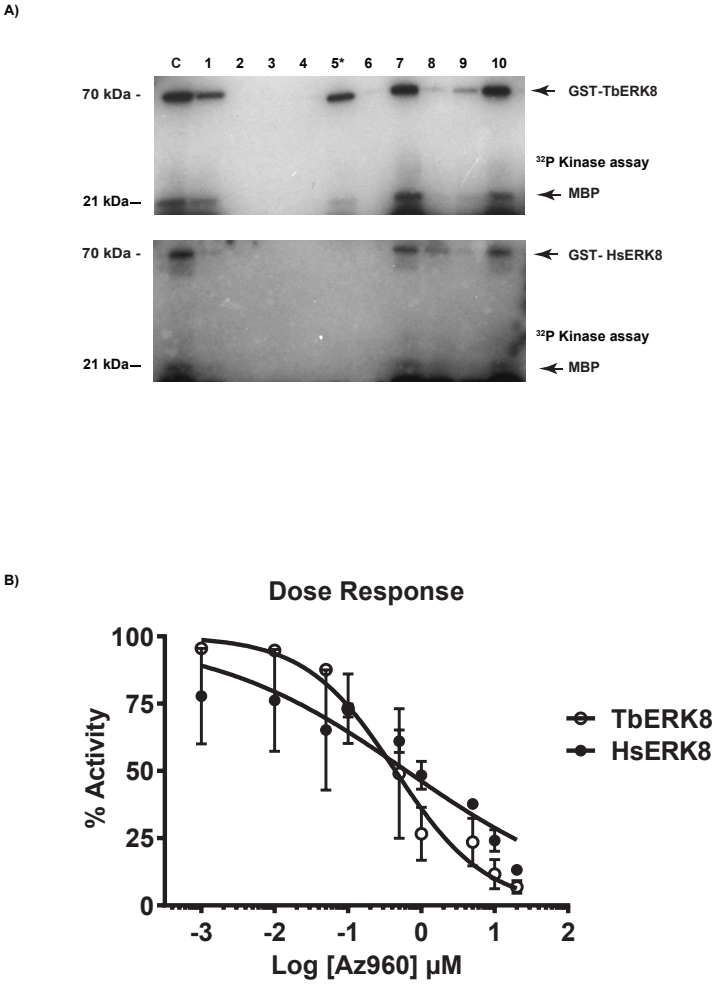

Figure 5.2 TbERK8 vs HsERK8 inhibition. (A) TbERK8 and HsERK8 were purified as GST fusion proteins. The hit compounds were tested on its ability to inhibit ERK8 autophosphorylation as well as MBP phosphorylation, at a final concentration of 5 µM. The reactions were resolved by SDS-Page and the gel dried and exposed to film. The films show the autophosphorylation of the ERK8s and MBP or lack thereof. (B) Graph showing the dose response of TbERK8 and HsERK8 in response to the inhibition of compound 5 (AZ 960).

5.4 Discussion

Due to the decreased effectiveness, toxic side effects and difficulty of administration of the current treatments for HAT, there is urgent need for new treatments. We have combined phenotypic screening and a target-based approach to identify AZ960, a TbERK8 inhibitor that has bioactivity against TbERK8.

A wide range of kinase inhibitors have been tested in *T. brucei* in recent years by phenotypic screens (168-170). Repurposing approved drugs is an efficient approach to get potentially new therapeutics for neglected diseases into clinical trials (171,172). SNS-032 (formerly BMS-387032) and NVP-BGT226, the two compounds that were highly selective towards HsERK8 are known CDK and PI3K/mTOR inhibitors respectively. SNS-032 stops cell cycle progression when it inhibits the CDK 2, 7 and 9 in solid tumours and has been through phase I study (Heath, 2008). NVP-BGT226 is known to cause apoptosis and cell death in breast cancer cells and inhibits cell growth in myeloma as well (164,173).

AZ960 is a potent and selective JAK2 inhibitor identified while studying the signal transducers and activators of Transcription 5 (STAT5) phosphorylation by JAKS (JAK/STAT signalling pathway) in leukaemia cells. This inhibition resulted in decreased levels of BCL-xL (174). AZ960 also makes the cells more sensitive to anti-leukaemia agents and is very effective against tumours (175-177). This compound acts as a tight binding ATP competitive inhibitor. Although the inhibitor was tested by Gozgit *et al*. (174) against another 83 kinases, ERK like proteins were not on the list. Several studies after have shown that inhibition of this interaction by the AZ960 results in apoptosis and growth arrest (175,176).

In this study we identified potent inhibitors that validate TbERK8 as a chemotherapeutic target in *T. brucei*. The molecules that hit both kinases show no specificity but we were also able to proof that the kinase domains from both organisms are different and molecules can have preference for one or the other, confirming TbERK8 as a good drug target. Future studies to improve the potency of AZ 960 are needed to further develop this molecule.

6. Concluding Remarks

This dissertation presents the study of the biological and biochemical role of TbERK8 in bloodstream form *T. brucei* and its relationship to TbPCNA. Our studies demonstrate that the biological and biochemical relationship between TbERK8 and TbPCNA have diverged from the human counterparts.

TbERK8 was confirmed to be a cytoplasmic as well as a nuclear protein in the parasite. And we showed that inserting a double mutation in the conserved Threonine (T) and Tyrosine (Y) of the activation loop, produces a dominant negative effect (Chapter 2). Due to previous studies suggesting that an interaction between ERK8 and PCNA takes place in human cells, we investigated the possible interactions in the parasite homologs. The biological role of TbPCNA was elucidated first (Chapter 3). We found this protein to be essential for parasite proliferation, depleting it resulted in a cell cycle arrest in S and G2/M suggesting that the absence of it during DNA replication inhibits the normal exit of cells from S-phase. The study of protein localization, unlike previously reported, shows TbPCNA localized to the nucleus during S-phase and around the cytoplasm/nucleus for M phase. The overexpression of TbPCNA in the parasites developed a lethal phenotype. We concluded that the tight regulation of this protein in the parasites is necessary for cell survival.

We further studied the interaction of these two proteins, showing that TbERK8 phosphorylated TbPCNA and did not form a tight binding complex as shown in human cell (Chapter 4). We also observed that the phosphorylation took place in three residues (T_{202}, S_{211} and S_{216}) localized to an insertion loop of TbPCNA that is only present in PCNA homologs of kinetoplastid parasites. Further studies where we demonstrated that this interaction is unique to the parasitic proteins and not human homologs suggest that this mechanism is restricted to parasites. Our last result in this study suggests that phosphorylation of TbPCNA by TbERK8 occurs *in vivo*.

Finally, we used a focus kinase inhibitor library to chemically validate TbERK8 as a drug target (Chapter 5). A phenotypic screen of 273 small molecule inhibitors was performed; we identified 10 molecules that were capable of killing the parasites and had never been tested in *Trypanosoma brucei*. The hits were studied for their ability to inhibit ERK8 from the parasite and humans. Six of the molecules were able to inhibit the parasite protein while AZ960, an ATP competitive inhibitor was more efficient at inhibiting TbERK8 than HsERK8. Two other compounds were selective toward HsERK8 only, meaning that they did not inhibit the parasite kinase.

Together these results validate TbERK8 as a drug target, biologically and chemically. The differences on the (1) mechanism of action, (2) *in vitro* kinase substrate preference and (3) selectivity of the inhibitor show that TbERK8 could be chemically exploited for the production of new treatments that could spare an effect on the human kinase.

Further studies will need to be done in the inhibitor AZ960 by using synthetic chemistry to make it more selective towards TbERK8, followed by toxicity studies of the inhibitors in human cells. With the resources that have been produced during the course of this dissertation, a crystal structure of TbERK8 bound to an inhibitor could not only be the first ERK8 structure solved but also elucidate more into the mechanism of action of the inhibitor of interest. More studies should also be done to confirm TbERK8 as the *in vivo* target of AZ960. Studies on TbPCNA are also on going on our group; differences between the parasite and human PCNA have been observed. T2AA, an inhibitor of HsPCNA does bind to TbPCNA with less affinity, a crystal structure of this protein can also be solved to shade some light into the structural differences, especially the unique insertion loop where the phosphorylation by TbERK8 occurs. Together all of these results could lead to the development of new drugs that could treat sleeping sickness with all the properties of a better drug. Cost effective, non-harmful to the host and easier to administrate.

References

1. Brun, R., Blum, J., Chappuis, F., and Burri, C. (2009) Human African trypanosomiasis. *The Lancet* **375**, 148-159
2. Alroy, K. A., Huang, C., Gilman, R. H., Quispe-Machaca, V. R., Marks, M. A., Ancca-Juarez, J., Hillyard, M., Verastegui, M., Sanchez, G., Cabrera, L., Vidal, E., Billig, E. M. W., Cama, V. A., Náquira, C., Bern, C., Levy, M. Z., and Working Group on Chagas Disease in, P. (2015) Correction: Prevalence and Transmission of <italic>Trypanosoma cruzi</italic> in People of Rural Communities of the High Jungle of Northern Peru. *PLoS Negl Trop Dis* **9**, e0003910
3. Reithinger, R., Dujardin, J.-C., Louzir, H., Pirmez, C., Alexander, B., and Brooker, S. (2007) Cutaneous leishmaniasis. *The Lancet Infectious Diseases* **7**, 581-596
4. Steverding, D. (2008) The history of African trypanosomiasis. *Parasites & Vectors* **1**, 3-3
5. WHO. (2013) Sustaining the drive to overcome the global impact of neglected tropical diseases. . *World Health Organization.*
6. Hammarton, T. C., Mottram, J. C., and Doerig, C. (2003) The cell cycle of parasitic protozoa: potential for chemotherapeutic exploitation. *Progress in Cell Cycle Research* **5**
7. Van Den Abbeele, J., Claes, Y., Van Bockstaele, D., Le Ray, D., and Coosemans, M. (1999) *Trypanosoma brucei* spp. development in the tsetse fly: characterization of the post-mesocyclic stages in the foregut and proboscis. *Parasitology* **118**, 469-478
8. Rico, E., Rojas, F., Mony, B. M., Szoor, B., MacGregor, P., and Matthews, K. R. (2013) Bloodstream form pre-adaptation to the tsetse fly in *Trypanosoma brucei*. *Frontiers in Cellular and Infection Microbiology* **3**, 78
9. Kennedy, P. G. E. (2004) Human African trypanosomiasis of the CNS: current issues and challenges. *The Journal of Clinical Investigation* **113**, 496-504
10. Jamonneau, V., Ilboudo, H., Kabore, J., Kaba, D., Koffi, M., Solano, P., Garcia, A., Courtin, D., Laveissiere, C., Lingue, K., Buscher, P., and Bucheton, B. (2012) Untreated human infections by *Trypanosoma brucei gambiense* are not 100% fatal. *PLoS Negl Trop Dis* **6**, e1691
11. Simarro, P. P., Cecchi, G., Franco, J. R., Paone, M., Diarra, A., Ruiz-Postigo, J. A., Fèvre, E. M., Mattioli, R. C., and Jannin, J. G. (2012) Estimating and Mapping the Population at Risk of Sleeping Sickness. *PLoS Negl Trop Dis* **6**, e1859
12. FRANCO, J. R., SIMARRO, P. P., DIARRA, A., RUIZ-POSTIGO, J. A., and JANNIN, J. G. (2014) The journey towards elimination of gambiense human African trypanosomiasis: not far, nor easy. *Parasitology* **141**, 748-760
13. Berrang-Ford, L., Lundine, J., and Breau, S. (2011) Conflict and human African trypanosomiasis. *Social Science & Medicine* **72**, 398-407
14. Simo, G., Fongho, P., Farikou, O., Ndjeuto-Tchouli, P. I. N., Tchouomene-Labou, J., Njiokou, F., and Asonganyi, T. (2015) Trypanosome infection rates in tsetse flies in the "silent" sleeping sickness focus of Bafia in the Centre Region in Cameroon. *Parasites & Vectors* **8**, 528
15. Lejon, V., Reiber, H., Legros, D., Djé, N., Magnus, E., Wouters, I., Sindic, C. J. M., and Büscher, P. (2003) Intrathecal Immune Response Pattern for Improved Diagnosis of Central Nervous System Involvement in Trypanosomiasis. *The Journal of Infectious Diseases* **187**, 1475-1483
16. Blum, J., Schmid, C., and Burri, C. (2006) Clinical aspects of 2541 patients with second stage human African trypanosomiasis. *Acta Tropica* **97**, 55-64
17. Checchi, F., Filipe, J., Haydon, D., Chandramohan, D., and Chappuis, F. (2008) Estimates of the duration of the early and late stage of gambiense sleeping sickness. *BMC Infectious Diseases* **8**, 16
18. Truc, P., Lejon, V., Magnus, E., Jamonneau, V., Nangouma, A., Verloo, D., Penchenier, L., and Büscher, P. (2002) Evaluation of the micro-CATT, CATT/*Trypanosoma brucei gambiense*, and LATEX/T b gambiense methods for serodiagnosis and surveillance of human African

trypanosomiasis in West and Central Africa. *Bulletin of the World Health Organization* **80**, 882-886
19. Miézan, T. W., Meda, H. A., Doua, F., Djè, N. N., Lejon, V., and Büscher, P. (2000) Single centrifugation of cerebrospinal fluid in a sealed pasteur pipette for simple, rapid and sensitive detection of trypanosomes. *Transactions of The Royal Society of Tropical Medicine and Hygiene* **94**, 293
20. Jamonneau, V., Solano, P., Garcia, A., Lejon, V., Djé, N., Miezan, T. W., N'Guessan, P., Cuny, G., and Büscher, P. (2003) Stage determination and therapeutic decision in human African trypanosomiasis: value of polymerase chain reaction and immunoglobulin M quantification on the cerebrospinal fluid of sleeping sickness patients in Côte d'Ivoire. *Tropical Medicine & International Health* **8**, 589-594
21. Deborggraeve, S., Claes, F., Laurent, T., Mertens, P., Leclipteux, T., Dujardin, J. C., Herdewijn, P., and Büscher, P. (2006) Molecular Dipstick Test for Diagnosis of Sleeping Sickness. *Journal of Clinical Microbiology* **44**, 2884-2889
22. Sullivan, L., Wall, S. J., Carrington, M., and Ferguson, M. A. J. (2013) Proteomic Selection of Immunodiagnostic Antigens for Human African Trypanosomiasis and Generation of a Prototype Lateral Flow Immunodiagnostic Device. *PLoS Negl Trop Dis* **7**, e2087
23. Nzou, S. M., Fujii, Y., Miura, M., Mwau, M., Mwangi, A. W., Itoh, M., Salam, M. A., Hamano, S., Hirayama, K., and Kaneko, S. (2016) Development of multiplex serological assay for the detection of human African trypanosomiasis. *Parasitology International* **65**, 121-127
24. SIMARRO, P. P., FRANCO, J., DIARRA, A., POSTIGO, J. A. R., and JANNIN, J. (2012) Update on field use of the available drugs for the chemotherapy of human African trypanosomiasis. *Parasitology* **139**, 842-846
25. Nok, A. (2003) Arsenicals (melarsoprol), pentamidine and suramin in the treatment of human African trypanosomiasis. *Parasitol Res* **90**, 71-79
26. Baker, N., de Koning, H. P., Mäser, P., and Horn, D. (2013) Drug resistance in African trypanosomiasis: the melarsoprol and pentamidine story. *Trends in Parasitology* **29**, 110-118
27. Delespaux, V., and de Koning, H. P. (2007) Drugs and drug resistance in African trypanosomiasis. *Drug Resistance Updates* **10**, 30-50
28. Legros, D., Evans, S., Maiso, F., Enyaru, J. C. K., and Mbulamberi, D. (1999) Risk factors for treatment failure after melarsoprol for *Trypanosoma brucei gambiense* trypanosomiasis in Uganda. *Transactions of the Royal Society of Tropical Medicine and Hygiene* **93**, 439-442
29. Bacchi, C., Nathan, H., Hutner, S., McCann, P., and Sjoerdsma, A. (1980) Polyamine metabolism: a potential therapeutic target in trypanosomes. *Science* **210**, 332-334
30. Brun, R., Schumacher, R., Schmid, C., Kunz, C., and Burri, C. (2001) The phenomenon of treatment failures in Human African Trypanosomiasis. *Tropical Medicine & International Health* **6**, 906-914
31. Priotto, G., Kasparian, S., Ngouama, D., Ghorashian, S., Arnold, U., Ghabri, S., and Karunakara, U. (2007) Nifurtimox-Eflornithine Combination Therapy for Second-Stage *Trypanosoma brucei gambiense* Sleeping Sickness: A Randomized Clinical Trial in Congo. *Clinical Infectious Diseases* **45**, 1435-1442
32. Na-Bangchang, K., Doua, F., Konsil, J., Hanpitakpong, W., Kamanikom, B., Kuzoe, F. . (2004) The pharmacokinetics of eflornithine (alphadifluoromethylornithine) in patients with late-stage T. b. gambiense sleeping sickness. *European Journal of Clinical Pharmacology* **60**, 269–278
33. Jansson, R., Malm, M., Roth, C., and Ashton, M. (2008) Enantioselective and Nonlinear Intestinal Absorption of Eflornithine in the Rat. *Antimicrobial Agents and Chemotherapy* **52**, 2842-2848
34. Kultz, D. (1998) Phylogenetic and functional classification of mitogen- and stress- activated protein kinases. *Journal of Molecular Evolution* **46**, 571–588
35. Yang, S. H., Sharrocks, A. D., and Whitmarsh, A. J. (2013) MAP kinase signalling cascades and transcriptional regulation. *Gene* **513**, 1-13

36. Pearson, G., Robinson, F., Gibson, T. B., Xu, B. E., Karandikar, M., Berman, K., and Cobb, M. H. (2001) Mitogen-activated protein (MAP) kinase pathways: Regulation and physiological functions. *Endocrine reviews* **22**, 153-183
37. Ricci, R., Ittner, A., Gehart, H., and Kumpf, S. (2010) MAPK signalling in cellular metabolism: stress or wellness? *EMBO reports* **11**, 834-840
38. Roux, P. P., and Blenis, J. (2004) ERK and p38 MAPK-Activated Protein Kinases: a Family of Protein Kinases with Diverse Biological Functions. *Microbiology and Molecular Biology Reviews* **68**, 320-320
39. Martin-Blanco, E. (2000) p38 MAPK signalling cascades: ancient roles and new functions. *BIOESSAYS* **22**, 637-645
40. Berriman, M., Ghedin, E., Hertz-Fowler, C., Blandin, G., Renauld, H., Bartholomeu, D. C., Lennard, N. J., Caler, E., Hamlin, N. E., Haas, B., Bohme, U., Hannick, L., Aslett, M. A., Shallom, J., Marcello, L., Hou, L., Wickstead, B., Alsmark, U. C., Arrowsmith, C., Atkin, R. J., Barron, A. J., Bringaud, F., Brooks, K., Carrington, M., Cherevach, I., Chillingworth, T. J., Churcher, C., Clark, L. N., Corton, C. H., Cronin, A., Davies, R. M., Doggett, J., Djikeng, A., Feldblyum, T., Field, M. C., Fraser, A., Goodhead, I., Hance, Z., Harper, D., Harris, B. R., Hauser, H., Hostetler, J., Ivens, A., Jagels, K., Johnson, D., Johnson, J., Jones, K., Kerhornou, A. X., Koo, H., Larke, N., Landfear, S., Larkin, C., Leech, V., Line, A., Lord, A., Macleod, A., Mooney, P. J., Moule, S., Martin, D. M., Morgan, G. W., Mungall, K., Norbertczak, H., Ormond, D., Pai, G., Peacock, C. S., Peterson, J., Quail, M. A., Rabbinowitsch, E., Rajandream, M. A., Reitter, C., Salzberg, S. L., Sanders, M., Schobel, S., Sharp, S., Simmonds, M., Simpson, A. J., Tallon, L., Turner, C. M., Tait, A., Tivey, A. R., Van Aken, S., Walker, D., Wanless, D., Wang, S., White, B., White, O., Whitehead, S., Woodward, J., Wortman, J., Adams, M. D., Embley, T. M., Gull, K., Ullu, E., Barry, J. D., Fairlamb, A. H., Opperdoes, F., Barrell, B. G., Donelson, J. E., Hall, N., Fraser, C. M., Melville, S. E., and El-Sayed, N. M. (2005) The genome of the African trypanosome *Trypanosoma brucei. Science* **309**, 416-422
41. Parsons, M., Worthey, E. A., Ward, P. N., and Mottram, J. C. (2005) Comparative analysis of the kinomes of three pathogenic trypanosomatids: Leishmania major, *Trypanosoma brucei* and Trypanosoma cruzi. *BMC Genomics* **6**, 1-19
42. Naula, C., Parsons, M., and Mottram, J. C. (2005) Protein kinases as drug targets in trypanosomes and Leishmania. *Biochimica et Biophysica Acta (BBA) - Proteins and Proteomics* **1754**, 151-159
43. Brumlik, M. J., Pandeswara, S., Ludwig, S. M., Murthy, K., and Curiel, T. J. (2011) Parasite Mitogen-Activated Protein Kinases as Drug Discovery Targets to Treat Human Protozoan Pathogens. *Journal of Signal Transduction* **2011**
44. Gupta CL, A. S., Kumar N, Ali J, Pathak N, Bajpai P. (2016) In Silico Elucidation and Inhibition Studies of Selected Phytoligands Against Mitogen-Activated Protein Kinases of Protozoan Parasites. *Interdisciplinary Sciences: Computational Life Sciences* **8**, 41-52
45. Müller, I. B., Domenicali-Pfister, D., Roditi, I., and Vassella, E. (2002) Stage-specific Requirement of a Mitogen-activated Protein Kinase by *Trypanosoma brucei*. *Molecular Biology of the Cell* **13**, 3787-3799
46. Domenicali Pfister, D., Burkard, G., Morand, S., Renggli, C. K., Roditi, I., and Vassella, E. (2006) A Mitogen-Activated Protein Kinase Controls Differentiation of Bloodstream Forms of *Trypanosoma brucei*. *Eukaryotic Cell* **5**, 1126-1135
47. Mackey, Z. B., Koupparis, K., Nishino, M., and McKerrow, J. H. (2011) High-throughput analysis of an RNAi library identifies novel kinase targets in *Trypanosoma brucei*. *Chemical biology & drug design* **78**, 454-463
48. Alsford, S., Turner, D. J., Obado, S. O., Sanchez-Flores, A., Glover, L., Berriman, M., Hertz-Fowler, C., and Horn, D. (2011) High-throughput phenotyping using parallel sequencing of RNA interference targets in the African trypanosome. *Genome Research* **21**, 915-924

49. Jones, N. G., Thomas, E. B., Brown, E., Dickens, N. J., Hammarton, T. C., and Mottram, J. C. (2014) Regulators of *Trypanosoma brucei* Cell Cycle Progression and Differentiation Identified Using a Kinome-Wide RNAi Screen. *PLoS Pathog* **10**, e1003886
50. Abe, M. K., Saelzler, M. P., Iii, R. E., Kahle, K. T., Hershenson, M. B., Michelle, M. L. B., and Rosner, M. R. (2002) ERK8, a New Member of the Mitogen-activated Protein Kinase Family. *Journal of Biological Chemistry* **277**, 16733-16743
51. Bogoyevitch, M. A., and Court, N. W. (2004) Counting on mitogen-activated protein kinases—ERKs 3, 4, 5, 6, 7 and 8. Elsevier Inc, NEW YORK
52. Iavarone, C., Acunzo, M., Carlomagno, F., Catania, A., Melillo, R. M., Carlomagno, S. M., Santoro, M., and Chiariello, M. (2006) Activation of the Erk8 Mitogen-activated Protein (MAP) Kinase by RET/PTC3, a Constitutively Active Form of the RET Proto-oncogene. *Journal of Biological Chemistry* **281**, 10567-10576
53. Klevernic, I. V., Martin, N. M. B., and Cohen, P. (2009) Regulation of the activity and expression of ERK8 by DNA damage. *FEBS letters* **583**, 680-684
54. Xu, Y.-M., Zhu, F., Cho, Y.-Y., Carper, A., Peng, C., Zheng, D., Yao, K., Lau, A. T. Y., Zykova, T. A., Kim, H.-G., Bode, A. M., and Dong, Z. (2010) Extracellular Signal-Regulated Kinase 8–Mediated c-Jun Phosphorylation Increases Tumorigenesis of Human Colon Cancer. *Cancer Research* **70**, 3218-3227
55. Rossi, M., Colecchia, D., Iavarone, C., Strambi, A., Piccioni, F., Verrotti di Pianella, A., and Chiariello, M. (2011) Extracellular Signal-regulated Kinase 8 (ERK8) Controls Estrogen-related Receptor α (ERRα) Cellular Localization and Inhibits Its Transcriptional Activity. *Journal of Biological Chemistry* **286**, 8507-8522
56. Chia, J., Tham, K. M., Gill, D. J., Bard-Chapeau, E. A., and Bard, F. A. (2014) ERK8 is a negative regulator of O-GalNAc glycosylation and cell migration. *eLife* **3**, e01828
57. Groehler, A. L., and Lannigan, D. A. (2010) A chromatin-bound kinase, ERK8, protects genomic integrity by inhibiting HDM2-mediated degradation of the DNA clamp PCNA. *The Journal of cell biology* **190**, 575-586
58. Liwak-Muir, U., Dobson, C. C., Naing, T., Wylie, Q., Chehade, L., Baird, S. D., Chakraborty, P. K., and Holcik, M. (2015) ERK8 is a novel HuR kinase that regulates tumour suppressor PDCD4 through a miR-21 dependent mechanism. *Oncotarget; Vol 7, No 2*
59. Ray, D., Dutta, S., Banerjee, S., Banerjee, R., and Raha, S. (2005) Identification, structure, and phylogenetic relationships of a mitogen-activated protein kinase homologue from the parasitic protist Entamoeba histolytica. *Gene* **346**, 41-50
60. Lacey, M. R., Brumlik, M.J., Yenni, R.E., Burow, M.E., Curiel, T.J. . (2007) Toxoplasma gondii Expresses Two Mitogen-Activated Protein Kinase Genes That Represent Distinct Protozoan Subfamilies. *Journal of Molecular Evolution* **64**, 4-14
61. Coulombe, P., and Meloche, S. (2007) Atypical mitogen-activated protein kinases: Structure, regulation and functions. *Biochimica et Biophysica Acta (BBA) - Molecular Cell Research* **1773**, 1376-1387
62. Jónsson, Z. O., and Hübscher, U. (1997) Proliferating cell nuclear antigen: More than a clamp for DNA polymerases. *BioEssays* **19**, 967-975
63. Mailand, N., Gibbs-Seymour, I., and Bekker-Jensen, S. (2013) Regulation of PCNA-protein interactions for genome stability. *Nat Rev Mol Cell Biol* **14**, 269-282
64. Park, S. Y., Jeong, M.S., Han, C.W., Yu, H.S., Jang, S.B. (2015) Structural and functional insight into proliferating cell nuclear antigen. *Journal of Microbiology and Biotechnology* **25**
65. Dieckman, L. M., Freudenthal, B. D., and Washington, M. T. (2012) PCNA structure and function: insights from structures of PCNA complexes and post-translationally modified PCNA. *Sub-cellular biochemistry* **62**, 281-299
66. Ulrich, H. D. (2009) Regulating post-translational modifications of the eukaryotic replication clamp PCNA. *DNA Repair* **8**, 461-469

67. Wang, S.-C., Nakajima, Y., Yu, Y.-L., Xia, W., Chen, C.-T., Yang, C.-C., McIntush, E. W., Li, L.-Y., Hawke, D. H., Kobayashi, R., and Hung, M.-C. (2006) Tyrosine phosphorylation controls PCNA function through protein stability. *Nat Cell Biol* **8**, 1359-1368
68. Ortega, J., Li, J. Y., Lee, S., Tong, D., Gu, L., and Li, G.-M. (2015) Phosphorylation of PCNA by EGFR inhibits mismatch repair and promotes misincorporation during DNA synthesis. *Proceedings of the National Academy of Sciences* **112**, 5667-5672
69. Zhao, H., Chen, M. S., Lo, Y. H., Waltz, S. E., Wang, J., Ho, P. C., Vasiliauskas, J., Plattner, R., Wang, Y. L., and Wang, S. C. (2014) The Ron receptor tyrosine kinase activates c-Abl to promote cell proliferation through tyrosine phosphorylation of PCNA in breast cancer. *Oncogene* **33**, 1429-1437
70. Zhao, H., Ho, P.-C., Lo, Y.-H., Espejo, A., Bedford, M. T., Hung, M.-C., and Wang, S.-C. (2012) Interaction of Proliferation Cell Nuclear Antigen (PCNA) with c-Abl in Cell Proliferation and Response to DNA Damages in Breast Cancer. *PLoS ONE* **7**, e29416
71. Dang, H. Q., and Li, Z. (2011) The Cdc45·Mcm2–7·GINS Protein Complex in Trypanosomes Regulates DNA Replication and Interacts with Two Orc1-like Proteins in the Origin Recognition Complex. *Journal of Biological Chemistry* **286**, 32424-32435
72. Calderano, S. G., de Melo Godoy, P. D., Motta, M. C. M., Mortara, R. A., Schenkman, S., and Elias, M. C. (2011) Trypanosoma cruzi DNA replication includes the sequential recruitment of pre-replication and replication machineries close to nuclear periphery. *Nucleus* **2**, 136-145
73. Kaufmann, D., Gassen, A., Maiser, A., Leonhardt, H., and Janzen, C. J. (2012) Regulation and spatial organization of PCNA in *Trypanosoma brucei*. *Biochemical and Biophysical Research Communications* **419**, 698-702
74. Bruning, J. B., and Shamoo, Y. (2004) Structural and Thermodynamic Analysis of Human PCNA with Peptides Derived from DNA Polymerase-δ p66 Subunit and Flap Endonuclease-1. *Structure* **12**, 2209-2219
75. Nett, I. R. E., Martin, D. M. A., Miranda-Saavedra, D., Lamont, D., Barber, J. D., Mehlert, A., and Ferguson, M. A. J. (2009) The Phosphoproteome of Bloodstream Form *Trypanosoma brucei*, Causative Agent of African Sleeping Sickness. *Molecular & Cellular Proteomics : MCP* **8**, 1527-1538
76. I, C. (1977) New culture medium for maintenance of tsetse tissues and growth of trypanosomatids. *J Protozool* **24**, 325-329
77. Hirumi, H., and Hirumi, K. (1989) Continuous cultivation of *Trypanosoma brucei* blood stream forms in a medium containing a low concentration of serum protein without feeder cell layers. *The Journal of parasitology* **75**, 985-989
78. Wirtz, E., Leal, S., Ochatt, C., and Cross, G. A. (1999) A tightly regulated inducible expression system for conditional gene knock-outs and dominant-negative genetics in *Trypanosoma brucei*. *Molecular and biochemical parasitology* **99**, 89-101
79. Motyka, S. A., Drew, M. E., Yildirir, G., and Englund, P. T. (2006) Overexpression of a cytochrome b5 reductase-like protein causes kinetoplast DNA loss in *Trypanosoma brucei*. *The Journal of biological chemistry* **281**, 18499-18506
80. Bryksin, A. V., and Matsumura, I. (2010) Overlap extension PCR cloning: a simple and reliable way to create recombinant plasmids. *Biotechniques* **48**, 463-465
81. Valenciano, A. L., Ramsey, A. C., and Mackey, Z. B. (2015) Deviating the level of proliferating cell nuclear antigen in *Trypanosoma brucei* elicits distinct mechanisms for inhibiting proliferation and cell cycle progression. *Cell Cycle* **14**, 674-688
82. Colecchia, D., Strambi, A., Sanzone, S., Iavarone, C., Rossi, M., Dall'Armi, C., Piccioni, F., Verrotti di Pianella, A., and Chiariello, M. (2012) MAPK15/ERK8 stimulates autophagy by interacting with LC3 and GABARAP proteins. *Autophagy* **8**, 1724-1740
83. Salic, A., and Mitchison, T. J. (2008) A chemical method for fast and sensitive detection of DNA synthesis in vivo. *Proceedings of the National Academy of Sciences* **105**, 2415-2420

84. Klevernic, Iva V., Stafford, Margaret J., Morrice, N., Peggie, M., Morton, S., and Cohen, P. (2006) Characterization of the reversible phosphorylation and activation of ERK8. *Biochemical Journal* **394**, 365-373
85. Bao, Y., Weiss, L. M., Ma, Y. F., Lisanti, M. P., Tanowitz, H. B., Das, B. C., Zheng, R., and Huang, H. (2010) Molecular cloning and characterization of mitogen-activated protein kinase 2 in Trypanosoma cruzi. *Cell Cycle* **9**, 2888-2896
86. Alsford, S., and Horn, D. (2008) Single-locus targeting constructs for reliable regulated RNAi and transgene expression in *Trypanosoma brucei*. *Molecular and biochemical parasitology* **161**, 10.1016/j.molbiopara.2008.1005.1006
87. Wang, Z., Morris, J. C., Drew, M. E., and Englund, P. T. (2000) Inhibition of *Trypanosoma brucei* gene expression by RNA interference using an integratable vector with opposing T7 promoters. *The Journal of biological chemistry* **275**, 40174-40179
88. Bell, S. P., and Dutta, A. (2002) DNA replication in eukaryotic cells. *Annual review of biochemistry* **71**, 333-374
89. Diffley, J. F. (2004) Regulation of early events in chromosome replication. *Current biology : CB* **14**, R778-786
90. Kumar, D., Mukherji, A., and Saha, S. (2008) Expression and subcellular localization of ORC1 in Leishmania major. *Biochem Biophys Res Commun* **375**, 74-79
91. Godoy, P. D. d. M., Nogueira-Junior, L. A., Paes, L. S., Cornejo, A., Martins, R. M., Silber, A. M., Schenkman, S., and Elias, M. C. (2009) Trypanosome Prereplication Machinery Contains a Single Functional Orc1/Cdc6 Protein, Which Is Typical of Archaea. *Eukaryotic Cell* **8**, 1592-1603
92. Johnson, A., and O'Donnell, M. (2005) Cellular DNA replicases: components and dynamics at the replication fork. *Annual review of biochemistry* **74**, 283-315
93. Moldovan, G. L., Pfander, B., and Jentsch, S. (2007) PCNA, the maestro of the replication fork. *Cell* **129**, 665-679
94. Berezney, R., Dubey, D. D., and Huberman, J. A. (2000) Heterogeneity of eukaryotic replicons, replicon clusters, and replication foci. *Chromosoma* **108**, 471-484
95. Miyachi, K., Fritzler, M. J., and Tan, E. M. (1978) Autoantibody to a Nuclear Antigen in Proliferating Cells. *The Journal of Immunology* **121**, 2228-2234
96. Vairapandi, M., Azam, N., Balliet, A. G., Hoffman, B., and Liebermann, D. A. (2000) Characterization of MyD118, Gadd45, and Proliferating Cell Nuclear Antigen (PCNA) Interacting Domains: PCNA IMPEDES MyD118 AND Gadd45-MEDIATED NEGATIVE GROWTH CONTROL. *Journal of Biological Chemistry* **275**, 16810-16819
97. Maga, G., and Hübscher, U. (2003) Proliferating cell nuclear antigen (PCNA): a dancer with many partners. *Journal of Cell Science* **116**, 3051-3060
98. Celis, J., and Celis, A. (1985) Cell cycle-dependent variations in the distribution of the nuclear protein cyclin proliferating cell nuclear antigen in cultured cells: subdivision of S phase. *Proc Natl Acad Sci U S A* **82**, 3262 - 3266
99. Grana, X., and Reddy, E. P. (1995) Cell cycle control in mammalian cells: role of cyclins, cyclin dependent kinases (CDKs), growth suppressor genes and cyclin-dependent kinase inhibitors (CKIs). *Oncogene* **11**, 211-219
100. Sherr, C. J. (1994) G1 phase progression: Cycling on cue. *Cell* **79**, 551-555
101. Zhang, H., Xiong, Y., and Beach, D. (1993) Proliferating cell nuclear antigen and p21 are components of multiple cell cycle kinase complexes. *Molecular Biology of the Cell* **4**, 897-906
102. Chan, P. K., Frakes, R., Tan, E. M., Brattain, M. G., Smetana, K., and Busch, H. (1983) Indirect immunofluorescence studies of proliferating cell nuclear antigen in nucleoli of human tumor and normal tissues. *Cancer Res* **43**, 3770-3777
103. Malkas, L. H., Herbert, B. S., Abdel-Aziz, W., Dobrolecki, L. E., Liu, Y., Agarwal, B., Hoelz, D., Badve, S., Schnaper, L., Arnold, R. J., Mechref, Y., Novotny, M. V., Loehrer, P., Goulet, R. J.,

and Hickey, R. J. (2006) A cancer-associated PCNA expressed in breast cancer has implications as a potential biomarker. *Proceedings of the National Academy of Sciences* **103**, 19472-19477
104. Witko-Sarsat, V., Mocek, J., Bouayad, D., Tamassia, N., Ribeil, J.-A., Candalh, C., Davezac, N., Reuter, N., Mouthon, L., Hermine, O., Pederzoli-Ribeil, M., and Cassatella, M. A. (2010) Proliferating cell nuclear antigen acts as a cytoplasmic platform controlling human neutrophil survival. *The Journal of Experimental Medicine* **207**, 2631-2645
105. Wirtz, E., Hoek, M., and Cross, G. A. (1998) Regulated processive transcription of chromatin by T7 RNA polymerase in *Trypanosoma brucei*. *Nucleic acids research* **26**, 4626-4634
106. Woodward, R., and Gull, K. (1990) Timing of nuclear and kinetoplast DNA replication and early morphological events in the cell cycle of *Trypanosoma brucei*. *J Cell Sci* **95 (Pt 1)**, 49-57
107. Gluenz, E., Povelones, M. L., Englund, P. T., and Gull, K. (2011) The Kinetoplast Duplication Cycle in *Trypanosoma brucei* Is Orchestrated by Cytoskeleton-Mediated Cell Morphogenesis. *Molecular and Cellular Biology* **31**, 1012-1021
108. Hammarton, T. C. (2007) Cell cycle regulation in *Trypanosoma brucei*. *Molecular and biochemical parasitology* **153**, 1-8
109. Naryzhny, S. N. (2008) Proliferating cell nuclear antigen: a proteomics view. *Cellular and molecular life sciences : CMLS* **65**, 3789-3808
110. Bravo, R., and Macdonald-Bravo, H. (1987) Existence of two populations of cyclin/proliferating cell nuclear antigen during the cell cycle: association with DNA replication sites. *J Cell Biol* **105**, 1549 - 1554
111. Bauer, G. A., and Burgers, M. J. (1990) Molecular cloning, structure and expression of the yeast proliferating cell nuclear antigen gene. *Nucleic acids research* **18**, 261-265
112. Branzei, D., Seki, M., and Enomoto, T. (2004) Rad18/Rad5/Mms2-mediated polyubiquitination of PCNA is implicated in replication completion during replication stress. *Genes to Cells* **9**, 1031-1042
113. Forsythe, G. R., McCulloch, R., and Hammarton, T. C. (2009) Hydroxyurea-induced synchronisation of bloodstream stage *Trypanosoma brucei*. *Molecular and biochemical parasitology* **164**, 131-136
114. Mackey, Z. B., Baca, A. M., Mallari, J. P., Apsel, B., Shelat, A., Hansell, E. J., Chiang, P. K., Wolff, B., Guy, K. R., Williams, J., and McKerrow, J. H. (2006) Discovery of trypanocidal compounds by whole cell HTS of *Trypanosoma brucei*. *Chemical biology & drug design* **67**, 355-363
115. Rogakou, E. P., Pilch, D. R., Orr, A. H., Ivanova, V. S., and Bonner, W. M. (1998) DNA double-stranded breaks induce histone H2AX phosphorylation on serine 139. *The Journal of biological chemistry* **273**, 5858-5868
116. Glover, L., and Horn, D. (2012) Trypanosomal histone gammaH2A and the DNA damage response. *Molecular and biochemical parasitology* **183**, 78-83
117. Tandon, R., Chandra, S., Baharia, R. K., Das, S., Misra, P., Kumar, A., Siddiqi, M. I., Sundar, S., and Dube, A. (2014) Characterization of the Proliferating Cell Nuclear Antigen of Leishmania donovani Clinical Isolates and Its Association with Antimony Resistance. *Antimicrobial Agents and Chemotherapy* **58**, 2997-3007
118. Jonsson, Z. O., Podust, V. N., Podust, L. M., and Hubscher, U. (1995) Tyrosine 114 is essential for the trimeric structure and the functional activities of human proliferating cell nuclear antigen. *The EMBO journal* **14**, 5745-5751
119. Kelman, Z., and O'Donnell, M. (1995) Embryonic PCNA: a missing link? *Current biology : CB* **5**, 814
120. Henderson, D. S., Wiegand, U. K., Norman, D. G., and Glover, D. M. (2000) Mutual correction of faulty PCNA subunits in temperature-sensitive lethal mus209 mutants of Drosophila melanogaster. *Genetics* **154**, 1721-1733

121. Engel, F. B., Hauck, L., Boehm, M., Nabel, E. G., Dietz, R., and von Harsdorf, R. (2003) p21CIP1 Controls Proliferating Cell Nuclear Antigen Level in Adult Cardiomyocytes. *Molecular and Cellular Biology* **23**, 555-565
122. Stelter, P., and Ulrich, H. D. (2003) Control of spontaneous and damage-induced mutagenesis by SUMO and ubiquitin conjugation. *Nature* **425**, 188-191
123. Ulrich, H. D., and Takahashi, T. (2013) Readers of PCNA modifications. *Chromosoma* **122**, 259-274
124. Nicolae, C. M., Aho, E. R., Vlahos, A. H., Choe, K. N., De, S., Karras, G. I., and Moldovan, G. L. (2014) The ADP-ribosyltransferase PARP10/ARTD10 interacts with proliferating cell nuclear antigen (PCNA) and is required for DNA damage tolerance. *The Journal of biological chemistry* **289**, 13627-13637
125. Gehen, S. C., Vitiello, P. F., Bambara, R. A., Keng, P. C., and O'Reilly, M. A. (2007) Downregulation of PCNA potentiates p21-mediated growth inhibition in response to hyperoxia. *American journal of physiology. Lung cellular and molecular physiology* **292**, L716-724
126. Tan, Z., Wortman, M., Dillehay, K. L., Seibel, W. L., Evelyn, C. R., Smith, S. J., Malkas, L. H., Zheng, Y., Lu, S., and Dong, Z. (2012) Small-Molecule Targeting of Proliferating Cell Nuclear Antigen Chromatin Association Inhibits Tumor Cell Growth. *Molecular Pharmacology* **81**, 811-819
127. Ebina, M., Steinberg, S. M., Mulshine, J. L., and Linnoila, R. I. (1994) Relationship of p53 overexpression and up-regulation of proliferating cell nuclear antigen with the clinical course of non-small cell lung cancer. *Cancer research* **54**, 2496-2503
128. Lörz, M., Meyer-Breiting, E., and Bettinger, R. (1994) Proliferating cell nuclear antigen counts as markers of cell proliferation in head and neck cancer. *Eur Arch Otorhinolaryngol* **251**, 91-94
129. Elias, J. M. (1997) Cell Proliferation Indexes: a Biomarker in Solid Tumors. *Biotechnic & Histochemistry* **72**, 78-85
130. Waseem, N. H., Labib, K., Nurse, P., and Lane, D. P. (1992) Isolation and analysis of the fission yeast gene encoding polymerase delta accessory protein PCNA. *The EMBO journal* **11**, 5111-5120
131. Maeshima, Y., Kashihara, N., Sugiyama, H., Makino, H., and Ota, Z. (1996) Antisense oligonucleotides to proliferating cell nuclear antigen and Ki-67 inhibit human mesangial cell proliferation. *Journal of the American Society of Nephrology* **7**, 2219-2229
132. Morita, Y., Kashihara, N., Yamamura, M., Okamoto, H., Harada, S., Maeshima, Y., Okamoto, K., and Makino, H. (1997) Inhibition of rheumatoid synovial fibroblast proliferation by antisense oligonucleotides targeting proliferating cell nuclear antigen messenger RNA. *Arthritis Rheum.* **40**, 1292-1297
133. Kontopidis, G., Wu, S.-Y., Zheleva, D. I., Taylor, P., McInnes, C., Lane, D. P., Fischer, P. M., and Walkinshaw, M. D. (2005) Structural and biochemical studies of human proliferating cell nuclear antigen complexes provide a rationale for cyclin association and inhibitor design. *Proceedings of the National Academy of Sciences of the United States of America* **102**, 1871-1876
134. Punchihewa, C., Inoue, A., Hishiki, A., Fujikawa, Y., Connelly, M., Evison, B., Shao, Y., Heath, R., Kuraoka, I., Rodrigues, P., Hashimoto, H., Kawanishi, M., Sato, M., Yagi, T., and Fujii, N. (2012) Identification of small molecule proliferating cell nuclear antigen (PCNA) inhibitor that disrupts interactions with PIP-box proteins and inhibits DNA replication. *The Journal of biological chemistry* **287**, 14289-14300
135. Mackey, Z. B., O'Brien, T. C., Greenbaum, D. C., Blank, R. B., and McKerrow, J. H. (2004) A cathepsin B-like protease is required for host protein degradation in *Trypanosoma brucei*. *The Journal of biological chemistry* **279**, 48426-48433
136. Lewis, T. S., Shapiro, P. S., and Ahn, N. G. (1998) Signal transduction through MAP kinase cascades. *Adv.Cancer Res.* **74**, 49-139
137. Kolch, W. (2000) Meaningful relationships: the regulation of the Ras/Raf/MEK/ERK pathway by protein interactions. *Biochemical Journal* **351**, 289-305

138. O'Neill, E., and Kolch, W. (2004) Conferring specificity on the ubiquitous Raf/MEK signalling pathway. *British journal of cancer* **90**, 283-288
139. Guttinger, A., Schwab, C., Morand, S., Roditi, I., and Vassella, E. (2007) A mitogen-activated protein kinase of *Trypanosoma brucei* confers resistance to temperature stress. *Molecular and biochemical parasitology* **153**, 203-206
140. Morand, S., Renggli, C. K., Roditi, I., and Vassella, E. (2012) MAP kinase kinase 1 (MKK1) is essential for transmission of *Trypanosoma brucei* by Glossina morsitans. *Molecular and biochemical parasitology* **186**, 73-76
141. Gulbis, J. M., Kelman, Z., Hurwitz, J., O'Donnell, M., and Kuriyan, J. (1996) Structure of the C-Terminal Region of p21WAF1/CIP1 Complexed with Human PCNA. *Cell* **87**, 297-306
142. Ron D, D. H. (1992) pGSTag--a versatile bacterial expression plasmid for enzymatic labeling of recombinant proteins. *Biotechniques* **13**, 866-869
143. Hellman, U., Wernstedt, C., Gonez, J., and Heldin, C. H. (1995) Improvement of an "In-Gel" digestion procedure for the micropreparation of internal protein fragments for amino acid sequencing. *Anal Biochem* **224**, 451-455
144. Olsen, J. V., de Godoy, L. M., Li, G., Macek, B., Mortensen, P., Pesch, R., Makarov, A., Lange, O., Horning, S., and Mann, M. (2005) Parts per million mass accuracy on an Orbitrap mass spectrometer via lock mass injection into a C-trap. *Mol Cell Proteomics* **4**, 2010-2021
145. Chalkley, R. J., Baker, P. R., Medzihradszky, K. F., Lynn, A. J., and Burlingame, A. L. (2008) In-depth analysis of tandem mass spectrometry data from disparate instrument types. *Mol Cell Proteomics* **7**, 2386-2398
146. Elias, J. E., and Gygi, S. P. (2007) Target-decoy search strategy for increased confidence in large-scale protein identifications by mass spectrometry. *Nat Meth* **4**, 207-214
147. Baker, P. R., Trinidad, J. C., and Chalkley, R. J. (2011) Modification site localization scoring integrated into a search engine. *Mol Cell Proteomics* **10**, M111 008078
148. Zhou, Y., and Landweber, L. F. (2007) BLASTO: a tool for searching orthologous groups. *Nucleic acids research* **35**, W678-W682
149. El-Sayed, N. M., Myler, P. J., Blandin, G., Berriman, M., Crabtree, J., Aggarwal, G., Caler, E., Renauld, H., Worthey, E. A., Hertz-Fowler, C., Ghedin, E., Peacock, C., Bartholomeu, D. C., Haas, B. J., Tran, A. N., Wortman, J. R., Alsmark, U. C., Angiuoli, S., Anupama, A., Badger, J., Bringaud, F., Cadag, E., Carlton, J. M., Cerqueira, G. C., Creasy, T., Delcher, A. L., Djikeng, A., Embley, T. M., Hauser, C., Ivens, A. C., Kummerfeld, S. K., Pereira-Leal, J. B., Nilsson, D., Peterson, J., Salzberg, S. L., Shallom, J., Silva, J. C., Sundaram, J., Westenberger, S., White, O., Melville, S. E., Donelson, J. E., Andersson, B., Stuart, K. D., and Hall, N. (2005) Comparative genomics of trypanosomatid parasitic protozoa. *Science* **309**, 404-409
150. Abe, M. K., Kahle, K. T., Saelzler, M. P., Orth, K., Dixon, J. E., and Rosner, M. R. (2001) ERK7 is an autoactivated member of the MAPK family. *The Journal of biological chemistry* **276**, 21272-21279
151. Hanks, S., Quinn, A., and Hunter, T. (1988) The protein kinase family: conserved features and deduced phylogeny of the catalytic domains. *Science* **241**, 42-52
152. Carrera, A. C., Alexandrov, K., and Roberts, T. M. (1993) The conserved lysine of the catalytic domain of protein kinases is actively involved in the phosphotransfer reaction and not required for anchoring ATP. *Proceedings of the National Academy of Sciences of the United States of America* **90**, 442-446
153. Saelzler, M. P., Spackman, C. C., Liu, Y., Martinez, L. C., Harris, J. P., and Abe, M. K. (2006) ERK8 Down-regulates Transactivation of the Glucocorticoid Receptor through Hic-5. *Journal of Biological Chemistry* **281**, 16821-16832
154. Ashwell, J. D. (2006) The many paths to p38 mitogen-activated protein kinase activation in the immune system. *Nat Rev Immunol* **6**, 532-540
155. Songyang, Z., Lu, K. P., Kwon, Y. T., Tsai, L. H., Filhol, O., Cochet, C., Brickey, D. A., Soderling, T. R., Bartleson, C., Graves, D. J., DeMaggio, A. J., Hoekstra, M. F., Blenis, J.,

Hunter, T., and Cantley, L. C. (1996) A structural basis for substrate specificities of protein Ser/Thr kinases: primary sequence preference of casein kinases I and II, NIMA, phosphorylase kinase, calmodulin-dependent kinase II, CDK5, and Erk1. *Molecular and Cellular Biology* **16**, 6486-6493

156. Lebedeva, S., Jens, M., Theil, K., Schwanhäusser, B., Selbach, M., Landthaler, M., and Rajewsky, N. (2011) Transcriptome-wide Analysis of Regulatory Interactions of the RNA-Binding Protein HuR. *Molecular Cell* **43**, 340-352
157. Mukherjee, N., Corcoran, David L., Nusbaum, Jeffrey D., Reid, David W., Georgiev, S., Hafner, M., Ascano Jr, M., Tuschl, T., Ohler, U., and Keene, Jack D. (2011) Integrative Regulatory Mapping Indicates that the RNA-Binding Protein HuR Couples Pre-mRNA Processing and mRNA Stability. *Molecular Cell* **43**, 327-339
158. Katsanou, V., Milatos, S., Yiakouvaki, A., Sgantzis, N., Kotsoni, A., Alexiou, M., Harokopos, V., Aidinis, V., Hemberger, M., and Kontoyiannis, D. L. (2009) The RNA-Binding Protein Elavl1/HuR Is Essential for Placental Branching Morphogenesis and Embryonic Development. *Molecular and Cellular Biology* **29**, 2762-2776
159. Najafabadi, H. S., Lu, Z., MacPherson, C., Mehta, V., Adoue, V., Pastinen, T., and Salavati, R. (2013) Global identification of conserved post-transcriptional regulatory programs in trypanosomatids. *Nucleic acids research* **41**, 8591-8600
160. Olsen, J. V., Blagoev, B., Gnad, F., Macek, B., Kumar, C., Mortensen, P., and Mann, M. (2006) Global, In Vivo, and Site-Specific Phosphorylation Dynamics in Signaling Networks. *Cell* **127**, 635-648
161. Wang, S.-C. (2014) PCNA: a silent housekeeper or a potential therapeutic target? *Trends in Pharmacological Sciences*
162. Mercer, L., Bowling, T., Perales, J., Freeman, J., Nguyen, T., Bacchi, C., Yarlett, N., Don, R., Jacobs, R., and Nare, B. (2011) 2,4-Diaminopyrimidines as Potent Inhibitors of *Trypanosoma brucei* and Identification of Molecular Targets by a Chemical Proteomics Approach. *PLoS Neglected Tropical Diseases* **5**, e956
163. Chang, K. Y., Tsai, S. Y., Wu, C. M., Yen, C. J., Chuang, B. F., and Chang, J. Y. (2011) Novel phosphoinositide 3-kinase/mTOR dual inhibitor, NVP-BGT226, displays potent growth-inhibitory activity against human head and neck cancer cells in vitro and in vivo. *Clin Cancer Res* **17**, 7116-7126
164. Baumann, P. S., Laura; Mandl-Weber, Sonja; Oduncu, Fuat; Schmidmaier, Ralf. (2012) Simultaneous targeting of PI3K and mTOR with NVP-BGT226 is highly effective in multiple myeloma. *Anti-Cancer Drugs* **23**, 131-138
165. Simioni, C., Cani, A., Martelli, A. M., Zauli, G., Alameen, A. A., Ultimo, S., Tabellini, G., McCubrey, J. A., Capitani, S., and Neri, L. M. (2015) The novel dual PI3K/mTOR inhibitor NVP-BGT226 displays cytotoxic activity in both normoxic and hypoxic hepatocarcinoma cells. *Oncotarget* **6**, 17147-17160
166. Bain, J., Plater, L., Elliott, M., Shpiro, N., Hastie, C. J., Mclauchlan, H., Klevernic, I., Arthur, J. Simon C., Alessi, Dario R., and Cohen, P. (2007) The selectivity of protein kinase inhibitors: a further update. *Biochemical Journal* **408**, 297-315
167. McNamara, C. W., Lee, M. C. S., Lim, C. S., Lim, S. H., Roland, J., Nagle, A., Simon, O., Yeung, B. K. S., Chatterjee, A. K., McCormack, S. L., Manary, M. J., Zeeman, A.-M., Dechering, K. J., Kumar, T. R. S., Henrich, P. P., Gagaring, K., Ibanez, M., Kato, N., Kuhen, K. L., Fischli, C., Rottmann, M., Plouffe, D. M., Bursulaya, B., Meister, S., Rameh, L., Trappe, J., Haasen, D., Timmerman, M., Sauerwein, R. W., Suwanarusk, R., Russell, B., Renia, L., Nosten, F., Tully, D. C., Kocken, C. H. M., Glynne, R. J., Bodenreider, C., Fidock, D. A., Diagana, T. T., and Winzeler, E. A. (2013) Targeting Plasmodium PI(4)K to eliminate malaria. *Nature* **504**, 248-253
168. Woodland, A., Thompson, S., Cleghorn, L. A. T., Norcross, N., De Rycker, M., Grimaldi, R., Hallyburton, I., Rao, B., Norval, S., Stojanovski, L., Brun, R., Kaiser, M., Frearson, J. A., Gray,

D. W., Wyatt, P. G., Read, K. D., and Gilbert, I. H. (2015) Discovery of Inhibitors of *Trypanosoma brucei* by Phenotypic Screening of a Focused Protein Kinase Library. *ChemMedChem* **10**, 1809-1820

169. Peña, I., Pilar Manzano, M., Cantizani, J., Kessler, A., Alonso-Padilla, J., Bardera, A. I., Alvarez, E., Colmenarejo, G., Cotillo, I., Roquero, I., de Dios-Anton, F., Barroso, V., Rodriguez, A., Gray, D. W., Navarro, M., Kumar, V., Sherstnev, A., Drewry, D. H., Brown, J. R., Fiandor, J. M., and Julio Martin, J. (2015) New Compound Sets Identified from High Throughput Phenotypic Screening Against Three Kinetoplastid Parasites: An Open Resource. *Scientific Reports* **5**, 8771
170. Diaz, R., Luengo-Arratta, S. A., Seixas, J. D., Amata, E., Devine, W., Cordon-Obras, C., Rojas-Barros, D. I., Jimenez, E., Ortega, F., Crouch, S., Colmenarejo, G., Fiandor, J. M., Martin, J. J., Berlanga, M., Gonzalez, S., Manzano, P., Navarro, M., and Pollastri, M. P. (2014) Identification and Characterization of Hundreds of Potent and Selective Inhibitors of *Trypanosoma brucei* Growth from a Kinase-Targeted Library Screening Campaign. *PLoS Negl Trop Dis* **8**, e3253
171. Wu, Z., Wang, Y., and Chen, L. (2013) Network-based drug repositioning. *Molecular BioSystems* **9**, 1268-1281
172. Sbaraglini, M. L., Vanrell, M.C., Bellera, C.L., Benaim, G., Carrillo, C., Talevi A., Romano P.S. (2016) Drug repositioning for neglected tropical protozoan diseases. *Current Topics in Medicinal Chemistry* **Epub ahead of print**
173. Sanchez, C., Ma, C., Crowder, R., Guintoli, T., Phommaly, C., Gao, F., Lin, L., and Ellis, M. (2011) Preclinical modeling of combined phosphatidylinositol-3-kinase inhibition with endocrine therapy for estrogen receptor-positive breast cancer. *Breast Cancer Research* **13**, R21
174. Gozgit, J. M., Bebernitz, G., Patil, P., Ye, M., Parmentier, J., Wu, J., Su, N., Wang, T., Ioannidis, S., Davies, A., Huszar, D., and Zinda, M. (2008) Effects of the JAK2 Inhibitor, AZ960, on Pim/BAD/BCL-xL Survival Signaling in the Human JAK2 V617F Cell Line SET-2. *Journal of Biological Chemistry* **283**, 32334-32343
175. Yang, J., Ikezoe, T., Nishioka, C., Furihata, M., and Yokoyama, A. (2010) AZ960, a Novel Jak2 Inhibitor, Induces Growth Arrest and Apoptosis in Adult T-Cell Leukemia Cells. *Molecular Cancer Therapeutics* **9**, 3386-3395
176. Ikezoe, T., Yang, J., Nishioka, C., Kojima, S., Takeuchi, A., Phillip Koeffler, H., and Yokoyama, A. (2011) Inhibition of signal transducer and activator of transcription 5 by the inhibitor of janus kinases stimulates dormant human leukemia CD34+/CD38− cells and sensitizes them to antileukemia agents. *International Journal of Cancer* **128**, 2317-2325
177. Takeuchi, A., Nishioka, C., Ikezoe, T., Yang, J., and Yokoyama, A. (2015) STAT5A regulates DNMT3A in CD34+/CD38− AML cells. *Leukemia Research* **39**, 897-905